THE ASTROPHYSICAL JOURNAL

AN INTERNATIONAL REVIEW OF SPECTROSCOPY AND ASTRONOMICAL PHYSICS

VOLUME 91 MAY 1940 NUMBER 4

THE RELATION BETWEEN ABSORPTION VELOCITY AND RATE OF DECLINE FOR GALACTIC NOVAE

DEAN B. McLAUGHLIN

ABSTRACT

The relations between times of decline of light and the velocities of the *principal* and *diffuse enhanced* absorption spectra are determined from observations of twenty-one galactic novae. These agree closely with relations between rates of development of spectra and the absorption velocities of six bright novae, as previously found by the author.

It is concluded that (1) the spectral stage is a function of the difference of magnitude from maximum; (2) the time of decline or of spectral change is *inversely proportional* to the *square* of the velocity of the principal spectrum; and (3), in the average case, the velocity of the diffuse enhanced spectrum is twice that of the principal spectrum.

The observed relations are radically different from that proposed by Zwicky, viz., the lifetime is *directly* proportional to the velocity. Such a relation, adjusted on a supernova, is fortuitously satisfied by some rapid common novae, but stars of slow and intermediate rate deviate very far from Zwicky's relation.

In an earlier paper[1] the writer demonstrated that there exists a close relation between the velocities of the absorption spectra and the rates of development through successive spectroscopic stages of the six bright galactic novae for which accurate data are available. It was noted incidentally that the rate of spectral change is related to the rate of decline of light of these objects. Evidently, therefore, it should be possible to find a corresponding relation between the velocities of the absorption spectra and the rate of fading. Such a relation has, in fact, been suggested by Zwicky,[2] but it will be

[1] *Ap. J.*, **85**, 362, 1937.

[2] *Pub. A.S.P.*, **48**, 191, 1936.

shown in this paper that the theoretical relation he proposes is quite incompatible with the observational data.

A number of the fainter novae have been observed with spectrographs only in a very fragmentary manner, so that little is known of the details of their spectroscopic history. They are, therefore, not usable in deriving a relation between velocity and rate of spectral change. But a single spectrogram will furnish a measure of the velocity which can be used in connection with a fairly good light-curve to furnish a datum for use in deriving a relation between velocity and rate of fading. It is not even necessary that the velocities be of high accuracy; an uncertainty of 10 per cent is of little consequence, and an error of 20 per cent would still leave the value within the actual scatter of the best determinations. Thus, observations made with low dispersion—even mere estimates—would be useful in a statistical study.

A search of the literature yielded twenty-one galactic novae for which measures or reliable estimates of velocity have been made or can be calculated from the published data. Besides these, there are four objects which it seems best to omit from the present discussion. These are the two repeating novae (T Pyxidis and RS Ophiuchi) and the two RT Serpentis stars (RT Serpentis and DO Aquilae). Spectra of several others exist and might furnish usable data if they were subjected to study. Brief notes on the spectroscopic material are given below. V_1 and V_2 are the velocities in km/sec of the "principal" and "diffuse enhanced" absorption spectra.

Nova Aquilae 1899 (Campbell, *Ap. J.*, **12**, 258, 1900). Visual observation in August, 1900. Emission lines very broad; perhaps twice as broad as in Nova Aurigae in August, 1892. Inferred $V_1 = 800$.

Nova Aquilae 1905 (Moore, *Ap. J.*, **23**, 261, 1906). $H\beta$ 40 A wide with sharp edges. Hy and $H\delta$ wider (probably blended with 4352 or 4363 and *N* III, respectively). Calculated $V_1 = 1230$.

Nova Aquilae 1918 (many references). Michigan plates: $V_1 = 1500$; $V_2 = 2200$.

Nova (DO) Aquilae 1925 (Merrill, *Pub. A.S.P.*, **38**, 387, 1926). Photograph reproduced; no data given. Many emission bands of [*Fe* II], about 12 A wide (estimated from reproduction).

Nova (EL) Aquilae 1927 (Humason, *Pub. A.S.P.*, **39**, 369, 1927). Many lines measured; mean $V_1 = 900$; $V_2 = 2100$.

Nova (v356) Aquilae 1936 (Wyse, *Pub. A.S.P.*, **48**, 305, 1936; McLaughlin, *Pub. Amer. Astr. Soc.*, **9**, 12, 1937). $V_1=450$; $V_2=960$.

Novae (v368) Aquilae 1936 (Wyse, *op. cit.;* McLaughlin, *op. cit.*). $V_1=1000$; ($V_2=1900$).

Nova Arae 1910 (*Harvard Ann.*, **76**, 37). No data on velocities or band widths.

Nova Aurigae 1891 (Campbell, *Pub. A.S.P.*, **4**, 231, 1892). Dark lines 12–14 A wide, with centers about 11 A to violet of strongest part of bright lines. Fine bright lines *central* in the absorption. These latter may be interpreted as continuum between two absorption components. Considering the phase of the nova, there is little doubt that this is the case and that the two components were the principal and the diffuse enhanced spectra. Inferred $V_1=400$; $V_2=800$.

RS Carinae 1895 (*Harvard Ann.*, **76**, 37). No data on velocities or band widths.

Nova Cygni 1920 (many references). Michigan plates (Baldwin, unpublished): $V_1=700$; $V_2=1400$.

Nova Geminorum 1903 (Reese and Curtis, *Ap. J.*, **18**, 299, 1903). Widths of emission bands a little discordant, but clearly indicate approximately $V_1=1600$.

Nova Geminorum 1912 (many references). Michigan plates: $V_1=800$; $V_2=1500$.

Nova Herculis 1934 (many references). Michigan plates: $V_1=315$; $V_2=800$.

Nova Lacertae 1910 (Frost, *Ap. J.*, **33**, 410, 1911; Wright, *Pub. A.S.P.*, **23**, 50, 1911). Two absorption components blended except at $H\delta$. Velocities approximately: $V_1=950$; 1200. Emission edges on Lick plate indicate probable component, $V_2=1800$. Values somewhat discordant.

Note added in proof.—Since the preceding statement was written, the author has measured the Yerkes plate, which was kindly loaned by Dr. Struve. The components with velocities of 950 and 1200 km/sec are separately measurable at $H\beta$, $H\gamma$, and $H\delta$. The component with $V = 1800$ is not confirmed; instead, absorption with $V = 2050$ is just suspected at all three lines. However, the effect of this change upon the solutions would be very slight.

Nova Lacertae 1936 (many references). Michigan plates: $V_1=1500$; $V_2=3000$. Both velocities increased greatly in later stages.

Nova Lyrae 1919 (Adams and Joy, *Pub. A.S.P.*, **32**, 154, 1920; Wright, *Pub. A.S.P.*, **32**, 167, 1920). Accordant values: $V_1=980$; $V_2=1900$.

Nova Monocerotis 1918 (Paddock, *Lick Obs. Bull.*, **9**, 170, 1918). Emission edges of $H\beta$ and $H\gamma$ indicate probable $V_1=1300$.

Nova Normae 1893 (*Harvard Ann.*, **76**, 37). No data on velocities or band widths.

RS Ophiuchi 1933 (many references). Michigan plates: no clear absorption components; emission bands vague, of uncertain width. Extreme edge $H\beta$ emission gives $V=1400$.

Nova Ophiuchi 1919 (Adams and Burwell, *Ap. J.*, **51**, 121, 1920; Wright, *Lick Obs. Pub.*, **14**, 1, 1920). Many lines measured: $V_1=330$.

Nova Persei 1901 (many references; Stratton, *Ann. Solar Phys. Obs., Cambr.*, **4**, 78, 1936). $V_1 = 1300$, increasing later.

Nova Pictoris 1925 (H. S. Jones, *Cape Ann.*, **10**, Part 9, 1931). $V_1 = 285$; $V_2 = 750$ (average of composite absorption).

T Pyxidis 1920 (Adams and Joy, *Pop. Astr.*, **28**, 514, 1920). Absorption velocities: (940); 1380; 1830.

Nova Sagittarii 1898 (Pickering, *Harvard Ann.*, **56**, 170). Bright hydrogen lines; broad 4640 band; *narrow* bright lines as in Nova Aurigae. The writer interprets these narrow lines as maxima in the emission bands. If the bands were truly narrow in this rapid nova, then it is entirely unique and deviates very far from the relation which is approximately satisfied by all other normal novae.

Nova Sagittarii 1910 (Wright, *Lick Obs. Bull.*, **6**, 65, 1912). Widths of emission bands indicate approximate velocity of 700 km/sec. No absorption lines were measured. Considering the phase and the slowness of this nova, it seems probable that this velocity is to be referred to the diffuse enhanced spectrum rather than to the principal spectrum. Hence, $V_2 = 700$.

Nova Sagittarii 1936.32 (Burwell, *Pub. A.S.P.*, **49**, 342, 1937; R. Jones, *Harvard Bull.*, No. 907). No data on velocities or band widths.

Nova (v726) Sagittarii 1936.37 (Mrs. Mayall, *Harvard Bull.*, No. 907). Emission bands 40 A wide. Calculated $V_1 = 1400$.

Nova (v630) Sagittarii 1936.7 (Adams, Joy, and Dunham, *Pub. A.S.P.*, **48**, 328, 1936). $V_1 = 2130$; $V_2 = 3590$.

RT Serpentis (Adams and Joy, *Pub. A.S.P.*, **40**, 252, 1928). Absorption lines show variable *positive* velocity.

Nova (XX) Tauri 1927 (Schwassmann and Wachmann, *A.N.*, **232**, 273, 1927). Displacements of absorption and emission lines, on objective-prism plates, seem ambiguous. Possible velocity 1200 km/sec? This star omitted from solutions.

Nova Velorum 1905 (*Harvard Ann.*, **76**, 37). No data on velocities or band widths.

There are fairly good light-curves for all the twenty-one novae which have furnished usable spectroscopic data. A discussion of the light-curves has been published elsewhere,[3] and the relevant data have been taken bodily from that paper. In a few cases a small amount of reconstruction was necessary on account of gaps in the series of observations. These are assigned lower weight in the present discussion. In no case is the information on the light-variation sufficiently poor to justify exclusion of a star for which an absorption velocity is available. The data used are the time intervals from

[3] *Pop. Astr.*, **47**, 410, 481, 538, 1939.

maximum to two and three magnitudes below maximum. In those curves which had large fluctuations the interval was measured from maximum to the *last date* on which the star was of the magnitude concerned. Smoothed curves would have yielded values slightly different, but not sufficiently so to justify a duplicate investigation by that method.

TABLE 1

DURATIONS OF DECLINE AND ABSORPTION VELOCITIES OF NOVAE

Nova	Duration of Decline		Relative Duration (N. Lac = 1)	Velocities		Weight
	2 Mag. Days	3 Mag. Days		V_1 Km/Sec	V_2 Km/Sec	
Aql 1899	25	33	4.4	800:	.....	0.3
Aql 1905	9	31	2.6	1230	.....	0.5
Aql 1918	4	8	0.85	1500	2200	1.0
Aql 1925 (EL)	8:	22:	2:	900	2100	0.5
Aql 1936 (v356)	150	.....	30	450	960	1.0
Aql 1936 (v368)	25:	50:	5.3:	1000	1900:	0.7
Aur 1892	80	90:	13	400:	800:	0.5
Cyg 1920	7	16	1.6	700	1400	1.0
Gem 1903	6	17	1.6	1600	.....	0.7
Gem 1912	16	37	3.6	800	1500	1.0
Her 1934	67	100	12.2	315	800	1.0
Lac 1910	20	37	4.1	950	1800:	0.5
Lac 1936	5	9	1.0	1500	3000	1.0
Lyr 1919	31	80	7.6	980	1900	0.7
Mon 1918	10	21	2.2	1300	.....	0.7
Oph 1919	120	150	20	330	.....	0.7
Per 1901	6	13	1.3	1300	.....	1.0
Pic 1925	80	150	16.4	285	750	1.0
Sgr 1910	220	320	40	.....	700:	0.3
Sgr 1936.37	14:	34:	3.3:	1400:	.....	0.3
Sgr 1936.7	4	9	0.9	2130	3590	1.0

The data on light-variation and velocities are collected in Table 1. The first column contains the designation of each nova; the second and third give the number of days required to decline through two and three magnitudes, respectively. In the fourth column the relative duration of decline is given, with the duration for Nova Lacertae 1936 as unit. These figures were obtained simply by dividing the times in the second column by 5, and those in the third by 9 (since the times for Nova Lacertae were 5 and 9 days), and taking the mean of the two resulting numbers for each nova. The fifth and sixth columns contain the velocities of the "principal" and "diffuse

enhanced" absorption spectra. In the seventh column is the weight given to each nova in the least-squares solutions.

The velocities in Table 1 are not homogeneous. They refer to various time intervals after maximum, and it is well known that

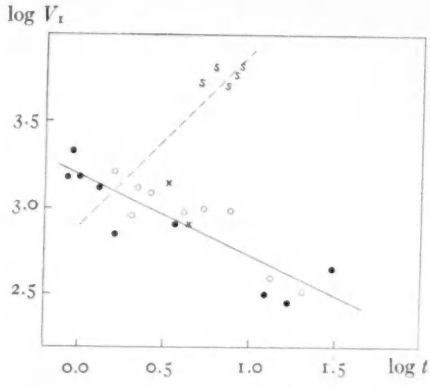

FIG. 1.—The relation between velocity of the "principal" absorption spectrum and the duration of decline for common novae and supernovae. Full circles, weight 1.0; open circles, weight 0.5 to 0.7; crosses, weight 0.3; *S*, supernovae. The full line represents the relation $\log V_1 = 3.19 - 0.47 \log t$. The dashed line represents Zwicky's relation: $\log v = 2.9 + \log t$.

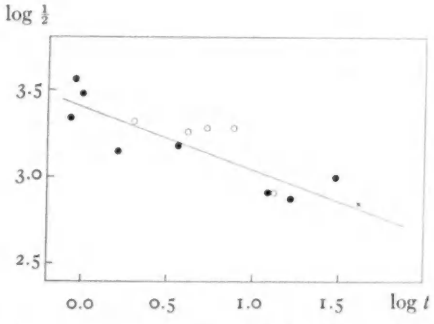

FIG. 2.—The relation between velocity of the "diffuse enhanced" absorption spectrum and the duration of decline for common novae. Full circles, weight 1.0; open circles, weight 0.5 to 0.7; crosses, weight 0.3. The full line represents the relation $\log V_2 = 3.40 - 0.36 \log t$.

the "principal" spectrum especially tends to increase its displacement with the passage of time. However, the increase is usually only moderate; Nova Lacertae 1936 was exceptional, in that the velocity nearly doubled in the course of two weeks. In each case the velocity

has been taken for the earliest phase possible, but no attempt has been made to allow for variation. The possible changes of displacement will operate to increase the scatter of the data, but they should not alter the general conclusions reached.

The data from Table 1 are plotted in Figures 1 and 2 for the "principal" and the "diffuse enhanced" spectra, respectively. In each figure the abscissa is the logarithm of the relative duration of decline, and the ordinate is the logarithm of the velocity. The points fall into bands which may be represented by expressions of the form[4]

$$\log V = a - b \log t , \tag{1}$$

where a and b are positive constants. The largest deviations from the bands of points are exhibited by Nova Cygni, whose decline of light was much too rapid for its absorption velocity. It is noteworthy that this star shows no such deviation from the relation between velocity and rate of development of the spectrum. It is clearly the rate of decline of light which is at fault.

The coefficients a and b were determined by the method of least squares. The resulting relations are as follows:

$$\log V_1 = 3.19 - 0.47 \log t \tag{2}$$

$$\log V_2 = 3.40 - 0.36 \log t \tag{3}$$

for the "principal" and "diffuse enhanced" spectra, respectively. The corresponding straight lines are drawn in Figures 1 and 2. When Nova Cygni is omitted from the solutions, the results are:

$$\log V_1 = 3.22 - 0.50 \log t \tag{2a}$$

$$\log V_2 = 3.43 - 0.39 \log t . \tag{3a}$$

The relations derived in the earlier paper,[1] connecting velocity with rate of spectral change, are given here for comparison:

$$\log V_1 = 3.19 - 0.54 \log t \tag{2b}$$

$$\log V_2 = 3.39 - 0.39 \log t . \tag{3b}$$

[4] Logarithms are to the base 10 in all formulae in this paper.

One other relation is readily derived from the velocities. The thirteen novae for which both V_1 and V_2 were measured give a mean value of precisely 2.0 for the ratio V_2/V_1. For individual stars the ratio ranges from 1.5 (Nova Aquilae 1918) to 2.6 (Nova Pictoris). This dispersion is, of course, real, since the velocities are quite accurately known in these cases. Two high values of V_2/V_1 among the slow novae and two low ones among the rapid novae are almost wholly responsible for the difference between the coefficients of log t in formulae (2) and (3).

The agreement of the formulae (2) and (3)—or, alternatively, (2*a*) and (3*a*)—obtained from the rates of decline of light, with the formulae (2*b*) and (3*b*), obtained from the rates of spectral change, is so close that we are justified in concluding that the spectral development is closely related to the decline of light. The principal results of this investigation may then be summarized in the following three general statements:

1. *The stage of the spectral development of a nova is, in the main, a function of the difference of magnitude from maximum.*

2. *The time interval from maximum to any given stage of the decline of light or the spectral development of a nova is approximately inversely proportional to the square of the velocity of the principal absorption spectrum.*

3. *The velocity of the diffuse enhanced spectrum is roughly twice that of the principal spectrum.*

The success of any physical model, or of any theory of the nature of the nova outburst, must be judged by its degree of accordance with these relations, whose derivation is purely empirical.

COMPARISON WITH ZWICKY'S RELATION

On the assumption that the liberation of energy in a nova outburst is instantaneous, Zwicky[5] developed the relation

$$\log t_{\Delta m} = \log v + \text{const} , \qquad (4)$$

connecting the lifetime $t_{\Delta m}$ of the nova, as a star brighter than magnitude $M_{\max} + \Delta m$, with the velocity of the ejected gases. He evaluated the constant by means of the supernova in NGC 4273

[5] *Proc. Nat. Acad. Sci.*, **22**, 457, 1936; *Pub. A.S.P.*, **48**, 191, 1936.

and found that several common novae apparently satisfied the relation. But the equation (4) states that the lifetime is *directly proportional to the first power* of the velocity, while the expression (2), which is based on a much larger body of observational data, states that the duration of decline is *inversely proportional to the square* of the velocity. Inasmuch as the light-curves of common novae and supernovae are of very similar form, we should expect (4) to be just as valid for comparison of times of decline as it is for lifetimes. We shall therefore use t in equation (4) to mean the duration of decline, in terms of the duration for Nova Lacertae.

TABLE 2

Supernova	Velocity Km/Sec	Duration of Decline (N. Lac = 1)
NGC 1003	6500	6
NGC 4273	6500	8.5
NGC 4303	5800	8:
IC 4182	5200	5
NGC 5253*	5000	7:

*Z Centauri.

Observational data are now available for five supernovae. In Table 2 the first column gives the designation of the galaxy in which the supernova appeared; the second contains the velocity as indicated by the widths of emission bands, from the recent tabulation by Whipple;[6] the third column contains the duration of decline, which was determined in the same manner as the similar data in Table 1, from the light-curves by Miss Hoffleit.[7]

When we use the mean values $v = 5800$, $t = 7$, equation (4) becomes

$$\log v = 2.9 + \log t . \qquad (5)$$

Now, by an odd coincidence, if we use the five bright rapid novae of the twentieth century,[8] the mean of their values of $\log t$ and $\log V_1$ gives precisely the same value of the constant! It was this

[6] *Proc. Amer. Phil. Soc.*, **81**, 256, 1939.

[7] *Proc. Amer. Phil. Soc.*, **81**, 271, 1939.

[8] Aquilae 1918, Cygni 1920, Geminorum 1912, Lacertae 1936, Persei 1901.

fortuitous agreement which gave apparent confirmation of Zwicky's equation (4). But the line representing (5) intersects the observed relation (2) at a large angle, as shown in Figure 1. For comparison with the common novae, the data for the five supernovae are indicated on Figure 1 by *S*.

The general conclusion which is indicated is that the supernovae are a class apart and that they cannot be simply linked with the common novae. Their rates of decline are of the same order as that of Nova Lyrae 1919, whose rate may be fairly taken as average. But the spectra of supernovae are evidently rather unlike those of average novae, and the velocities are of a different order. The assignment of an individual star to the category of supernovae solely on the basis of its rate of decline is, therefore, wholly fallacious. Other evidence, however, may tend to confirm the supernova character of a star, in the absence of spectroscopic data. Thus, the brilliant novae of 1572 and 1604 were probably supernovae, since the lack of any identifiable star in the position of either of them requires a distance which makes their luminosities comparable with those of typical extragalactic supernovae. Their rates of decline were such as to agree with this classification.

There seems to be little hope of reconciling the diametrically opposed relations (2) and (5). It might be suggested that for velocities up to 2000 km/sec the lifetime decreases with increasing velocity, after which the reverse is true, but there is no observational evidence to support such a two-branch hypothesis. Objects showing velocities and other spectral characteristics intermediate between common novae and supernovae are entirely unknown. Likewise, there is a minimum of frequency at luminosities intermediate between the two classes.[9] Finally, it appears questionable whether a continuous relation, such as (5), can be expected to apply to the physics of two classes of bodies between which there exists such a profound discontinuity. In other words, a radical difference in the physical causes of the two types of novae seems to be indicated.

THE OBSERVATORY
UNIVERSITY OF MICHIGAN
October 25, 1939

[9] However, it must be admitted that this could be an effect of observational selection.

THE WOLF-RAYET SPECTROSCOPIC BINARY HD 193576*

O. C. WILSON

ABSTRACT

Spectrographic orbits have been derived for the double-lined binary HD 193576. The Wolf-Rayet component is of type WN5, while that of the absorption-line component is somewhat uncertainly estimated as B1. The minimum masses of the Wolf-Rayet and B-type components are 9.74⊙ and 24.8⊙, respectively.

A curious feature of the results is that the γ-axes for the two stars differ by 90 km/sec, the two values being +56 and −34 km/sec, respectively, for the Wolf-Rayet and the B components. Neither erroneous wave lengths nor blends seem to afford an explanation of this difference. Since a velocity for the system of −34 km/sec is much more in keeping with the velocities of other early-type stars in the vicinity of HD 193576 than is one of +56 km/sec, it is probable that the emission bands of the Wolf-Rayet star are shifted toward the red by an amount equal to the difference between the γ-axes. The nature of the red shift is discussed in the following *Contribution*.

The significance of certain rather minor periodic variations in the *He* II 4686 band is discussed. In particular, no evidence for an eclipse is found in the spectrographic material, and, therefore, no est mate of the inclination of the orbit plane is possible.

The absolute magnitude of the system has been previously derived from the intensities of the interstellar H and K lines. It is found necessary to assume the stars to be 1–2 mag. brighter in order to bring the density of the B-type component into line with the known densities of other massive stars of early type. When this is done, the density of the Wolf-Rayet star is found to be of the same order as that of the sun, if it has a surface temperature of 80,000°. Also, the Wolf-Rayet star appears to be about 4 mag. brighter than would be estimated from its mass on the basis of the empirical mass-luminosity relation.

The Wolf-Rayet star HD 193576 was recently announced to be a spectroscopic binary on the basis of spectrograms obtained at Mount Wilson in 1937 and 1938.[1] The velocity range was large, and, in addition, the absorption-line spectrum of the other component was visible. For these reasons the star offered a unique opportunity of determining at least a lower limit for the mass of a Wolf-Rayet star, a quantity about which we have hitherto had no knowledge. Accordingly, 40 spectrograms of the star were secured during the summer of 1939. This material, together with the earlier plates, has sufficed to yield good spectroscopic orbits for both components of the system. These orbits, however, possess certain features which

* *Contributions from the Mount Wilson Observatory, Carnegie Institution of Washington*, No. 623.

[1] *Pub. A.S.P.*, **51**, 55, 1939.

may lead to a conception of the nature of a Wolf-Rayet star rather widely divergent from that generally accepted at present. Thus it became necessary to examine existing data on the spectra of other Wolf-Rayet stars to seek for evidence bearing on the conclusions derived for HD 193576. Confirmatory evidence is possibly present in published measures of Wolf-Rayet spectra; and certain, as yet unpublished, measures by the writer have a direct bearing on the matter. In view of these facts it seemed best to divide the work into two parts. The present paper discusses the observations of HD 193576 and the deductions which follow directly from them, with a minimum of assumption. The succeeding paper combines the conclusions of this one with all available data in an attempt to form an acceptable picture of a Wolf-Rayet star.

The observations.—The emission portion of the spectrum of HD 193576 is of spectral type WN5. The bands are those due to *He* II, *N* IV, and *N* V almost exclusively. Careful inspection of the plates fails to reveal any certain evidence of the presence of bands due to *H* or *He* I. (These remarks apply only to the photographic region.) By far the strongest band—and, in fact, the dominating feature of the entire blue-violet region—is λ 4686 *He* II. In the absence of photometric measures it is impossible to make a definite statement, but this band must exceed any of the others in strength by a factor of at least 10–20 and is much the most suitable for measurement. In addition to its great intensity, and partly, perhaps, as a consequence of it, λ 4686 is, in all probability, entirely free of disturbing blends. None can be detected on any of the spectrograms, and there are no *N* IV or *N* V emissions listed by Edlén[2] in the vicinity. Hence, it seems fair to suppose that measures of this band may legitimately be reduced to velocities by using the laboratory wave length, 4685.81 A.

The *N* V bands at λ 4603 and λ 4619 were also measured on practically all plates. They are much weaker than λ 4686 and give a definite impression of being considerably narrower. However, since they occur in a region which is relatively free of other faint bands, they are generally suitable for measurement, especially on plates whose density is near the optimum value. Edlén[2] gives for these

[2] *Zs. f. Ap.*, **7**, 378, 1933.

bands the wave lengths 4603.2 and 4619.4 A, and these values were used to reduce the measures to velocities. These wave lengths of Edlén, however, were not directly measured in the laboratory but were deduced from measures of lines in the far ultraviolet region of the spectrum and may be appreciably in error. Consequently, the velocities derived from λ 4603 and λ 4619 were placed on the same footing as those from λ 4686 by applying to each a correction, $-\Delta V$, where

$$\Delta V_{4603} = \overline{V_{4603} - V_{4686}} = +8 \text{ km/sec}$$

and

$$\Delta V_{4619} = \overline{V_{4619} - V_{4686}} = -19 \text{ km/sec}.$$

In passing, we may apply these corrections to Edlén's wave lengths and obtain, perhaps, slightly improved values. Thus, from 48 and 43 spectrograms, respectively, we find the wave lengths, referred to λ 4685.81 of *He* II,

$$N\,\text{V} \quad 3S - 3P_2, \qquad \lambda = 4603.32 \text{ A},$$

$$N\,\text{V} \quad 3S - 3P_1, \qquad \lambda = 4619.10 \text{ A}.$$

In deriving the velocities, the measures of the three bands were given equal weight.

The exact classification of the star producing the absorption spectrum is not possible, but it is important to determine its spectral type as closely as we can. The outstanding absorption features are *Hβ*, *Hγ*, and *Hδ*. These lines are not very strong, but all three are easily visible on suitable spectrograms. All the plates were first measured by using only *Hγ* in absorption, and λλ 4603, 4619, and 4686 in emission. *Hβ* was omitted because of the poorer quality of the spectra in that region and because of considerable interference due to the λ 4859 *He* II band of the Wolf-Rayet component, while *Hδ* was considered too difficult. The latter line, in general, does not show as clearly as does *Hγ*. However, to strengthen the material, the plates were all measured a second time (for the absorption lines only), and *Hδ* and λ 4471 *He* I were then included wherever possible. *Hδ* was measured on 39 plates, and λ 4471 on 27.

The latter is a very difficult line to measure and yields velocities in only rough agreement with $H\gamma$ and $H\delta$. Nevertheless, I believe that λ 4471 is present, a belief greatly strengthened by the appearance of a feeble absorption at about λ 4026 on plates with good density at that wave length. In forming the mean velocities for a plate, each measure of $H\gamma$ and $H\delta$ was given weight 2, while the measure of λ 4471 was assigned weight 1. Thus, since $H\gamma$ was measured twice, the three lines $H\gamma$, $H\delta$, and λ 4471 had, in effect, the weights 4, 2, and 1, respectively.

A careful search was made for the *He* II absorption lines at λ 4542 and λ 4200 on spectrograms for which the velocity differences between absorption and emission components were greatest. The results are rather inconclusive; but it may be definitely stated that, if the Pickering series is present at all, it must be very considerably weaker than the Balmer series. This point is very important, for, if the Pickering series were present in appreciable strength, the wave lengths of the lines which we have assumed to be $H\gamma$ and $H\delta$ might be rather seriously affected by blending and thus yield erroneous velocities for the absorption component. As it stands, the weight of the evidence is that we are entirely justified in using the normal hydrogen wave lengths to derive velocities, and this has been the procedure followed.

It is thus evident that no very certain classification of the spectrum of the absorption-line star can be made. I am inclined to place it somewhere in the range B0–B3, although, as far as the observations go, it might easily lie somewhat outside these limits at either end. For the sake of definiteness, B1 is adopted with the understanding that it is subject to considerable uncertainty.

The velocity measures, all from Mount Wilson spectrograms except the first two,[3] are collected and summarized in Tables 1 and 2. The phases, which are in fractions of a period, have been computed with the period and zero point to be described below. When several plates were obtained in sequence on the same night, only the Julian day and the phase of the mean time of observation are recorded. The velocities from individual spectrograms have been tabulated,

[3] I am greatly indebted to Dr. C. S. Beals for his kindness in sending me these early Victoria spectrograms of this star.

TABLE 1

OBSERVED RADIAL VELOCITIES OF HD 193576

PLATE	JULIAN DAY	PHASE (FRACTION OF PERIOD)	V_{Em}	V_{Abs}	NORMAL POINT NO.	
					Em.	Abs.
	2,420,000+		km/sec	km/sec		
DAO 8241	3342.781	0.281	+316	−161	.....	.....
DAO 9152	3612.910	.408	+255	−100	.....	.....
V 1985	8770.882	.887	−138	+ 97	8	8
V 1989	8771.905	.130	+257	−119	1	1
γ 21581	9240.623	.402	+199	.....	4	.....
21582			+230			
γ 21588	9241.615	.637	−164	.....	6	.....
21589			−231			
γ 21593	9243.611	.111	+353	.....	.....	.....
γ 21942	9445.891	.131	+281	−157	1	1
21943			+300	−153		
21944			+298	−118		
γ 21999	9471.823	.288	+391	.....	3	3
22000			+315	−194		
22001			+338	−170		
22002			+341	−149		
22003			+339	−164		
22004			+354	−132		
γ 22005	9472.774	.513	+ 20	+ 5	5	5
γ 22006	9474.792	.992	− 16	+ 31	9	9
22007			+ 52	+ 9		
22008			+ 40	−110		
22009			+ 79	− 75		
C 7375	9509.736	.288	+364	−111	3	3
7376			+426	−112		
7377			+356	−140		
C 7380	9510.772	.534	+ 75	− 5	5	5
7381			+ 21	−102		
7382			+ 8	− 25		
7383			− 19	− 12		
γ 22130	9511.746	0.766	−256	+ 73	7	7
22131			−261	+ 66		
22132			−259	+109		
22133			−282	+ 93		
22134			−254	+ 50		

TABLE 1—*Continued*

Plate	Julian Day	Phase (Fraction of Period)	V_{Em}	V_{Abs}	Normal Point No.	
					Em.	Abs.
	2,420,000+		km/sec	km/sec		
γ 22136	9513.678	0.224	+344	−141	2	2
γ 22145	9533.760	.991	+105	.....	.....	.....
γ 22146	9534.755	.227	+390	−116	2	2
22147			+381	−120		
γ 22150	9535.698	.451	+108	− 94	4	4
22151			+146	− 87		
γ 22156	9536.795	.712	−296	+105	7	7
γ 22161	9537.677	.921	− 92	+ 52	8	8
γ 22166	9540.698	.638	−162	+ 57	6	6
22167			−195	+ 69		
C 7394	9541.656	.866	−115	+104	8	8
7395			−115	+ 97		
γ 22176	9542.654	0.102	+185	− 94	1	1
22177			+263	−104		

however, to illustrate the accuracy attained. Plates γγ 21581–21593, inclusive, were taken with a short-focus camera and were unsuitable for measurement of the absorption lines. The dispersion of the other spectrograms is about 46 A/mm at λ 4600, and the two missing values of V_{Abs} are due to underexposure. The figures in the last two columns of Table 1 indicate for each plate, or group of plates, the normal point in Table 2 in which the observation has been placed. Some of the phases of the normal points in Table 2 differ slightly for the two components, owing to the more complicated weighting of the absorption velocities; the numbers of lines measured was not the same on all spectrograms, and, as already noted, velocities are lacking for several plates. Lastly, the normal points themselves were weighted, very roughly, in proportion to the number of measures included, as shown in the last column of Table 2.

The purely observational details of this work are presented at considerable length, since otherwise the unusual results that follow

from them might raise a question as to the possibility of observational or computational deficiencies.

Results.—The Mount Wilson observations by themselves gave for the binary a period of 4^d2125. The representation of the two Victoria velocities required only a slight change, to the value 4^d21238. This period was therefore assumed to be correct and was adopted for the ensuing calculations. It was then observed that the velocities fitted a simple sine-curve very closely, with no indication

TABLE 2

NORMAL POINTS

No.	Emission			Absorption			Weight
	Phase	Vel.	O−C	Phase	Vel.	O−C	
		km/sec	km/sec		km/sec	km/sec	
1	0.122	+260	−10	0.122	−124	− 4	1
2	.226	+371	+10	.226	−127	+29	½
3	.288	+359	+ 3	.288	−148	+ 6	1
4	.435	+156	−23	.451	− 90	−17	½
5	.530	+ 17	+18	.528	− 25	−10	1
6	.648	−186	− 8	.638	+ 63	+ 7	½
7	.756	−268	−16	.757	+ 82	− 2	1
8	.885	−115	+33	.884	+ 89	+45	½
9	0.992	+ 43	+ 1	0.992	− 36	− 5	½

of appreciable eccentricity. Hence, since in any case the measured velocities include fairly large accidental errors, it was deemed sufficient, for the present, to assume $e = 0$.

The Wolf-Rayet velocities from the nine normal points of Table 2 were therefore fitted to a curve of the form

$$V_W = \gamma_W + K_W \sin(\phi - \phi_0),$$

the corrections to the preliminary graphical values of γ_W, K_W, and ϕ_0 being found by the method of least squares. Lastly, the quantities γ_B and K_B were determined by another least-squares solution from the observations of the B-type star on the assumption that ϕ_0 has the value found from the Wolf-Rayet observations. The zero point of phase was chosen to be the point where the velocity-curve of the Wolf-Rayet star crosses from the minus to the plus side of its

γ-axis. These solutions led to the following elements of the system (with probable errors):

$$\begin{aligned} P &= 4^{d}.21238\,, \\ e &= 0.0 \text{ (assumed)}\,, \\ K_{W} &= 308.4 \pm 6.0 \text{ km/sec}\,, \\ \gamma_{W} &= +56.4 \pm 4.4 \text{ km/sec}\,, \\ K_{B} &= 120.7 \pm 5.8 \text{ km/sec}\,, \\ \gamma_{B} &= -33.6 \pm 4.4 \text{ km/sec}\,. \end{aligned}$$

The phases are to be computed from the formula

$$\text{JD} = 2428771.357 \pm 0.0135 + 4^{d}.21238E\,.$$

The representation of the observations by these elements is shown in Figure 1. The corresponding minimum masses and dimensions of the system are

$$\begin{aligned} m_{W} \sin^{3} i &= 9.74\odot\,, \\ m_{B} \sin^{3} i &= 24.8\odot\,, \\ a_{W} \sin i &= 1.7849 \cdot 10^{7} \text{ km}\,, \\ a_{B} \sin i &= 0.7012 \cdot 10^{7} \text{ km}\,, \\ (a_{W} + a_{B}) \sin i &= 2.4861 \cdot 10^{7} \text{ km} = 35.8R\odot\,. \end{aligned}$$

The most striking result thus far is the difference of 90 km/sec between the γ-axes for the two stars. The explanation of this fact must involve the answers to two questions: (*a*) Which of the γ-axes most nearly represents the velocity of the system? (*b*) How account for the deviation of one or both γ-axes from this velocity?

Question (*a*) cannot be answered with complete certainty. The best that can be done is to make the reasonable assumption that the velocity of HD 193576 lies somewhere within the observed range of the known radial velocities of neighboring early-type stars. From Moore's *Catalogue of Radial Velocities*[4] I have taken the radial velocities of all stars of spectral type $B3$ or earlier within the region $\alpha = 19^{h}45^{m}$ to $20^{h}45^{m}$ and $\delta = +35^{\circ}$ to $+45^{\circ}$. There are twenty-

[4] *Pub. Lick Obs.*, **18**, 1932.

nine such stars,[5] and their radial velocities range from +4 to −59.7 km/sec, with a mean of −16.2 km/sec. A velocity of −34 km/sec for HD 193576 is obviously much more in line with the velocities of other early-type stars in its vicinity than is one of +56 km/sec. Naturally, this comparison does not prove that the center-of-mass

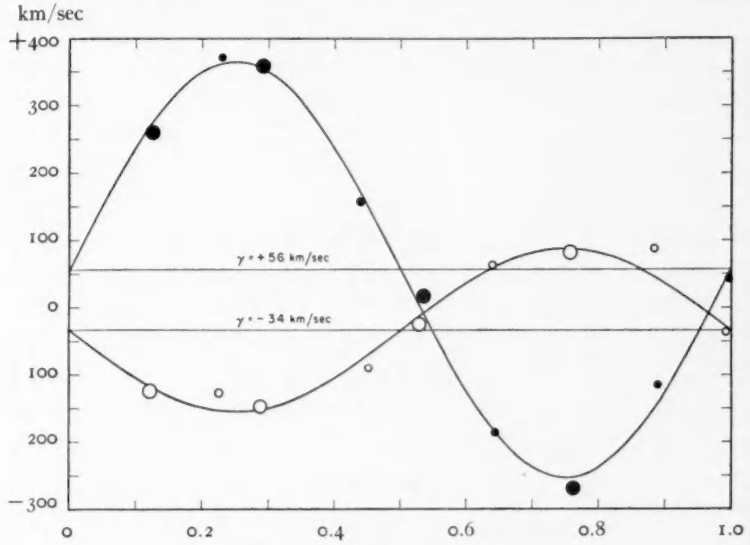

FIG. 1.—Velocity-curves of HD 193576

velocity of the binary is represented by the γ-axis of the B-type star, but the conclusion does seem highly probable.[6]

The answers to questions (*a*) and (*b*) thus suggested are: (*a*) The radial velocity of the binary is that given by the γ-axis of the B-type

[5] Unfortunately, the mean apparent magnitude of these stars is only 7.0, whereas that of HD 193576 is 8.0, and they may therefore be less distant than the latter. This discrepancy is unavoidable at present.

[6] It might be supposed that an appeal to galactic rotation would give an indication of the true velocity. In the Cygnus region, however, there appear to be objections to this procedure. Thus, L. Berman, in his discussion of the planetary nebulae (see *Lick Obs. Bull.*, **17**, 65, 1937), finds a preponderance of negative radial velocities in this part of the sky and states that Trumpler finds a similar effect for the galactic clusters. According to galactic rotation about the usually accepted center, the radial velocities in this region (freed from solar motion) should be positive. Perhaps these facts offer further support for the view that the γ-velocity of the B-type star (−17 km/sec when the solar motion is removed) is approximately the velocity of the system.

component. (*b*) The γ-axis of the Wolf-Rayet star at +56 km/sec indicates a red shift of the emission bands of about 90 km/sec. A discussion of the possible causes of this red shift, as well as evidence for its presence in other Wolf-Rayet spectra, is given in the following *Contribution.*

Variations in the λ 4686 He II band.—Certain variations of a periodic nature in the λ 4686 band of *He* II now require comment. On practically all the spectrograms utilized for the orbit determinations, λ 4686 was necessarily overexposed and shows little in the way of detail. Enough was visible, however, to justify some shorter exposures, which have since been made near phases 0.0, 0.5, and 0.75. The character of the λ 4686 band is illustrated by the microphotometer tracings of these plates shown in Figure 2. The available spectrograms at phase 0.25 indicate that the band is essentially the same at that phase as at 0.75.

Qualitatively, it may be stated that, when the velocities of approach or recession are greatest, the λ 4686 band is rounded and essentially symmetrical, while at phases 0.0 and 0.5, when the Wolf-Rayet star is in front of, and behind, the B-type, respectively, the band slopes slightly downward toward the violet at the former phase and toward the red at the latter. In addition, when the band is not symmetrical, there appears to be a slightly depressed or flattened region near its center. The total band width, of the order of 40 A, does not seem to vary appreciably throughout the cycle. Probably no attempted explanation of these facts should be taken too seriously as yet. However, if the atoms producing the emission bands are being ejected from the Wolf-Rayet star, the observations suggest that, while the velocity of ejection is essentially constant in all directions, either the ejection or the excitation is somewhat greater in the direction of the B-type star than in the opposite direction. Quantitative photometry of the bands in the future may, of course, lead to a different interpretation.

It is not yet known whether accurate photometry will show HD 193576 to be an eclipsing binary; but at present it is not listed as a variable, and, judged by the spectroscopic results, there is probably no eclipse. Thus, although phases 0.40–0.63 have been fairly well covered (Table 1), none of the plates shows any sign of the ab-

sorption lines that might be expected if the Wolf-Rayet star passed behind the atmosphere of the B-type (ζ Aurigae effect); and, moreover, the variations in the λ 4686 band, already described, do not appear susceptible of explanation in terms of an eclipse. Thus, for the present, the inclination of the orbit plane is indeterminate, and future photometric measures of the star are highly desirable.

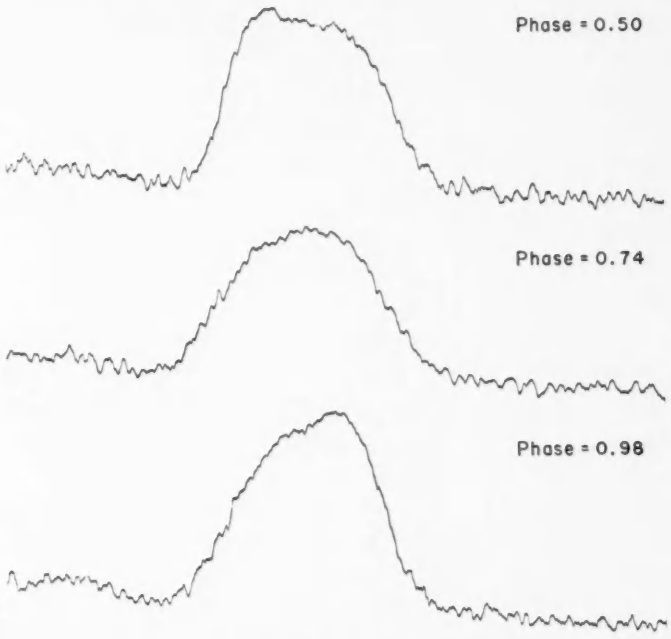

FIG. 2.—Microphotometer tracings of λ 4686 *He* I

Distance and absolute magnitude; temperatures and densities.—The distance and the absolute magnitude of HD 193576 have been found from intensities of the interstellar H and K lines to be 740 parsecs and -1.7 photovisual, respectively.[7] It was hoped that these values might be improved by utilizing the radial velocity from the H and K lines and the theory of galactic rotation. The velocity from H and K for 11 spectrograms is -8.6 km/sec. With the values of the ampli-

[7] R. F. Sanford and O. C. Wilson, *Mt. W. Contr.*, No. 613; *Ap. J.*, **90**, 235, 1939. Only the line intensities are given here, but the method of deriving the other quantities is indicated.

tude and of the center for galactic rotation given by Merrill and Sanford,[8] the calculated distance is 1130 parsecs. It is very doubtful, however, if interstellar-line velocities can be given much weight as criteria of distance for individual stars, at least in the Cygnus region. Table 3, containing results for eight Wolf-Rayet stars in Cygnus, illustrates the point. The velocities and line intensities are from Mount Wilson data.[9] For four of the stars the velocities cannot be used at all to derive distances (excess negative velocities again; see footnote 5), while whatever agreement there is for the remaining stars is probably fortuitous. Hence, we rely only on the intensities and adopt $M_{pv} = -1.7$ for HD 193576. Since both spectra are visible—at least in the photographic region—it is legitimate to assume as a first approximation that the two stars are of equal brightness and, therefore, that $M_{pv} = -1.0$ for each of the components. This result may indicate that the Wolf-Rayet star is somewhat fainter than the average for stars of its type, since the mean values of M_{pv} for six WC and twelve WN stars have been found to be -2.8 and -2.1, respectively.[7] However, the uncertainty of a determination of luminosity for an individual object by the method of interstellar line intensities is such as to give doubtful weight to a discrepancy of 1 mag.

Similarly, the B-type star appears to be too faint for its type, if the latter has been estimated correctly. Estimates of absolute magnitudes of early-type stars indicate that for those of class B1, $M_{pv} \sim -3.0$.[8,10] Thus, both members of the system seem to be fainter by 1–2 mag. than the means for their respective types. This result can readily be explained on the basis of an error in the derived distance or of an excessive absorption effect operating on the star, or as the result of a combination of the two. In any event there is no very serious discrepancy between the spectral types and the observed luminosities of the two stars.

When, on the other hand, the masses of the two stars are com-

[8] *Mt. W. Contr.*, No. 585; *Ap. J.*, **87**, 118, 1938.

[9] *Mt. W. Contr.*, No. 576; *Ap. J.*, **86**, 274, 1937, and *Contr.* No. 613.

[10] Stebbins, Huffer, and Whitford, *Mt. W. Contr.*, No. 617; *Ap. J.*, **90**, 209, 1939.

pared with their luminosities, through the medium of Kuiper's empirical mass-luminosity relation,[11] the situation appears less favorable. If the Wolf-Rayet star radiates as a black body, its bolometric correction must be at least of the order of -5 mag., whence $M_{bol} \sim -6$. For a mass of $10\odot$, Kuiper's diagram indicates an absolute bolometric magnitude of about -4, and thus the Wolf-Rayet star appears to be about 2 mag. too luminous for its mass. From Kuiper's data on the stellar temperature scale,[12] the effective temperature

TABLE 3

DISTANCES OF WOLF-RAYET STARS IN CYGNUS FROM INTENSITIES AND VELOCITIES OF INTERSTELLAR LINES

Star	Reduced *Ca* II Velocity	Distance from Velocity	Distance from Line Intensity
HD 190918	+4 km/sec	540 psc	1430 psc
191765	+8	1080	890
192103	−4	.....	1000
192163	0	.....	990
192641	+1	135	700
193077	−2	.....	840
193576	+8	1130	740
193793	−1	.....	1210

and bolometric correction of the B-type star may be taken as 23,000° and -2.5, respectively, and hence the value of M_{bol} is approximately -3.5. For a mass of $25\odot$, however, the mass-luminosity relation yields about —6.5 for the absolute bolometric magnitude, and the B-type component is therefore some 3 mag. fainter than would be estimated from its mass. Evidently, any effect—such as erroneous distance, for example—which would act to change the absolute magnitudes of both stars by the same amount in the same sense, would be of no help in resolving this difficulty. Beyond pointing out the foregoing facts, it is probably not profitable to attempt any deductions based upon them at present in view of the theoretical uncertainties in the mass-luminosity relation in the region of masses exceeding $10\odot$.[13]

[11] *Ap. J.*, **88**, 472, 1938. [12] *Ibid.*, p. 429. [13] *Ibid.*, p. 490.

The radius of the B-type star may be computed with sufficient accuracy by means of the well-known equation

$$\log R = \frac{5900^\circ}{T} - 0.20M_v - 0.02 .$$

With $T = 23{,}000^\circ$ and $M_v = -1$, we find $R = 2.8R\odot$. For a mass of $25\odot$ the density is found to be $\rho_B = 1.14\rho_\odot$—a value considerably higher than the known densities of massive early-type stars. Thus, for example, the early B-type components of V Puppis of masses $19\odot$ have densities of about $0.05\rho_\odot$; and the O9 components of Y Cygni, of masses $17\odot$, have densities about $0.09\rho_\odot$.[14]

There are two ways in which the density of the B-type component of HD 193576 may be reduced to consistency with these figures. Either the temperature must be assumed lower than $23{,}000^\circ$ or the star is considerably more luminous than was previously supposed. From the formula for $\log R$ it follows that, if $M_v = -1$ be retained, T must be reduced to approximately $10{,}000^\circ$ to give a density of the right order. So low a value seems definitely to be ruled out by the character of the spectrum. If, on the other hand, the value of M_v be changed from -1 to -3, the radius turns out to be $7R\odot$, and the density is $0.073\rho_\odot$. Since, as noted previously, the absolute magnitudes derived from the interstellar lines seemed to make both stars too faint for their spectral types, this way of resolving the difficulty is much more satisfactory. If it is adopted, the B-type star must have an absolute bolometric magnitude of about -5.5, which is in reasonable agreement with the value to be expected on the basis of the mass-luminosity relation. The one outstanding discrepancy is that the Wolf-Rayet component, on the assumption of a bolometric correction of -5, then turns out to be about 4 mag. too luminous for its mass. However, if anomalous results are admitted for one of the components, it will probably be safer to place the burden on the Wolf-Rayet star rather than on the B-type star. Wolf-Rayet spectra differ so widely from those of nor-

[14] Table I*a* of Moore's "Fourth Catalogue of Spectroscopic Binary Stars," *Lick Obs. Bull.*, **18**, 1, 1936.

mal stars that it would not be surprising if the objects in which they originate were found to be abnormal in other respects as well.

As a final step in the discussion of the binary, it is of interest to see what deductions concerning the radius and density of the Wolf-Rayet component follow from the assumption that it radiates as a black body. For this purpose the radius and temperature of the B-type star are assumed to be $7R\odot$ and 23,000°, respectively; and the continuous spectrum of the Wolf-Rayet star is supposed to come from a body whose effective temperature is 80,000°. The latter value appears to be a reasonable estimate for a high-excitation object of the kind under consideration.[15] Since both spectra are visible in the photographic region, it is assumed that $I_B = I_W$ for λ 4300, and hence that $j_W R_W^2 = j_B R_B^2$ where the j's are the surface brightnesses at that wave length. Inserting the Planck function and the foregoing values of the parameters into the equation, we find $R_W = 0.4R_B = 2.8R\odot$ and, therefore, $\rho_W = 0.46\rho_\odot$. It should be noted that if the absolute magnitudes derived from the interstellar-line intensities had not been revised ρ_W would have been about fifteen times larger than the value quoted. Thus, if the assumption that the Wolf-Rayet star radiates as a black body is justified, which may be open to question, its density may be said to be of the same order as that of the sun. Further discussion of the system must necessarily be upon a more speculative plane and is therefore reserved for the following *Contribution*.

In conclusion I wish to express my appreciation of helpful discussion with several members of the Observatory staff and in particular to thank W. H. Christie and G. Strömberg for securing several plates at critical phases.

Carnegie Institution of Washington
Mount Wilson Observatory
November 1939

[15] C. H. Payne, *Zs. f. Ap.*, **7**, 1, 1933, Table VIII.

PHYSICAL CHARACTERISTICS OF THE WOLF-RAYET STARS*

O. C. WILSON

ABSTRACT

The red shift of the emission bands of the Wolf-Rayet component of HD 193576, noted in the preceding *Contribution*, suggests that similar displacements may be a common feature of Wolf-Rayet spectra. Examination of the wave lengths derived by Beals from measures of a number of Wolf-Rayet stars lends strong support to this view, at least for stars of the nitrogen sequence. A discussion of the possible origins of such a shift leads to the conclusion that only two of them are at all likely. One of these possibilities, namely, that the red shift is due to a weakening of the violet sides of the bands by absorption of the light of the central star in the expanding envelope, does not require any modification of the current view as to the nature of a Wolf-Rayet star. The other possible interpretation is that the observed displacements represent a gravitational red shift. If the latter is correct, the radii of the gaseous envelopes in which the emission bands arise cannot exceed approximately one-tenth that of the sun, and the nuclei themselves must be considerably smaller and extremely dense. Some elementary computations of the physical conditions in these small gaseous envelopes do not lead to any inherent impossibilities. The one grave objection appears to lie in the extraordinarily high surface temperatures demanded of the nuclei in order to produce the observed continuous spectra. In fact, it is suggested that, if the gravitational interpretation is adopted, the continuous spectra cannot be the black-body radiations of the nuclei at all but must be fluorescent spectra arising in the inner portions of the gaseous envelopes.

The data available at present are insufficient to decide between the two possible interpretations of the red shift. It may only be said that the absorption explanation does not receive much support, since visual inspection of spectrograms indicates that absorption components on the violet edges of *He* II bands are quite rare. Probably careful photometric investigation of the contours of emission bands in Wolf-Rayet spectra will, in the future, decide the question.

In the preceding *Contribution* a straightforward discussion of the Wolf-Rayet binary HD 193576 was based upon the spectrographic orbits of the two components and upon the absolute magnitudes derived from the intensities of interstellar H and K. Consideration of the density of the B-type star suggested a revision of the absolute magnitudes obtained directly from observation. Apart from this, the only restrictive assumptions were the customary one of black-body radiation for both components, together with reasonable values for the effective temperatures. The only unusual result of the computations was the rather high mean density, of the order of that of the sun, found for the Wolf-Rayet star.

* *Contributions from the Mount Wilson Observatory, Carnegie Institution of Washington*, No. 624.

The red shift.—One interesting feature of the orbits was the difference of 90 km/sec between the γ-axes of the two components. Arguments were presented which tended to show that this difference was due to a red shift of the emission bands of the Wolf-Rayet star, and it was tacitly assumed to be ignorable in deriving the masses and dimensions of the system. It is now necessary, however, to examine the red shift in more detail and, if possible, to discover its origin. Presumably the Wolf-Rayet member of the binary is a normal star of type WN5; in any event, the spectrum appears identical with the spectra of other WN5 stars available to the writer. Therefore, it is not unlikely that the red shift is a feature common to all such spectra and, if so, that evidence of it should be present in published wave-length determinations. The only extensive measures of Wolf-Rayet spectra are those of Beals,[1] and a difficulty arises at this point, since Beals gives only the mean wave lengths from a number of Wolf-Rayet stars of various types. Hence, it is impossible from his data, to draw perfectly unambiguous conclusions as to wave lengths in any one Wolf-Rayet group.

Probably no choice of material from Beals's tabulation would be universally acceptable, but there are three criteria of selection upon which all investigators will doubtless agree. In the first place, only the stronger bands should be used, since for them the accuracy of measurement will be higher and the effects of blends with weak unrecognized bands will be minimized. Secondly, only those bands should be considered whose laboratory wave lengths have been directly measured and not merely computed from term values obtained by measures of lines in the far ultraviolet. Lastly, bands which are obviously distorted by blends should be avoided. All the bands listed by Beals as having intensity 5 or greater, which reach their maximum strengths in subdivisions WN5 or WN6 (OW5 and OW6 in Beals's table), and which, in the writer's opinion, satisfy the preceding selection criteria, are given in Table 1.

In commenting upon the table, it must first be remarked that the *He* II bands are common to stars of both the carbon and the nitrogen sequences; hence the stellar wave lengths given for these bands

[1] *Pub. Dominion Ap. Obs.*, **4**, 271, 1930. In this paper Beals also gives a discussion of the similarities of the spectra of Wolf-Rayet stars and novae.

include, to an unknown extent, contributions from WC stars. The possible blends in WC stars which might affect these bands are indicated in the last column, and it is impossible to estimate what effect, if any, they may have on the mean wave lengths. Next,

TABLE 1

WAVE LENGTHS AND IDENTIFICATIONS IN WOLF-RAYET SPECTRA

STAR		LAB. λ	ELEMENT	REMARKS
λ	Int.			
3483.....	10	3478.69 3482.98 3484.90	*N* IV	3479 strongest, 3485 weakest in laboratory
4339.7.....	8	4338.71 4340.47	*He* II *Hγ*	Probably mostly *He* II
4542.2.....	8	4541.63	*He* II	
4605.4.....	5	4603.3	*N* V	See note below
4622.2.....	5	4619.1	*N* V	See note below
4686.6.....	40	4685.81	*He* II	Possible blend with λ 4685.4 *C* IV in carbon stars
4860.8.....	7	4859.36 4861.33	*He* II *Hβ*	Probably mostly *He* II
5414.....	9	5411.5	*He* II	Blend with *O* VI 5410 or *O* V 5417 in carbon stars?
6563.....	20	6560.16 6562.79	*He* II *Hα*	Probably mostly *He* II

NOTE.—The "laboratory" wave lengths for λ 4603 and λ 4619, and *N* V are those found by measurement of many spectrograms of HD 193576 (*Mt. W. Contr.*, No. 623). They are referred to *He* II 4685.81 as standard and, if there are no differential shifts between *He* II and *N* V in the star, are probably close to the values that would result from actual laboratory measurement. Also, since these bands can be clearly observed only in stars of type WN_5, their inclusion in the table seems justified.

attention must be directed to the fact that hydrogen is probably very weak, or missing entirely, in nearly all Wolf-Rayet spectra, as has already been pointed out by Beals.[1] Hence the normal wave lengths to be attributed to the bands measured near *Hα*, *Hβ*, and *Hγ* should undoubtedly be much closer to those of the Pickering

series of *He* II than to those of the corresponding Balmer lines. The members of the Pickering series not listed in Table 1 are known to be badly blended.

In view of the preceding statements, a comparison of the stellar and laboratory wave lengths in Table 1 seems to afford fairly good evidence that the emission bands of *He* II and *N* V, and possibly those of *N* IV, in Wolf-Rayet spectra are shifted to the red by an amount of the order of 1 A. Every one of the nine bands shows the effect to a greater or less degree, and there is not a single example of a violet shift; hence, neither mere accidental errors of measurement nor possible blends with weak unknown bands provide a likely explanation. Inasmuch as fifteen of the twenty-eight Wolf-Rayet stars observed at Victoria are of types WN5 or WN6, and since the bands chosen are those which reach their maxima in these subdivisions, the foregoing evidence for the red shift may be presumed to refer chiefly to stars of the nitrogen sequence. The question of similar shifts in the spectra of the carbon stars cannot readily be answered from the published data; blends appear to be a much more serious difficulty in the WC spectra, although extended measurement of selected specimens may settle the point.

In connection with the carbon stars, however, the measures by Wright of HD 184738 (BD+30°3639, Campbell's hydrogen envelope star) must be mentioned. The spectrum is noteworthy because the emission bands are considerably narrower than those of the typical Wolf-Rayet spectrum and because more of them are bordered on the violet by absorption components than is generally the case. Wright[2] called attention to the red shift of some of the bands and attributed it to the encroachment of the absorption components on the violet edges. This explanation may very well be the correct one, but the star should be reobserved with higher dispersion, in order to see whether, in the light of modern knowledge of the identifications and wave lengths, the amount of the shift bears any relation to the intensity of the displaced absorption, and hence whether the presence of the absorption components is sufficient to account for the observed shifts. The matter is especially important because HD 184738 is surrounded by a small emission-line nebula whose

[2] *Pub. Lick Obs.*, **13**, 1918; see p. 224.

radial velocity has been measured by Campbell and Moore.[3] In all probability the velocity of the star is identical with that given by the nebular lines; thus the absolute values of any wave-length displacements of features of the star's spectrum may be accurately determined. Curiously enough, the measures of Campbell and Moore, combined with Wright's, indicate a red shift of the stellar emission bands of about 85 km/sec, a value very similar to that found for HD 193576 in the preceding *Contribution*. In view of the very different spectra of the two stars, however, no stress should be placed upon this agreement for the present.

Interpretation of the red shift.—The results of the study of HD 193576 in the preceding *Contribution*, together with the data contained in Table 1, provide sufficiently impressive evidence of the existence of a red shift of at least some of the Wolf-Rayet emission bands to justify further discussion. The possible causes of wave-length shifts in emission bands, which may be assumed to originate in a shell or envelope ejected by a central star, are the following: (1) motion of the star and envelope as a whole; (2) purely geometrical effects (occultation, unsymmetrical ejection); (3) Stark effect; (4) absorption effects; and (5) relativistic gravitational displacement. We now consider these possibilities in the foregoing order, although they are not, of course, mutually exclusive.

1. To explain the observed red shift in the case of the Wolf-Rayet stars on the basis of stellar motions is equivalent to postulating a large positive K-term for these objects. Moreover, the red shift has been obtained differentially for HD 193576 (and possibly also for HD 184738). For these reasons, we feel justified in rejecting this explanation.

2. Matter ejected symmetrically by a Wolf-Rayet star would be partly occulted by the stellar nucleus. If the shell were not too large, relative to the latter, an appreciable fraction of the receding gases would be obscured, and the centers of gravity of the emission bands would appear to be shifted to the violet. Only if the shell were collapsing, could occultation provide a red shift; and this possibility seems definitely to be ruled out by the fact that, when displaced absorption components are visible, they invariably occur on the

[3] *Pub. Lick Obs.*, **13**, 150, 1918.

violet edges of the emission bands. Similarly, considerations of probability dispose of the suggestion that some kind of unsymmetrical ejection could be responsible for a statistical effect such as that shown in Table 1.

3. The possibility of a Stark-effect interpretation can probably also be eliminated. In the first place, most of the evidence for the red shift depends upon measures of bands due to *He* II. For lines of *He* II (as also for *H*) the first-order Stark effect produces patterns which are symmetrical about the normal wave lengths, and there is no shift in the mean positions. This fact definitely rules out the first-order Stark effect, but the possibility of the second-order effect must be examined. Thus, for example, Foster[4] found that the average second-order shifts toward the red amounted to 0.40 and 0.73 A for $H\delta$ and $H\epsilon$, respectively, for a field strength of 65 kv/cm. For analogous *He* II lines the shifts for the same field strength should be less by a factor 1/16, since the theoretical expression for the displacement in λ contains the factor E^{-4}, where E is the nuclear charge. Extremely large fields would therefore be required to yield the observed Wolf-Rayet red shift. Moreover, it appears that bands of *N* V, and possibly of *N* IV, undergo a shift of the same order as those of *He* II, and the probability that such a result would be given by second-order Stark effect is very small. Lastly, if the second-order effect were large in *He* II, the first-order effect, as a source of band width, would be much greater still and would conflict with the observations of Beals, which show that the band widths in *He* II (and other) series follow the rule that $\Delta\lambda \propto \lambda$. We thus conclude that a successful explanation of the Wolf-Rayet red shift in terms of the Stark effect is unlikely.

4. The possibility that absorption effects are the source of the red shift cannot be disposed of at the present time, although a general discussion of the matter is appropriate at this point. In the first place, absorption effects may be divided roughly into two kinds: (*a*) absorption of radiation emitted in one part of the shell, or envelope, by atoms in another part; and (*b*) absorption of radiation emitted by the central star, producing a depression in its continuous spectrum.

[4] *Ap. J.*, **63**, 191, 1926.

The theoretical discussion of the effect of absorption upon the band contours in expanding shells is a difficult matter. It has been carried out in a general form in a paper by Araki and Kurihara,[5] but the final results are so complicated and depend in such intimate fashion upon the distributions of velocity and excitation throughout the envelope that no very satisfactory general conclusions appear possible. However, it may be noted that, on the assumption of a relatively large thin shell, Araki and Kurihara derive symmetrical band contours. It appears likely that the greatest effect will be due to the absorption of light from the continuous spectrum of the star, which, in an expanding envelope, must always produce an apparent weakening of the violet side of an emission band. Whether this effect is competent to account for the Wolf-Rayet red shift cannot be decided at present, and an appeal to observation must be made. If it is found, by careful photometry, that the *He* II bands in Wolf-Rayet spectra are both symmetrical and displaced, then it must be considered very unlikely that absorption effects are the cause of the shift.[6]

Pending a photometric investigation, the best that can be done is to estimate, by visual inspection of spectrograms, the frequency of occurrence of absorption components displaced to the violet. Spectra are available at Mount Wilson for fourteen stars of the nitrogen sequence, although some of the plates are not suitable for some of the bands of interest. Inspection of this material leads to the following results: Displaced *He* I λ 3889 absorption is definitely present for three stars, possibly present for three, and definitely absent for seven. Displaced components for λ 4603 and λ 4619 are possibly or probably present in five stars and are estimated as absent in two. For *He* II λ 4686, absorption is possibly present in

[5] *Zs. f. Ap.*, **13**, 89, 1936.

[6] Not many contours of suitable Wolf-Rayet bands have been published, although Beals has given accurate measures for λ 4686 in HD 192163 (*M.N.*, **92**, 196, 1932) and in HD 191765 (*Pub. Dominion Ap. Obs.*, **6**, No. 9, 1934). In the first, the band is definitely asymmetrical in the sense to be expected from violet absorption. The *He* I bands are relatively strong in this star, however, and are accompanied by displaced absorption components. Thus, it is not impossible that the presence of *He* I λ 4713 may be the source of the distortion of λ 4686. In HD 191765 Beals's measures do not give any certain evidence of a lack of symmetry, although they clearly show a red shift of roughly 100 km/sec.

only two stars and definitely or probably absent in eleven. Absorption components of the other *He* II bands, λλ 4859, 4542, and 4339, are estimated as probably present in one star and missing in eleven. In addition, it may be noted that a displaced absorption appears to be very common for the band measured by Beals at λ 4598 in stars of class WN6 and still, apparently, unidentified.

Although it is far from conclusive, the preceding evidence is rather against the idea that the red shift of the *He* II bands is due to absorption on the violet edges. The evidence in the case of the *N* V bands λ 4603 and λ 4619 may not be as decisive in favor of the presence of absorption as it appears. These bands are quite narrow; and, if there are weak bands somewhat to the violet of λ 4603, the resulting gap may give the appearance of a weak absorption. Likewise, the absorption accompanying λ 4619 lies between the latter and λ 4603 and hence must be regarded as very uncertain. All that may be said is that the available data tend against the absorption explanation and that the question can be settled only by a careful photometric investigation.

5. The last and most interesting possibility is that the red shift is of gravitational origin, and, if future observation requires its acceptance, will lead to a rather startling conception of the nature of a Wolf-Rayet star. As an illustration, consider the data presented in the preceding *Contribution* for HD 193576: mass = 9.74⊙; red shift = ΔV = 90 km/sec. These figures permit a computation of the mean radius of the *He* II envelope by means of the equation

$$R = \frac{mG}{10^5 c \Delta V},$$

where G and c are the gravitational constant and the velocity of light in cgs units. The foregoing values for m and ΔV lead to the result that

$$R_{\text{shell}} = 4.77 \cdot 10^9 \text{ cm} = 0.069 R\odot,$$

i.e., somewhat less than the radius of Jupiter. Since the minimum mass of the star was used, the computed value of R_{shell} is probably somewhat smaller than the true one. Nevertheless, for any reasonable inclination of the orbit plane, the radius of the envelope in

which the bright bands are formed must be quite small, compared to solar dimensions.

The radius of the stellar nucleus itself must, of course, be smaller than that of the envelope, although no very precise estimate of it is possible. However, if r and R are the radii of the nucleus and shell, respectively, it is possible to arrive at an upper limit for the ratio r/R by consideration of the widths and displacements of the displaced absorption components which are visible in some spectra. If, as all the evidence indicates, the emission bands originate in a rapidly expanding spherical envelope, the absorption component is then produced by that portion of it which is projected upon the nucleus. The width of the absorption line must be at least as great as the velocity spread of the matter within the absorbing region; but, since the width may be partially due to other causes (e.g., turbulence), only an upper limit for r in terms of R may be deduced. Thus, if V and ΔV be the displacement and width of such an absorption component and if r/R is not too large, it can easily be shown that

$$\frac{r}{R} \leq \sqrt{\frac{2\Delta V}{V}}.$$

Measures of three Wolf-Rayet stars yield the data of Table 2. The displacements were measured for the *He* I lines λλ 5876, 4471, 4026, and 3889, and the widths of absorption for λ 5876 and λ 3889. Several plates were measured for each star. Also, since the geometrical dilution factor is given by $W_G \sim \frac{1}{4}(r/R)^2$, upper limits for this quantity are included in the last column of the table.

It is difficult to say how much significance is to be attached to the numerical results of Table 2. In the first place, many Wolf-Rayet stars do not show displaced absorption components and may conceivably differ essentially from those that do. Moreover, even when *He* I absorptions are present, it is unlikely that they are formed in the region where the *He* II emission bands originate. Hence, the only conclusion to be drawn is that the observations, as they stand, indicate that the gaseous envelopes are probably fairly compact about the nuclei and that, as a very rough estimate, the radius of the nucleus cannot exceed approximately one-half that of the enve-

lope. For HD 193576 these considerations may be omitted and a minimum density for the nucleus computed by taking the radius of the latter equal to that found for the *He* II envelope. It turns out that $\rho_W \geq 2.97 \cdot 10^4 \rho_\odot = 4.2 \cdot 10^4$ gm/cm^3, which is a very decided lower limit, of course, since the radius of the nucleus must certainly be appreciably less than that of the envelope.

It remains only to make a few elementary computations on the physical conditions within the gaseous envelopes demanded by the gravitational explanation of the red shift and to point out the one really serious difficulty to which it leads. We must first inquire whether it is possible for a gaseous envelope of only about one-

TABLE 2

WIDTHS AND DISPLACEMENTS OF ABSORPTION COMPONENTS

HD	V	ΔV	r/R (Upper Limit)	W_G (Upper Limit)
	km/sec	km/sec		
191765	1620	185	0.48	0.057
192103	1120	280	.71	.125
192163	1410	205	0.53	0.072

tenth the radius of the sun to radiate the large amount of energy in discrete emission lines which is called for by the known absolute magnitudes of the Wolf-Rayet stars. For this purpose, the values $R = 0.1R\odot$ and $M_{pv} = -2$, in accord with the mean absolute magnitude found for the WN stars,[7] are adopted.

A black body of the size of the sun, at a temperature of 6000° K will radiate $2.4 \cdot 10^{31}$ erg/sec in a band 40 A wide near λ 4700. For the sun, $M_{pv} = +4.8$; hence the Wolf-Rayet star is some 7 mag. brighter, and we may take its total radiation in the photographic region to exceed that of the sun by a factor of roughly 600. On the assumption that the λ 4686 *He* II band is ten times as intense, on the average, over its 40 A width, as the continuous spectrum in the vicinity, the star must radiate in λ 4686 alone at a rate of about $1.5 \cdot 10^{35}$ erg/sec, which is equivalent to $3.5 \cdot 10^{46}$ quanta per second. In order to radiate a strong line, an atom must be permitted to remain in the upper state for a time interval of the order

[7] *Mt. W. Contr.*, No. 613; *Ap. J.*, **90**, 235, 1939.

of 10^{-8} sec, and thus a rather effective upper limit to the rate at which a *He* II ion can radiate quanta of λ 4686 will be 10^8 per second. Accordingly, the minimum number of *He* II ions responsible for the observed λ 4686 bands must be of the order of 10^{38}. For an envelope of radius $R = 0.1R\odot$, the minimum density is only of the order of 10^8 per cm^3, which is not excessively high.

It is important, also, to establish an upper limit to the total ionic density, which may be done on the basis of some recent work by Inglis and Teller,[8] who investigated the termination of spectral series as brought about by static Stark effect due to charged particles. If N is the density of charged particles, n the quantum number of the line where the series terminates, and a_0 the Bohr radius, these quantities are related by the equation

$$Nn^{7.5} = 0.027a_0^{-3}.$$

For high temperatures ($T > 10^5/n$), which is probably the case in a Wolf-Rayet envelope, N represents the density of positive ions only. In the spectrum of HD 193576, for example, the Pickering series can probably be followed in emission as far as λ 3887, for which $n = 16$. Hence an upper limit to the density of positive ions in the envelope of this star is $N \leq 1.7 \cdot 10^{14}$, which is sufficiently in excess of the lower limit for *He* II to permit of ample flexibility. The situation would have been very embarrassing for the gravitational red-shift hypothesis had the maximum allowable density of all positive ions turned out to be less than the minimum density of *He* II required to yield the observed bands.

Presumably the density of free electrons, n_e, cannot exceed that of the positive ions by more than a fairly small factor at most; so we adopt 10^{14} per cm^3 for n_e and investigate the ionization of *He* II in the envelope. Probably the *He* II bands represent a recombination spectrum, and the density of α-particles is considerably greater than that of singly ionized *He* atoms. The equation of ionization from *He* II to *He* III may be written

$$\frac{n_3}{n_2} n_e = W \cdot 2.4 \cdot 10^{15} \cdot T^{3/2} e^{-(6.3 \cdot 10^5)/T}.$$

[8] *Ap. J.*, **90**, 439, 1939.

The proper choice of the dilution factor W is uncertain, but in view of the results in Table 2 it may reasonably be given the value 0.1. Then, on setting $n_e = 10^{14}$, the equation becomes

$$\frac{n_3}{n_2} = 2.4T^{3/2}e^{-(6.3 \cdot 10^5)/T},$$

and we find

T	n_3/n_2
50,000°	91.5
100,000	$1.4 \cdot 10^5$

Thus, for most of the helium to be doubly ionized, the temperature in the shell would be within the range $5 \cdot 10^4$ to $5 \cdot 10^5$ degrees, and, perhaps, rather closer to the higher value. Such a temperature would be entirely reasonable.

Although the gravitational hypothesis has met no serious difficulties up to this point, one obvious objection must now be mentioned. In the preceding *Contribution* the fact that both spectra of HD 193576 are visible, together with the assumption of reasonable temperatures for both components, permitted a calculation of the radius of the Wolf-Rayet star. If it is now assumed that the radius of the Wolf-Rayet star is less than one-tenth that of the sun, the same line of reasoning requires that it have an effective temperature of at least 10^8 degrees. This value is so high as to merit no confidence at all; and, if the Wolf-Rayet stars are as small as the gravitational interpretation of the red shift demands, there appears to be only one alternative, namely, that the observed continuous spectra are not black-body radiations. They must, in fact, be a fluorescence effect produced by physical processes which degrade large amounts of far ultraviolet radiation in the inner parts of the gaseous envelopes and thus permit the true stellar nuclei to have more reasonable surface temperatures. I do not know whether any of the processes, such as free-free transitions, for example, which are generally supposed to bring about such a result, could have the high efficiency that would probably be necessary in this instance, or even whether they would take place at all. Nevertheless, examples of the kind of process needed are not unknown in astrophysics, a case in point being the well-known Crab nebula.[9] In this nebula the

[9] I am indebted to Dr. R. Minkowski for this reference.

total intensity of the continuous spectrum throughout the nebulosity certainly exceeds by several magnitudes the intensity of the central star in the observable wave lengths. There may, of course, be no direct physical analogy with the Wolf-Rayet stars, but the possibility may at least be considered as suggestive.

Conclusion.—To summarize briefly, it may be said that there seem to be two alternative viewpoints as to the nature of the Wolf-Rayet stars. In the first, as exemplified in the preceding *Contribution*, they are to be looked upon as having radii some two or three times that of the sun and surface temperatures of the same general order as those found by Beals from applications of Zanstra's theory, i.e., between 50,000° and 100,000°. Their densities are almost certainly fairly high for massive stars and may exceed somewhat the density of the sun. The radii of the gaseous envelopes in which the bright bands originate probably do not exceed those of the nuclei by a factor of more than 10 or so, at most. Otherwise, in the case of HD 193576, a more decided effect of the orbital motion upon the band structure might be anticipated than is actually observed. From this standpoint the red shift of the bands must almost certainly be caused by absorption within the expanding envelope.

The alternative view, based upon the interpretation of the red shift as a gravitational effect, leads to the conclusion that the entire Wolf-Rayet structure, including the envelope, has a radius of only a tenth or so that of the sun. The nuclei would be extremely dense and would, in fact, form the massive analogues of the well-known white dwarfs. There may be very good theoretical reasons for rejecting this picture. From the observational side, it is probable that a decision can be made by a careful study of the contours of the emission bands.

Finally, the nuclei of the planetary nebulae must be mentioned briefly in connection with the problems discussed here. It has long been known that these are very probably objects of small radius and correspondingly high density.[10, 11] Measures of absorption lines in the spectra of two nuclei have been made by Cillié[12] in an attempt to observe the anticipated gravitational red shift, although his re-

[10] D. H. Menzel, *Pub. A.S.P.*, **38**, 295, 1926.

[11] H. Zanstra, *M.N.*, **93**, 131, 1932.

[12] *M.N.*, **94**, 48, 1933.

sults can hardly be considered as conclusive. The only measures of the nuclear emission bands are those of Wright.[13] Inspection of the data contained in Table 12 of Wright's paper seems to afford some evidence that the emission bands originating in the planetary nuclei are appreciably shifted toward the red. A definite decision must, however, wait for further observations with the higher dispersions made available by instrumental and photographic advances since Wright's pioneering work.

CARNEGIE INSTITUTION OF WASHINGTON
MOUNT WILSON OBSERVATORY
December 1939

[13] *Pub. Lick Obs.*, **13**, 1918.

RADIATION MEASUREMENTS ON THE ECLIPSED MOON*

EDISON PETTIT

ABSTRACT

Instruments.—The measurements were made on the lunar eclipse of October 27, 1939, with a thermocouple attached to the 20-inch telescope of 40 inches focal length.

Sensitivity.—The deflection on total radiation at the end of totality was 54 mm, more than 36 times that previously observed.

Method.—Both cover glass and water cell were used to determine the temperatures.

Temperatures.—For a point near the center of the disk which was chosen for measurement, the temperature fell from 371° to 200° K during the first partial phase and slowly dropped to 175° K during totality. At the beginning of totality the temperature falls at the rate of 30° C per hour, but at the end of the first hour the rate is 7° C per hour.

Lunar radiation.—The rate of radiation is nearly proportional to the energy received, except for very low temperatures. A computation of the equivalent thickness of the radiating layer from the known physical constants of lava and the radiation data shows that about 2.6 cm will satisfy the conditions.

Measurements of radiation from the eclipsed moon were reported in a previous paper.[1] This work was done with the 100-inch telescope at the lunar eclipse of June 14, 1927, the observations being made on a point 48″ from the limb. At that eclipse 17 sets of measures were made of free, water-cell, and cover-glass deflections. The free deflection, which was 617 mm at the start, dropped to 1.48 mm at the end of totality; the sensitivity of the equipment was varied by changing the electrical circuit of the thermocouple. The experience gained in these observations showed the desirability of the following alterations in procedure: (1) secure a greater number of observations, particularly during the partial phases; (2) greatly increase the deflections during the total phase; (3) vary the sensitivity by diaphragming the telescope; (4) make the observations near the center of the disk where the initial temperature is highest (near the boiling-point of water). These improvements were attempted with a mirror of aperture ratio F 2.5 in the Snow telescope at the lunar eclipse of November 26, 1928; but an unexpected difficulty arose

* *Contributions from the Mount Wilson Observatory, Carnegie Institution of Washington*, No. 627.

[1] Pettit and Nicholson, *Mt. W. Contr.*, No. 392; *Ap. J.*, **71**, 102, 1930.

when false deflections were observed, due to radiation from the instrument, which were greater than the deflections at mid-eclipse.

THE OBSERVATIONS

The completion of the 20-inch reflector in 1934–35 provided means of reopening the problem. This instrument has the same 20-inch mirror of aperture ratio F 2 (diameter 50.5 cm, focal length 101 cm) as was used in the radiation measures at the solar eclipse[2] of January 24, 1925. Both Cassegrain and Newtonian arrangements are provided; the latter was used for the present measurements.

The lunar eclipse of October 27, 1939, took place under conditions which justified a repetition of the measures of 1927. Figure 1 shows the circumstances of the eclipse, with the thermocouple projected upon the moon. As in 1927, the moon was tangent to the shadow at mid-phase, but the thermocouple receivers, now in a 101-cm focus telescope, are effectively 12.5 times as large in linear dimensions as those formerly used at the 100-inch telescope. The path of the receiver across the earth's shadow is indicated by the line with hours marked in Pacific Standard Time.

The thermocouple employed in these measurements is one of several made for the solar eclipse of 1932 and designed for quick thermal response. The receivers are of gold leaf, blackened by a deposit of bismuth in a partial vacuum, 0.55 mm mercury (Pfund's method[3]), and attached to the junctions with white lead thinned with turpentine after removing the oil with alcohol. These gold-leaf receivers, 0.1 μ thick, make a very fast thermocouple when blackened with bismuth or platinum black. Tested with a Moll 0.2-second galvanometer, full deflection is realized in about 1.7 seconds. If the receivers are blackened with camphor smoke or with a lamp-black mixture in alcohol, the time of full deflection rises to 9 seconds, probably owing to the low conductivity of the coating. The receivers, 0.8 mm square, were separated 4.3 mm between centers. The separation of the platinum lead-wires which carry the receivers is only a little smaller

[2] Pettit and Nicholson, *Mt. W. Contr.*, No. 299; *Ap. J.*, **62**, 202, 1925.

[3] *J. Opt. Soc. Amer.*, **23**, 375, 1933. The infrared partial transmission of bismuth black was compensated by using the normal infrared lunar planetary heat as a standard of radiation, as later described.

than the image of the moon. The settings were made by placing the lunar image symmetrically upon the lead-wires, which were in the north-south direction as shown in Figure 1, and shifting the thermocouple in declination so that the receiver A was first just off the north limb of the moon, then in the position shown in the figure, with the moon nearly in contact with the other receiver. The measure-

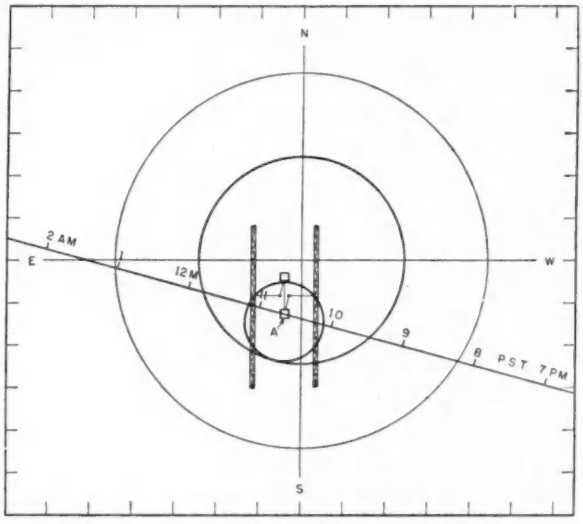

FIG. 1.—Circumstances of the lunar eclipse of October 27, 1939. The small circle is the lunar image projected upon the thermocouple. The heavy line, graduated into hours, shows the path of the hot-junction receiver A through the penumbra and umbra of the earth's shadow. The margin is graduated into units of 1000 seconds of arc.

ments were thus referred to a point on the disk 12'.6 = 0.83 lunar radii from the north point of the moon and covered an area of $3.9 \cdot 10^4$ square seconds of arc. A microscope cover glass 0.16 mm thick and a water cell 1 cm thick with quartz windows 1 mm thick could be put into the beam close in front of the rock-salt window of the thermocouple. The use of the water cell required a half-revolution of the focusing device.

The image of a straight-filament lamp reflected by the galvanometer, in an adjoining room at a distance of 4 m, was formed upon a translucent scale 500 mm long, set near the telescope where it could

be read by the observer. The aperture of the telescope was covered by a paper shield having a sector-shaped opening of 45° angle which, with allowance for the eccentric shadow of the Newtonian flat, illuminated an area of 1/9.1 of the uncovered mirror. This opening was in turn closed by a hinged cover provided with a circular opening having an area of 1/21.3 of the uncovered mirror.

The observing procedure was as follows: (*a*) the moon was set in right ascension symmetrically upon the lead-wires as in Figure 1; (*b*) junction *A* was moved just off the limb of the moon; (*c*) the mean and sidereal times were recorded, and the zero of the galvanometer image adjusted; (*d*) the thermocouple junction *A* was set upon the image as in Figure 1 by direct observation; (*e*) the deflection was noted; (*f*) junction *A* was moved off the image by a half-turn of the declination worm, and the zero deflection was recorded; (*g*) the cover glass was thrown in, and the deflection again observed as in (*a*) to (*f*); (*h*) the water cell was exchanged for the cover glass, the telescope focused, and the measurements repeated; (*i*) the mean time was noted, the water cell removed, and the telescope focused. This complete cycle of operations yielded a set of three single deflections to which we will refer as free, cover glass, and water cell; there were also the sidereal and mean times of the free, the mean time of the water-cell, and by interpolation the mean time of the cover-glass deflections. Four to five minutes were required to complete the cycle.

The changing of the diaphragm involved no great loss of time, except when the paper shield was returned to the telescope after the deflection had again become uncomfortably large (*l*, Table 1) during the last partial phase. Then the sector aperture had to be carefully adjusted to admit a beam of moonlight which just fitted the corresponding mirror sector. This involved 10 minutes' work. During this period the free radiation deflection rose from 294 to 1046 mm (equivalent). This loss of observational material during a critical period of the eclipse can be avoided by the use of pins to define the position of the diaphragm upon the telescope tube, for example, but this simple device was not available at the time of the eclipse.

During the eclipse the sky was very clear, the galvanometer zero very steady, and the temperature varied only from 13°.1 to 12°.0 C

throughout the 6 hours of observing. The 39 sets of measurements made during this interval are detailed in Table 1, except the sidereal times which were used only for sec Z in Table 2.

TABLE 1

RADIATION MEASUREMENTS ON THE LUNAR ECLIPSE OF OCTOBER 27, 1939

	P.S.T. (Begin)	Free	*Cg*	*Wc*	P.S.T. (End)		P.S.T. (Begin)	Free	*Cg*	*Wc*	P.S.T. (End)
		mm	mm	mm				mm	mm	mm	
a	7^h24^m...	199	93	48	7^h33^m		9^h48^m...	97	6.5	2	9^h53^m
		204	.....	.....	.....		54....	87.5	6	1.5	58
	41....	207	94	53	47		10 01....	77.5	4	1.2	10 06
		212	.....	.....	.....	*g*	08....	75	4	1.0	14
	55....	215	99	55	8 04		16....	70	6	0.7	20
		219	.....	.....	.....		26....	65.5	5	1.0	30
b	8 10....	223	101	56	18		38....	60.5	3	1.0	43
		220	.....	.....	.....		52....	57.5	3	1.0	58
	25....	205	90	48	30		11 05....	54	3.5	1.0	11 11
	31....	193	84	45	35		20....	54.5	7	2	24
	37....	173	75	36	41		29....	55	9	4	35
	44....	144	61	32	48		39....	61	18	5	43
c	49....	128	52	27	54		45....	95	51	32	*j* 50
	53....	103	42	21	9 00		52....	294	190	99	*k* 57
	9 01....	82	.....	.....	.....	*l*	12 07....	115	71	43	12 11
d	(04)...	184	76	35	07		14....	190	99	60	19
	08....	130	49	23	13		23....	284	141	88	30
	14....	92	27	13	18		33....	396	186	112	40
	20....	61	14	7	23	*m*	44....	222	100	35	53
e	30....	140	17	5	*f* 34	*n*	1 14....	248	111	59	1 20
	35....	114	13	2	40		1 32....	249	108	58	*o* 1 38
	42....	102	13	3	(46)						

a.—4-inch diaphragm (×21.32), $t = 13°.1$ C. *b*.—$t = 13°.0$ C. *c*.—$t = 12°.5$ C. *d*.—Sector diaphragm (×9.096). *e*.—Diaphragm removed, telescope clear. *f*.—Receiver *A* just inside umbra. *g*.—$t = 12°.5$ C. *j*.—Receiver *A* just inside umbra. *k*.—Just outside umbra. *l*.—Sector diaphragm replaced. *m*.—4-inch diaphragm. *n*.—$t = 12°.0$ C. *o*.—$t = 12°.5$ C.

REDUCTION OF THE MEASUREMENTS

The immediate objective of the observations is a determination of the temperature variation during the eclipse, which must be obtained from a combination of the free (F), cover-glass (Cg), and water-cell (Wc) observations. Each set of such observations must therefore refer to the same instant. Both atmospheric extinction and the march of the eclipse tend to make the cover-glass and water-cell measures differ slightly from those corresponding to a free deflection

in a given set, but the former is negligible within the 4-minute period of observation and at maximum sec $Z = 2$ (Table 2).

TABLE 2

RADIOMETRIC MAGNITUDES AND TEMPERATURES OF THE MOON DURING ECLIPSE, OCTOBER 27, 1939

P.S.T.	sec Z	Free	Cg	Wc	$m_r'(Cg)$	$m_r''(Wc)$	T_{Cg}	T_{Wc}	$\sigma_{cal}T^4$
		mm	mm	mm					
7^h24^m...	2.02	4239	1960	1010	1.63	1.50	365°K	372°K	1.54
41....	1.84	4409	2040	1105	1.62	1.55	367	368	1.51
55....	1.70	4580	2098	1162	1.60	1.55	368	368	1.51
8 10....	1.62	4750	2148	1210	1.57	1.53	371	369	1.54
25....	1.51	4366	1955	1120	1.68	1.66	361	358	1.38
31....	1.46	4111	1828	1005	1.75	1.69	356	356	1.32
37....	1.43	3685	1625	885	1.86	1.80	347	348	1.21
44....	1.40	3067	1365	752	2.08	2.03	330	332	0.99
49....	1.38	2726	1180	655	2.18	2.14	324	325	0.91
55....	1.36	2194	975	540	2.48	2.41	305	308	0.72
9 01....	1.34	1747	785	418	2.72	2.63	291	295	0.61
04....	1.33	1674	692	368	2.68	2.61	293	296	0.62
08....	1.32	1183	540	287	3.16	3.07	267	271	0.43
14....	1.29	837	305	173	3.34	3.32	258	259	0.36
20....	1.26	555	150	98	3.63	3.67	245	243	0.29
30....	1.23	140	21	19	4.93	5.06	200	197	0.13
35....	1.22	114	13	2	5.01	5.00	196	198	0.12
42....	1.21	102	13	3	5.24	5.15	192	195	0.12
48....	1.19	97	6.5	2	5.23	5.19	193	194	0.12
54....	1.18	87	6	1.5	5.34	5.29	190	191	0.11
10 01....	1.16	77.5	4	1.2	5.46	5.41	187	188	0.10
08....	1.15	75	4	1.0	5.50	5.46	186	187	0.10
16....	1.14	70	6	0.7	5.62	5.53	183	185	0.09
26....	1.13	65.5	5	1.0	5.68	5.61	182	183	0.09
38....	1.11	65.5	3	1.0	5.74	5.71	181	181	0.09
52....	1.10	57.5	3	1.0	5.80	5.77	180	180	0.09
11 05....	1.09	54	3.5	1.0	5.88	5.84	178	179	0.08
20....	1.08	54.5	7	2	5.96	5.88	176	178	0.08
29....	1.07	55	9	4	6.01	5.95	175	176	0.08
39....	1.07	61	13	5	5.97	5.86	176	178	0.08
45....	1.07	95	38	15	5.83	5.59	179	184	0.09
52....	1.08	294	131	58	4.70	4.48	207	213	0.16
12 07....	1.09	1046	570	292	3.60	3.42	246	255	0.32
14....	1.09	1729	770	465	2.78	2.83	287	284	0.55
23....	1.10	2584	1210	705	2.40	2.40	310	309	0.76
33....	1.10	3604	1610	942	1.98	1.99	338	335	1.05
44....	1.11	4729	2045	1133	1.65	1.61	364	362	1.43
1 14....	1.15	5282	2370	1275	1.54	1.49	373	373	1.58
1 32....	1.18	5304	2330	1248	1.53	1.46	374	375	1.61

To reduce each set of observations to the same instant, the measures in Table 1 were first brought to a common scale by applying the diaphragm factors 21.32 and 9.096 wherever these diaphragms were used, as noted in the table. In this use of diaphragms to diminish the

radiation to be measured there is always the question whether different parts of a reflecting surface geometrically represent the whole. Experience shows, however, that variations of reflectivity are of minor importance, especially if the surface is new and clean. In the region of planetary heat any divergences are small indeed.

These corrected deflections were then plotted on a very large scale and the cover-glass and water-cell deflections were read from the curves for the times corresponding to the free deflections. These results are given in Table 2.

To reduce the observations to a common air mass, sec Z for the moon was determined from the formula[4]

$$\sec Z = \sec \{Z_0 + \sin^{-1} [(3601 - 120 \cos Z_0)^{-1/2} \sin Z_0]\} , \qquad (1)$$

where Z is the apparent zenith distance for the observer and Z_0 the geocentric value obtained from the *Ephemeris* positions of the moon. This equation assumes a lunar distance of 60 terrestrial radii, but the error reaches only ± 0.1 for sec $Z_0 = 8$, where $\Delta \sec Z_0 = 1.21$. The equation is, therefore, entirely satisfactory for radiation measurements, and the correction to sec Z_0 can be read from a convenient table computed once for all.

The atmospheric extinction was determined by plotting against air mass the logarithms of the free, water-cell, and cover-glass deflections before and after eclipse. These gave nearly the same results, atmospheric extinction = 0.24 mag., as compared with 0.16 mag., which usually prevails on Mount Wilson[1] for planetary heat as well as for reflected sunlight. This quantity has little actual importance because of the low value of maximum sec Z during the eclipse.

TEMPERATURES DURING THE ECLIPSE

In the discussion of the distribution of temperature over the lunar surface,[1] it was found that values determined from atmospheric absorptions given by the Smithsonian observers[5] and black-body formulae were much higher than those to be expected from the solar constant corrected for light reflected from the moon. From the meas-

[4] E. Pettit, *Mt. W. Contr.*, No. 504; *Ap. J.*, **81**, 17, 1935.

[5] F. E. Fowle, *Smithsonian Miscellaneous Collections*, **68**, No. 8, 1917.

urement of this latter quantity the temperature of the subsolar point was found to be 374° K; further, m_r', the radiometric magnitude per square second of the planetary heat reaching the observer, was 1.54.

This led to a readjustment of the atmospheric transmission-curve, from which a series of corrections $\Delta m_r'$ was obtained as a function of temperature.

Now, the temperature of a planet can be obtained from F and Cg by the equation

$$\left.\begin{aligned} m_r + {}^1_4{}^0 \log \bar{b} - {}^1_4{}^0 \log \left(F - \frac{Cg}{tr}\right) - (a \sec Z - b \sec z) + {}^1_4{}^0 \log AS^2 \\ = 26.12 - 10 \log T + \Delta m_r - {}^1_4{}^0 \log \left(1 - \frac{Tr}{tr}\right) = m_r' , \end{aligned}\right\} \quad (2)$$

where m_r is the radiometric magnitude and $\bar{b}$ the deflection for a comparison star, a and b the extinction coefficients, and Z and z the zenith distances of the planet and star, respectively. A is the area of the thermocouple receiver, S the scale of the telescope field in seconds of arc, T the absolute temperature of the planet, Δm_r the absorption of the atmosphere for the planetary heat at that temperature, and Tr and tr the transmissions of the cover glass for planetary heat and reflected light, respectively.

The second member of equation (2), all terms of which are functions of temperature, was used to compute a table of m_r' for different temperatures. The correction $\Delta m_r'$ obtained from the lunar measurements must now be added to these tabular data before the equation is used to determine temperatures, and this has been done in Table 3, which includes Δm_r and Tr.

We may write an equation similar to (2) for the water cell by substituting Wc for Cg; tr is then the transmission of the water cell for reflected light, and Tr its transmission for planetary heat. The second member of equation (2) will be the same, save the last term, which contains the ratio of Tr to tr. It was shown[1] that for the cover glass $tr = 0.90$, whence the last term of the second member of equation (2) becomes

$$f(T) = -{}^1_4{}^0 \log (1 - 1.11\, Tr) , \quad (3)$$

which was used to compute m_r' in Table 3. When the water cell is used, the water-cell absorption for a Ko-type star is 0.70 mag., hence for reflected light from the moon, which has the same color as a Ko star, $tr = 0.52$. On the other hand, Tr is zero, whence $f(T)$ is zero, and the corresponding m_r', which we shall call m_r'' for the water cell, is computed by applying equation (3) with reversed sign to Table 3. The term $f(T)$ is normally positive because of the sign of Tr, hence the values of m_r'' in Table 3 are somewhat smaller than m_r'.

TABLE 3

T	Δm_r	Tr	m_r'	m_r''
100° K.....	6.35	0.0	11.98	11.98
150.....	.....	.....	7.42	7.42
200.....	2.12	.0	4.95	4.95
250.....	.....	.....	3.52	3.52
300.....	1.39	.013	2.56	2.55
350.....	.....	.....	1.82	1.77
400.....	1.28	0.063	1.27	1.19

It was considered that the temperatures and radiation over the moon's surface were so completely determined in a previous study[1] that no comparison star was needed for calibration in equation (2). At the point observed the temperature[6] was 372° K, which can be obtained from the subsolar temperature 374° and the distribution-curve.[1] For this temperature $m_r' = 1.56$ mag. (Table 3), which we may use for m_r, corresponding to the planetary heat

$$\tfrac{1}{4}^0 \log \left(F - \frac{Cg}{tr} \right) = 8.56 \text{ mag.}, \qquad (4)$$

when the moon was highest and out of eclipse at $1^h\ 14^m$. At that time sec $Z = 1.15$ (Table 2) = sec z (equation [2]). The first four and the last observations in Table 2 are also out of eclipse. If these are corrected to sec $z = 1.15$ by use of the atmospheric extinction, 0.24 mag., we find the additional values 8.51, 8.50, 8.53, 8.56, and 8.57 mag., respectively. The average of these, including the above value 8.56, is 8.54 mag. Since there is some uncertainty in the at-

[6] Pettit and Nicholson, *Sci. M.*, **30**, 558, 1930.

mospheric extinction and the deflections are large, it seems preferable to use the value at least zenith distance given in equation (4). The difference of 0.02 mag. would affect the temperatures in Table 2 by a quantity not exceeding 2° C.

This use of planetary heat in the normal lunar radiation to calibrate the eclipse measures also voids the effects of infrared partial transmission of the bismuth black on the thermocouple receivers. Zinc black would have no such defect, but recoating was not possible under the circumstances.

Substituting the foregoing constants into equation (2), we find equations (5) and (6) which apply to these eclipse observations with the cover glass and the water cell, respectively,

$$m_r' = 10.12 - \tfrac{10}{4} \log (F - 1.11\, Cg) - 0.24\, (\sec Z - 1.15) \qquad (5)$$

and

$$m_r'' = 10.12 - \tfrac{10}{4} \log (F - 1.91\, Wc) - 0.24\, (\sec Z - 1.15)\,. \qquad (6)$$

The term $10/4 \log AS^2$ has disappeared, since we used $m_r = 1.56$ mag. for the deflection with the entire thermocouple junction without reduction to 1 square second of arc of planetary heat.

Equations (5) and (6) have been used to obtain the quantities m_r' and m_r'' in Table 2. The temperatures T_{Cg} and T_{Wc}, also shown in Table 2, were then found from Table 3. These two sets of temperatures are not independent, since both depend on the same free deflection. The first, however, depends on the transmission of the cover glass, which is nearly complete for reflected light but which also transmits some planetary heat, while the second depends only on the partial transmission of reflected light by the water cell. The transmission data are therefore quite different in the two cases. Examination of Table 2 or Figure 2 shows that the temperatures obtained with the two screens are sensibly the same. The coefficient of Wc in equation (6) should, of course, be a variable, increasing as the temperature falls, since the light from the eclipsed moon is red; but during the central phase, where the effect is most marked, the deflections with the water cell are excessively small and have no marked effect on the result. There is at present no suitable criterion

for making this correction. The last column in Table 2 gives the energy in cal cm^{-2} min^{-1} radiated at the moon's surface computed from σT^4, where T is the average of T_{Cg} and T_{Wc}.

Figure 2 is a plot of the temperatures from cover-glass and water-cell observations (T_{Cg} and T_{Wc}) and the energy emitted and the energy received by the moon during the eclipse of October 27, 1939, compared with the temperature-curve for the eclipse of June 14, 1927.

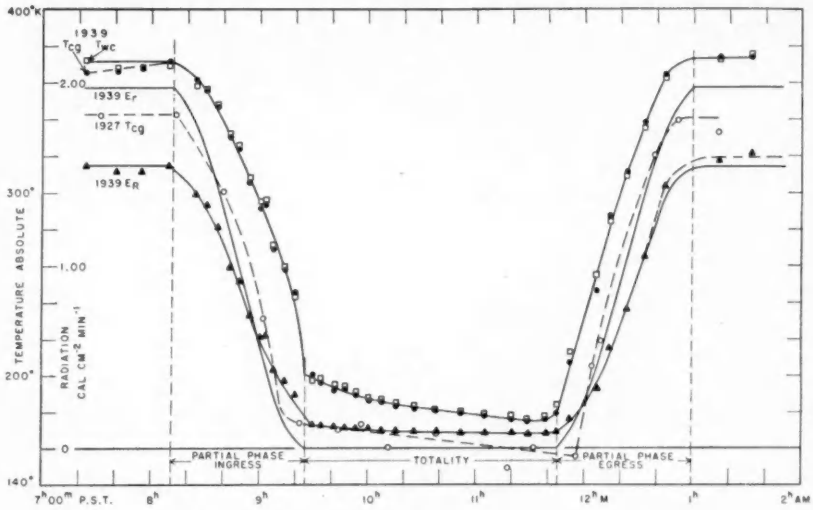

FIG. 2.—Radiation and temperature of the moon near the subsolar point (1939) compared with the temperature near the limb (1927).

It will be noted that the two temperature-curves are very similar, save that the temperatures during the 1939 eclipse were higher, since the point measured was nearer the subsolar point. The two curves at central phase are approximately parallel, but the 1927 curve is rectilinear so far as can be judged from the scattered observations, while the detailed observations of 1939 show a distinct decrease in rate of fall of temperature during the first hour, after which it is practically constant. We may therefore combine the temperature data of the two eclipses at central phase and obtain a description of the fall of temperature over a longer interval than is available for either eclipse alone as follows: When totality begins near the subsolar point the temperature of the moon is 200° K and is falling at the rate

of 30° per hour; the rate itself is decreasing, however. At the end of the first hour the temperature is 182°, and falling at the rate of 7° per hour. This rate would be sensibly constant (though, of course, slowly decreasing) for the next $3\frac{3}{4}$ hours, if the eclipse were to continue, and at the end of the whole period of $4\frac{3}{4}$ hours of totality the temperature would be 156° K. The slight curvature at the end of totality in the 1939 curve is due to the large size of the thermocouple receiver and should not be regarded as real. Probably at no other point on the curve do the dimensions of the receiver have any effect.

TEMPERATURE AND ENERGY RELATIONSHIPS

Figure 3 is a plot of the energy emitted by the moon against the energy received, taken from Figure 2, both of which apply to the lunar surface. The arrows show the direction of the cycle of events, ingress of the moon into the shadow, passage through the umbra, and egress from the penumbra. The time is also indicated. This plot shows that the rate of radiation is nearly proportional to the energy received, save for temperatures below 270° where the radiation falls below 0.70 cal cm^{-2} min^{-1}.

The heat characteristics of the lunar surface substance may be tested in a rather simple manner. Let us consider the exchange of energy to space at the central phase of the eclipse. The specific heat S of the surface material is

$$S = \frac{\sigma T^4 t}{\Delta T d B}, \tag{7}$$

where σT^4 is the energy exchange in cal cm^{-2} min^{-1} during the interval t, and ΔT the weighted mean temperature change during that interval within a layer of density d and thickness B. The most important constituent of the lunar surface is probably lava or pumice, which has a conductivity of only 0.008 watt cm^{-2} deg^{-1}. The thickness B within which a temperature change occurs must therefore be very small. An approximate value of B may be found from equation (7) by using simply $\Delta T = 3.^{\circ}5$ per hour, which is one-half the value found for the lunar surface. This value of ΔT would follow if the change in temperature were mostly at the radiating surface of the layer and if the temperature gradient within the layer were nearly

uniform, for example. For lava[7] $S = 0.20$, $d = 2.8$; further, $\sigma = 8.23 \cdot 10^{-11}$ cal cm^{-2} min^{-1}, $T = 180°$ K, $t = 60$ min. We thus obtain $B = 2.6$ cm, for the layer of the lunar surface immediately in-

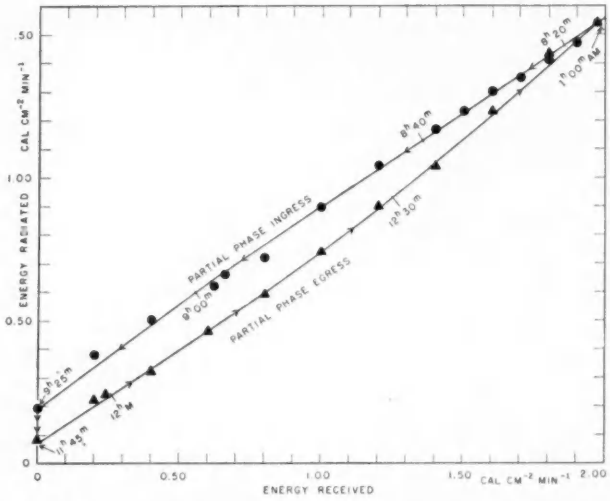

FIG. 3.—Radiation coming from the sun received by the moon near the subsolar point (1939) as a function of that radiated into space.

volved in the exchange of radiation during an eclipse. Both ΔT, which depends on the character of the temperature gradient within the layer, and S, which has been taken for ordinary temperatures, may be less than the values assumed here, but this uncertainty will not considerably affect the order of magnitude of B.

MOUNT WILSON OBSERVATORY
CARNEGIE INSTITUTION OF WASHINGTON
December 1939

[7] Landolt-Bornstein, *Physikalisch-chemische Tabellen*, **3**, 392.

THE EXCITATION TEMPERATURE OF THE SOLAR REVERSING LAYER FROM *CN* (λ 3883)

LEON BLITZER

ABSTRACT

The intensities, in equivalent milliangstroms, of fourteen doublets in the *R* branch of the *CN* (O − O) band have been measured from plates taken for the author with the 75-foot spectrograph of the 150-foot tower telescope on Mount Wilson. Theoretical curves of growth for *CN* were computed for a number of separations of the doublet lines, and from these curves values of log *Nf* corresponding to the measured equivalent widths were determined. Because of the very strong iron absorptions in this region, the equivalent widths were in all cases measured from the blending background. Thackeray's corrections to the true continuous background were then applied to the *Nf* values. On the assumption of thermal equilibrium in the solar reversing layer, the excitation temperature was found to be 4490° ± 100° K (p.e.).

I. INTRODUCTION

It is well known that the temperature of a diatomic gas in thermal equilibrium can be determined from a knowledge of the molecular constants and the relative intensities of the rotational lines in its band spectrum. In recent years two determinations of the temperature of the solar reversing layer have been made from the intensities of the lines of the *CN* (O − O) band at λ 3883. Birge,[1] by estimating the position of the line of maximum intensity, found a temperature of 4000° K; and Roach,[2] from Rowland intensities, arrived at a temperature of 5630° K. In view of the difference in the two results, it is of interest to redetermine the temperature from a quantitative photometry of the lines in the band.

II. OBSERVATIONAL MATERIAL

The observational material for this work consisted of seven solar spectrograms, covering the region λλ 3500–3900, kindly made by Dr. G. F. W. Mulders with the 75-foot spectrograph of the 150-foot tower telescope on Mount Wilson. The theoretical resolving power is 150,000, and the linear dispersion is 3 mm per angstrom. Care was taken to select an undisturbed region of the solar disk. Each plate had three to five exposures, for which the durations ranged from 40 minutes to 4 hours, as well as a set of nine calibration spectra exposed 30 minutes through a vibrating step-slit. Two plates covering

[1] *Ap. J.*, **55**, 273, 1922. [2] *Ap. J.*, **89**, 99, 1939.

the region λλ 3725–3890 and including all the identified *CN* (O – O) solar lines were used in this investigation.

Tracings were made with the Moll microphotometer of the Steward Observatory. The analyzing slit included an effective spectral width of 0.011 mm, or 0.0037 A, which is about one-seventh of the spectrographic resolution. Equivalent widths were determined by graphical integration of the areas defined by the line profiles plotted on an intensity scale.

III. MEASUREMENT OF INTENSITY

The near ultraviolet region of the solar spectrum is so crowded with strong iron absorptions that the *CN* lines never appear to absorb from the true continuous background but rather from the wings of the stronger atomic lines. Because of the impossibility of determining the equivalent widths from the true background, Thackeray's method[3] of reduction was used; that is, the equivalent widths were in all cases measured relative to the blending background, and corrections were then applied to the values of log Nf arrived at from theoretical curves of growth for *CN* (cf. Sec. V below). Here N is the number of molecules per square centimeter over the photosphere which are active in producing the line, and f is the absolute intensity factor for the transition. Corrections were made from a graphical interpolation of Thackeray's empirical Δ log Nf as a function of r_λ (see Thackeray's Table IV for the center of the solar disk), where the quantity r_λ is the ratio of intensity of the blending wing to that of the continuous background.

Uncertainty in the intensity of the blending background was minimized by utilizing only those lines for which the intensity of the blending background was nearly the same on both sides of the measured line. But the continuous spectrum itself, by virtue of complex absorptions, is depressed by a probably appreciable though indeterminable amount. However, since absorptions were measured from the blending background, and since the corrections from Thackeray's results (see cols. 4 and 6, Table 1) are generally small, the net effects of background errors, at least on the Nf values, are probably not very great.

[3] *Ap. J.*, **84**, 433, 1936; *Mt. W. Contr.*, No. 555.

Tracings across the sharp density-boundaries of the calibration exposures failed to show any evidence of Eberhard effect.

TABLE 1

Notation	λ (Lab.)	Total *EW* (Milliangstroms)	log *Nf*	r_1	Corrected log *Nf*	log *Nf*/*i*	*E*″(cm^{-1})
R_{12} (7½).....	3869.921	36.6	11.78	0.78	11.86	10.63	121
R_{12} (13½).....	65.151	38.8	11.82	.83	11.87	10.41	370
R_{12} (14½).....	64.300	35.6	11.76	.95	11.77	10.28	425
R_{12} (27½).....	51.285	47.4	11.90	.88	11.94	10.18	1482
R_1 (40½).....	35.202	21.9	11.35	.42	11.98	10.06	3177
R_2 (40½).....	35.147						
R_1 (47½).....	25.307	24.5	11.39	.50	11.79	9.80	4355
R_2 (47½).....	25.237						
R_1 (49½).....	22.322	42.4	11.71	.77	11.79	9.79	4725
R_2 (49½).....	22.259						
R_1 (51½).....	19.278	31.4	11.53	.68	11.68	9.66	5111
R_2 (51½).....	3819.213						
R_1 (65½).....	3796.184	19.9	11.29	.66	11.45	9.33	8234
R_2 (65½).....	96.104						
R_1 (74½).....	79.806	16.1	11.19	.95	11.20	9.02	10633
R_2 (74½).....	79.732						
R_1 (75½).....	77.919	11.3	11.00	.90	11.03	8.85	10919
R_2 (75½).....	77.842						
R_1 (77½).....	74.107	12.6	11.05	.87	11.09	8.89	11501
R_2 (77½).....	74.030						
R_1 (86½).....	56.332	6.3	10.73	.93	10.74	8.50	14308
R_2 (86½).....	56.263						
R_1 (88½).....	52.258	4.8	10.60	0.76	10.69	8.44	14973
R_2 (88½).....	3752.187						

IV. MEASURED LINES

The *R* branch of the λ 3883 band consists of a series of close doublets belonging to two parallel subbranches, R_1 and R_2. Up to quantum number $J'' = 30\frac{1}{2}$, the R_1 and R_2 lines have never been resolved. The unresolved pairs are, therefore, denoted in this paper by R_{12} (J''), and the mean wave lengths are used. Moreover, as a re-

sult of the blending of the Doppler wings, even the doub'ets of higher quantum number are not completely resolved. Consequently, we are restricted to the use of the total equivalent width for each available doublet.

Of the nearly one hundred doublets of this branch listed in the *Revised Rowland*, only fourteen were sufficiently free from close blending with atomic lines to be suitable in this study. These are given in Table 1. The notations for branch and quantum number in column 1 are from Jevons[4] and correspond to the laboratory wave lengths of Uhler and Patterson[5] in column 2. Identifications of the *CN* lines were made by comparing the laboratory wave lengths with the solar wave lengths from the *Revised Rowland*. In column 3 are tabulated the total equivalent widths, corrected for the ghosts of the grating. For the order of the grating used, Mulders[6] has found this correction to be 3 per cent.

V. CURVES OF GROWTH

As was mentioned previously, none of the *CN* doublets used in this investigation has been completely resolved. Moreover, the separations of the component lines vary with J''(see col. 2). Since the resultant equivalent width of two partially blended lines depends upon the separation of the lines, it is necessary, in order to determine the Nf values, to compute in each case a curve of growth corresponding to the observed or computed (as for the first four doublets) separation.

The procedure was to compute, by means of the formulae given by Unsöld,[7] the optical depths for *CN* ($\mu = 26$) in the sun at 4500° K and at λ 3800 for various distances from the center of an absorption line, and for various values of Nf. For any desired separation of a pair of lines the optical depths along the overlapping portion were obtained by adding linearly the component optical depths in each wave length. It was then possible to determine the intensities relative to the background along the resultant doublet and, by graphical

[4] *Proc. R. Soc.*, A, **112**, 407, 1926.

[5] *Ap. J.*, **42**, 434, 1915.

[6] Personal communication.

[7] *Physik der Sternatmosphären*, eqs. (69.3), (69.4), (69.5), and (69.6), Berlin: Julius Springer, 1938.

integration, the equivalent width. Repeating the foregoing for a suitable set of values of Nf, we thus have a curve of growth for any desired separation. Since the resultant curves of growth in the regions used were rather close together, it proved adequate to compute such curves only for doublet separations of 0.017, 0.034, 0.065, and 0.077 A.

VI. DETERMINATION OF TEMPERATURE

The equation relating the relative intensity of a rotational line to the temperature of the absorbing gas may be written as

$$I = Nf = C_1 i e^{-hcE''/kT}, \tag{1}$$

where C_1 is a constant for the band; i, the "relative intensity factor" for the line, which is proportional to the statistical weight of the initial level and to the probability of the transition; and E'', the rotational energy (in cm^{-1}) of the initial level.

On taking logarithms and substituting for the known constants, equation (1) is reduced to the simplified form

$$\log \frac{Nf}{i} = \log C_1 - \frac{0.628E''}{T}, \tag{2}$$

where[8]

$$0.628 = \frac{0.4343\ hc}{k}$$

and[9]

$$E'' = B_v'' J''(J'' + 1) = 1.8904\ J''(J'' + 1). \tag{3}$$

Values of $\log Nf$ taken from the appropriate curves of growth are tabulated in column 4. Thackeray's corrections corresponding to the measured values of r_1 were then added to give the corrected $\log Nf$ values (col. 6). Values of $\log i$ were computed from the formulae

[8] Attention is called to an error in *Ap. J.*, **89**, 99, 1939, eq. 9, in which hc was inadvertently placed in the denominator. However, the calculation of the constant was carried out correctly.

[9] The numerical value for B_v'' is from Sponer, *Molekülspektren*, p. 39, Berlin: Julius Springer, 1935.

given by Jevons[10] and applied to column 6 to give column 7. The values of E'' in column 8 were computed from equation (3).

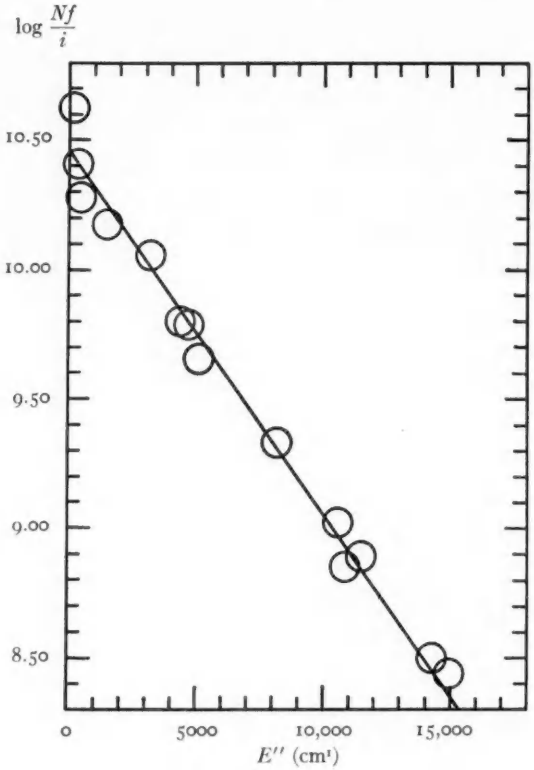

FIG. 1.—Variation of $\log \frac{Nf}{i}$ with E''. All observations have equal weights. The radii of the circles are equal to the probable error in the ordinate.

Equation (2) is linear in $\log Nf/i$ and E'', the slope involving the temperature T. In Figure 1 are plotted the values of $\log Nf/i$ against E'', together with the least-squares solution of equation (2). The resulting slope is -0.1399 ± 0.0030 (p.e.), and the corresponding temperature is $4490^\circ \pm 100^\circ$ K.

[10] *Report on Band Spectra of Diatomic Molecules*, p. 137, Cambridge: University Press, 1932.

The low temperature found in this paper is not without precedent. It is in good agreement with Miss Adam's recent determination[11] of 4550° K from the C_2 (Swan) band and in fair agreement with the *atomic* determinations of 4400° K (*Ti* I) by King[12] and 4150° K (*Fe* I) and 4350° K (*Ti* I) by Menzel, Baker, and Goldberg.[13] In this connection should also be mentioned the higher values of Richardson[14] of 5670° K (mean) from C_2 (Swan) and 5080° K from *CH* (λ 4314); Roach's[2] two determinations, from Rowland intensities, of 5630° K from *CN* (λ 3883) and 4640° K from *OH* (λ 3064); and Birge's[1] early value of 4000° K from *CN* (λ 3883).

It is a pleasure to record my deepest thanks and appreciation to Dr. Franklin E. Roach for suggesting this problem and guiding its prosecution. I am grateful to Dr. G. F. W. Mulders for the spectrograms upon which this study is based. My thanks are also due to Dr. A. Unsöld for valuable criticisms and suggestions. To Dr. E. F. Carpenter I am indebted for the generous help extended in the solution of the photometric problems.

DEPARTMENT OF PHYSICS
AND
STEWARD OBSERVATORY
UNIVERSITY OF ARIZONA
October 1939

[11] *M.N.*, **98**, 544, 1938. [12] *Ap. J.*, **87**, 40, 1938. [13] *Ap. J.*, **87**, 81, 1938.
[14] *Ap. J.*, **73**, 216, 1931; *Mt. W. Contr.*, No. 422; and *Trans. I.A.U.*, **4**, 55, 1932.

THE EFFECT OF CONTINUOUS BALMER ABSORPTION UPON THE EQUIVALENT WIDTHS OF STELLAR ABSORPTION LINES*

OTTO STRUVE AND FRANCES SHERMAN

ABSTRACT

Continuous Balmer absorption on the violet side of λ 3647 tends to weaken the absorption lines of various elements. From the equivalent widths of 48 lines of *Ti* II the ratio of the continuous absorption coefficients on both sides of λ 3647 is found to be 16 in η Leonis, 10 in α Cygni and α Lyrae, and 2 in υ Sagittarii. The hydrogen abundance is very great in η Leonis, α Cygni, and α Lyrae but is surprisingly low in υ Sagittarii.

Several years ago R. W. Shaw[1] pointed out that the lines of *Ti* II in α Lyrae, between λ 3480 and λ 3647, are abnormally weak. This effect is caused by continuous hydrogen absorption on the violet side of the Balmer limit. The problem is related to that of blended absorption lines investigated by Swings and Struve,[2] by Thackeray,[3] and by Wilson and Thackeray.[4] The theory of the problem has been discussed by Swings and Chandrasekhar,[5] especially for the important case of a stratified atmosphere.

Table 1 contains the equivalent widths of 48 lines of *Ti* II selected from the spectrum of α Cygni[6] as being almost free of blends. The lines were measured on plates standardized with a tube sensitometer which was equipped with an ultraviolet filter giving maximum sensitivity in the region between λ 3300 and λ 3900. The standardization is, therefore, entirely adequate.

The results in the table depend upon measurements of four plates of α Cygni, three of η Leonis, three of α Lyrae, and three of υ Sagittarii. Eastman Process emulsion was used for the exposures, and the star's image was permitted to trail along the slit giving greatly widened spectra. The observations were secured with the quartz Cassegrain spectrograph attached to the 82-inch reflector of the McDonald

* *Contributions from the McDonald Observatory, University of Texas*, No. 19.

[1] *Ap. J.*, **82**, 87, 1935.

[2] *Ap. J.*, **83**, 238, 1936.

[3] *Ap. J.*, **84**, 433, 1936.

[4] *Pub. A.S.P.*, **48**, 329, 1936.

[5] *M.N.*, **97**, 24, 1936.

[6] *Ap. J.*, **90**, 699, 1939.

TABLE 1

EQUIVALENT WIDTHS OF *Ti* II LINES

Multiplet	Wave Length	log Lab. Int.	E.P. of Low Level	Designation	α Cygni	η Leonis	α Lyrae	υ Sagittarii
1.....	3282.34	1.40	1.2	$b^4P_{1/2}-y^4D^\circ_{1/2}$	0.114 A	0.048 A	0.039 A	.....
2.....	3287.67	1.60	1.9	$b^2G_{3/2}-z^2H^\circ_{4/2}$	.182	.063	.057	.....
3.....	3308.82	0.90	0.1	$b^4F_{3/2}-z^4F^\circ_{4/2}$	.103	.040	.040	.....
	3326.78	1.30	0.1	$1/2-2/2$	.098	.048	.030	.....
	3329.5	1.85	0.1	$3/2-3/2$	.259	.081	.121	.....
	3343.78	1.00	0.1	$4/2-3/2$	.080	.052	.029	.....
	3346.7	1.18	0.1	$3/2\ 2/2$	.092	.040	.014	.....
4.....	3315.33	1.00	1.2	$b^4P_{1/2}-z^4S^\circ_{1/2}$	.094	.052	.024	.....
	3321.71	1.40	1.2	$1/2\ 1/2$	.132	.044	.026	.....
	3332.11	1.48	1.2	$2/2\ 1/2$	.154	.053	.033	.....
5.....	3337.85	0.30	1.2	$a^2P_{1/2}-y^2F^\circ_{2/2}$	.040	.040	.034	.....
6.....	3341.84	2.00	0.6	$a^2F_{2/2}-z^2G^\circ_{3/2}$	.535	.130	.111	.....
7.....	3361.19	2.10	0.0	$a^4F_{3/2}-z^4G^\circ_{4/2}$	.426	.178	.190	.....
	3383.77	2.10	0.0	$1/2\ 2/2$	.333	.170	.147	0.174 A
	3387.85	1.70	0.0	$3/2\ 3/2$	.286	.098	.132	.....
	3409.82	0.60	0.0	$3/2\ 2/2$	.023	.034	.031	.041
8.....	3352.07	0.70	1.2	$a^2P_{1/2}-z^2P^\circ_{1/2}$	.028	.028	.013	.....
	3366.18	0.90	1.2	$1/2\ 1/2$	.054	.016	.052	.160
9.....	3362.65	0.00	1.2	$b^4P_{1/2}-z^2P^\circ_{1/2}$	.033	.009	.028	.123
10.....	3388.76	0.90	1.2	$a^2P_{1/2}-y^2D^\circ_{2/2}$	.030	.033	.018	.....
11.....	3452.48	0.60	2.0	$b^2P_{1/2}-y^2P^\circ_{1/2}$	.037	.027	.....	.100
	3465.65	0.48	2.1	$1/2\ 1/2$	.032	.034	.....	.....
12.....	3444.33	1.48	0.2	$b^4F_{4/2}-z^4G^\circ_{5/2}$	.222	.078	.094	.251
	3461.50	1.30	0.1	$3/2\ 4/2$	.134	.062	.051	.125
	3477.19	1.18	0.1	$2/2\ 3/2$	.132	.044	.032	.113
	3491.06	1.00	0.1	$1/2\ 2/2$	.114	.046	.028	.....
13.....	3404.96	0.00	1.2	$b^4P_{1/2}-y^2D^\circ_{1/2}$	.018	.014	.026	.016
14.....	3509.85	0.48	1.9	$b^2G_{4/2}-y^2G^\circ_{3/2}$	.028	.028	.022	.070
	3510.85	1.78	1.9	$3/2\ 3/2$	.147	.077	.054	.194
15.....	3520.26	1.30	2.0	$b^2P_{1/2}-x^2D^\circ_{1/2}$	.090	.030	.031	.131
	3535.41	1.60	2.1	$1/2\ 2/2$	.119	.056	.042	.....
16.....	3561.58	0.48	0.6	$a^2F_{2/2}-z^4D^\circ_{2/2}$	.037	.019	.032	.160
	3573.74	1.30	0.6	$2/2\ 1/2$	.040	.012	.018	.056
	3587.15	1.08	0.6	$3/2\ 3/2$	.039	.033	.024	.....
	3596.06	1.78	0.6	$3/2\ 2/2$	0.104	0.064	0.034	0.141

TABLE 1—*Continued*

Multiplet	Wave Length	log Lab. Int.	E.P. of Low Level	Designation	α Cygni	η Leonis	α Lyrae	υ Sagittarii
17.....	3624.84	1.85	1.2	$a^2P_{1\frac{1}{2}}-z^2S^\circ_{1\frac{1}{2}}$	0.148 A	0.042 A	0.036 A	0.186 A
	3641.34	2.00	1.2	$1\frac{1}{2}$ $1\frac{1}{2}$	.148	.042	.066	.146
18.....	3659.76	1.78	1.6	$b^2D_{2\frac{1}{2}}-y^2F^\circ_{3\frac{1}{2}}$	.042	.021	.026	.104
19.....	3685.20	2.40	0.6	$a^2F_{3\frac{1}{2}}-z^2D^\circ_{2\frac{1}{2}}$	.536	.258	.132	.289
20.....	3759.30	2.30	0.6	$a^2F_{3\frac{1}{2}}-z^2F^\circ_{3\frac{1}{2}}$	.540	.368	.167	.302
	3761.32	2.30	0.6	$2\frac{1}{2}$ $2\frac{1}{2}$	.600	.317	.150	.391
21.....	3741.65	1.70	1.6	$b^2D_{2\frac{1}{2}}-y^2D^\circ_{2\frac{1}{2}}$	.284	.140	.088	.196
	3757.69	1.48	1.6	$1\frac{1}{2}$ $1\frac{1}{2}$	.298	.126	.150	.170
	3776.06	0.78	1.6	$2\frac{1}{2}$ $1\frac{1}{2}$	.100	.....	.....	.089
22.....	3786.33	0.00	0.6	$a^2F_{3\frac{1}{2}}-z^4F^\circ_{4\frac{1}{2}}$	.054	.062	.042	.085
23.....	3900.54	1.85	1.1	$a^2G_{4\frac{1}{2}}-z^2G^\circ_{4\frac{1}{2}}$	.406	.192	.112	.274
	3913.47	1.78	1.1	$3\frac{1}{2}$ $3\frac{1}{2}$	.381	.169	.120	0.246
	3932.02	0.30	1.1	$4\frac{1}{2}$ $3\frac{1}{2}$	0.110	0.038	0.084	.....

Observatory,[6] and the linear dispersion was 22 A/mm at λ 3300 and 40 A/mm at λ 3933.

Because of the very large drop of intensity in the continuous spectrum at λ 3647 in A-type stars, some of the plates were overexposed on the red side of the limit, while others were underexposed on the violet side. But nearly all entries in the table depend upon at least two separate plates, and many depend upon three plates.

Although the lines are relatively free of blending in α Cygni and, presumably, in η Leonis, this is not true for α Lyrae and, especially, for υ Sagittarii. The blending in α Lyrae is probably not serious. But in υ Sagittarii many lines had to be omitted because of serious blends, while others, although included, are somewhat suspicious. These suspicious lines are shown in Figure 4 with question marks. We are indebted to Dr. Jesse Greenstein for the use of his spectrograms of υ Sagittarii[7] and for valuable information concerning blended lines in this unusual spectrum.

The logarithms of the laboratory intensities were taken from Miss Moore's *A Multiplet Table of Astrophysical Interest*. These intensi-

[7] See the following article in this *Journal*, p. 438.

ties, obtained in the condensed spark, were estimated on a uniform scale by Miss Moore, on the basis of a selected list of standards prepared by A. S. King.[8] They represent the observable photographic density on King's spectrograms and tend to be low for the long and short wave lengths of Russell's list of *Ti* II lines.[8] Since this list covers the range from λ 2500 to λ 6700, it is reasonable to suppose that the intensities are quite homogeneous over the range used in this work.

TABLE 2

MULTIPLET ELECTRON CONFIGURATIONS OF *Ti* II

Multiplet	Configurations	Multiplet	Configurations
1	$3d^2(^3P)4s\ b^4P - 3d^2(^3P)4p\ y^4D^\circ$	13	$3d^2(^3P)4s\ b^4P - 3d^2(^1D)4p\ y^2D^\circ$
2	$3d^2(^1G)4s\ b^2G - 3d^2(^1G)4p\ z^2H^\circ$	14	$3d^2(^1G)4s\ b^2G - 3d^2(^1G)4p\ y^2G^\circ$
3	$3d^3\ b^4F - 3d^2(^3F)4p\ z^4F^\circ$	15	$3d^2(^3P)4s\ b^2P - 3d^2(^3P)4p\ x^2D^\circ$
4	$3d^2(^3P)4s\ b^4P - 3d^2(^3P)4p\ z^4S^\circ$	16	$3d^2(^3F)4s\ a^2F - 3d^2(^3F)4p\ z^4D^\circ$
5	$3d^3a^2P - 3d^2(^1D)4p\ y^2F^\circ$	17	$3d^3\ a^2P - 3d^2(^3P)4p\ z^2S^\circ$
6	$3d^2(^3F)4s\ a^2F - 3d^2(^3F)4p\ z^2G^\circ$	18	$3d^3\ b^2D - 3d^2(^1D)4p\ y^2F^\circ$
7	$3d^2(^3F)4s\ a^4F - 3d^2(^3F)4p\ z^4G^\circ$	19	$3d^2(^3F)4s\ a^2F - 3d^2(^3F)4p\ z^2D^\circ$
8	$3d^3\ a^2P - 3d^2(^1D)4p\ z^2P^\circ$	20	$3d^2(^3F)4s\ a^2F - 3d^2(^3F)4p\ z^2F^\circ$
9	$3d^2(^3P)4s\ b^4P - 3d^2(^1D)4p\ z^2P^\circ$	21	$3d^3\ b^2D - 3d^2(^1D)4p\ y^2D^\circ$
10	$3d^3\ a^2P - 3d^2(^1D)4p\ y^2D^\circ$	22	$3d^2(^3F)4s\ a^2F - 3d^2(^3F)4p\ z^4F^\circ$
11	$3d^2(^3P)4s\ b^2P - 3d^2(^3P)4p\ y^2P^\circ$	23	$3d^3\ a^2G - 3d^2(^3F)4p\ z^2G^\circ$
12	$3d^3\ b^4F - 3d^2(^3F)4p\ z^4G^\circ$		

Table 2 contains the electron configurations of the multiplets used. Of the 23 multiplets, 10 belong to the group $3d^24s - 3d^24p$, 9 belong to the group $3d^3 - 3d^24p$, and 4 involve combinations between doublets and quartets. Since these intersystem multiplets are strong (see, for example, multiplet 16 in Table 1), the use of theoretical line intensities based upon the assumption of *LS* coupling may lead to large errors. Table 3 lists those lines of Table 1 which belong to the transition array $3d^24s - 3d^24p$. The theoretical strengths, *S*, of the individual multiplets were taken from the tables by Goldberg,[9] and the relative intensities of the separate lines of each multiplet, *s*, were taken from the tables by White and Eliason.[10] The correlation of the theoretical intensities and the laboratory values is not satisfactory. The stellar data agree better with the laboratory intensities than

[8] H. N. Russell, *Ap. J.*, **66**, 291, 1927.

[9] *Ap. J.*, **82**, 1, 1935.

[10] *Phys. Rev.*, **44**, 753, 1933.

with the theoretical intensities. Hence, we have used the former throughout this work, in spite of the fact that the conditions of excitation in the spark may not have been similar to those in the stars. The excitation potentials of the lower levels of the lines used range from 0.0 to 2.1 volts. Hence it is possible that there are systematic differences between low-level lines and high-level lines. However, an inspection of groups of lines which lie close together in the spectrum shows that this effect is negligible for our present purpose.

TABLE 3

COMPARISON OF THEORETICAL INTENSITIES AND OF LABORATORY INTENSITIES

λ	Int. $\frac{S_S}{\Sigma_S}$	Lab. Int.	Multiplet
3282.34	0.83	25	1, quartet
3287.67	4.88	40	2, doublet
3315.33	0.33	10	4, quartet
3321.71	0.67	25	
3332.11	1.00	30	
3341.84	3.87	100	6, doublet
3361.19	4.60	125	7, quartet
3383.77	2.57	125	
3387.85	0.54	50	
3409.82	0.02	4	
3452.48	1.33	4	11, doublet
3465.65	0.66	3	
3509.85	0.11	3	14, doublet
3510.85	3.88	60	
3520.26	1.67	20	15, doublet
3535.41	3.00	40	
3685.20	2.86	250	19, doublet
3759.30	3.87	200	20, doublet
3761.32	2.87	200	

We have plotted, in Figures 1–4, for each star the measured equivalent width against the logarithm of the laboratory intensity. The lines were divided in four groups: large filled circles represent all lines in the region λλ 3932–3685; crosses represent the region λλ 3659–3561; open circles represent the region λλ 3535–3444; small filled circles represent the region λλ 3465–3282. In all four stars the lines of the region λλ 3932–3658 are strongest, and those immediately to the violet of the Balmer limit are weakest. The effect is most pronounced in η Leonis, but it is also conspicuous in α Cygni and in α Lyrae. It is least noticeable in υ Sagittarii. For convenience, we

have drawn curves through the four groups of points in each diagram, except that in α Lyrae and υ Sagittarii we have omitted the curve for the lines of region $\lambda\lambda$ 3465–3282.

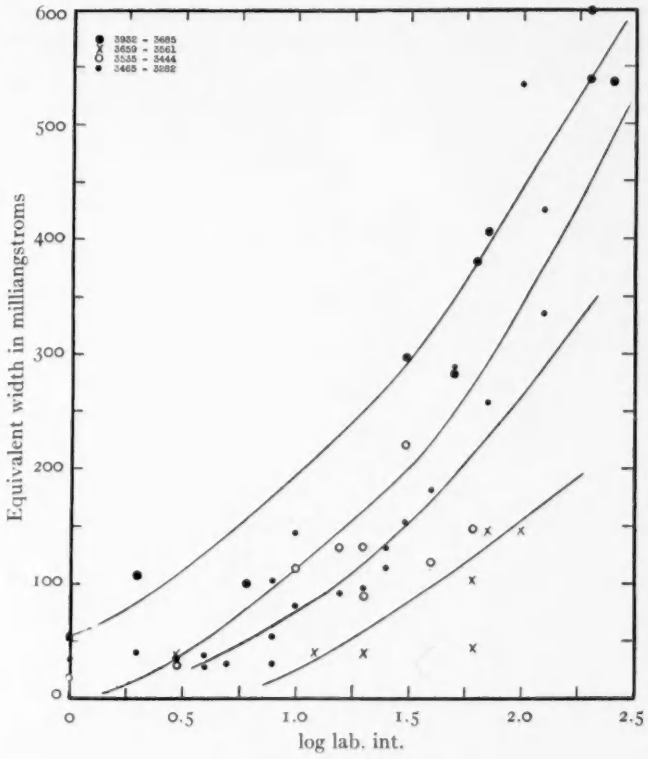

FIG. 1.—α Cygni

The weakening of spectral lines on the violet side of λ 3647 is produced by the continuous Balmer absorption in the atmosphere of the star. If the ratio, η, of the mass absorption coefficient within the line $(\sigma_\nu + \kappa_\nu)$ to the mass absorption coefficient for continuous radiation, κ, is constant, then the intensity within the line, at any frequency ν, is given by Eddington's formula[11]

$$\frac{H_\nu^1}{H} = \frac{1 + \frac{2}{3}\sqrt{3(1+\eta)(1+\epsilon\eta)}}{1 + \eta + \frac{2}{3}\sqrt{3(1+\eta)(1+\epsilon\eta)}},$$

[11] *M.N.*, **89**, 624, 1929.

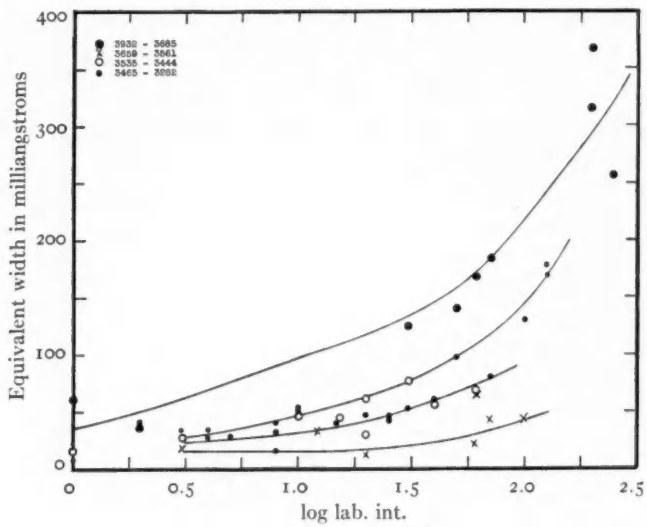

FIG. 2.—η Leonis

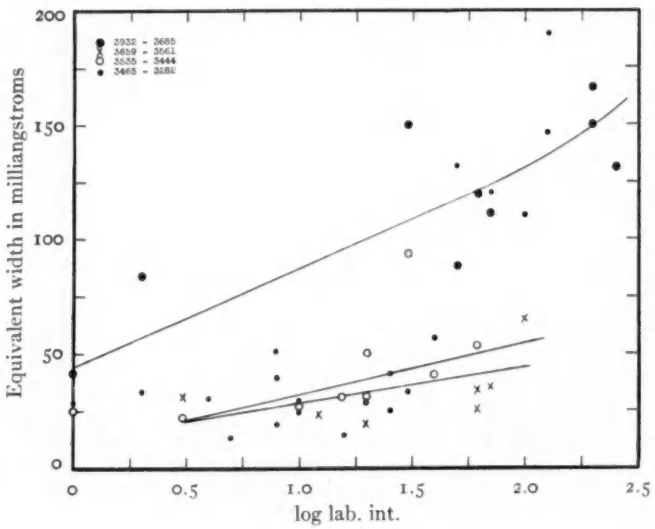

FIG. 3.—α Lyrae

where ϵ measures the fraction of the radiation absorbed by κ_ν to that absorbed by σ_ν. The absorption coefficients appear in this expression only in the form of η. We can consider that the mass absorption coefficient within the line, consisting of the scattering coefficient σ_ν and the pure absorption coefficient κ_ν, is proportional to the number of active atoms per gram of gas.

$$\sigma_\nu + \kappa_\nu = N(\sigma_{at} + \kappa_{at}) .$$

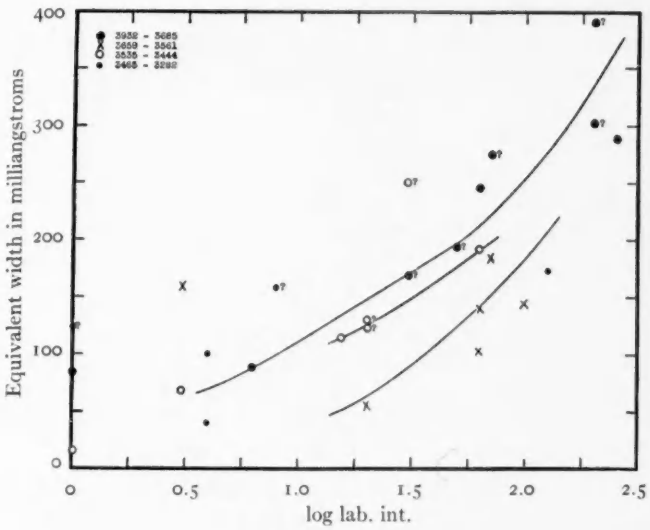

FIG. 4.—v Sagittarii

Accordingly, if κ increases by a factor of γ as we pass from one region of the spectrum to another, we can interpret the changes as producing exactly the same intensity H^1_ν/H as that which would have been produced had N been decreased by the factor γ.

From Figure 2 we infer that the equivalent width of a line of average laboratory intensity ($\log I = 1.5$), on the red side of λ 3647, is $W = 0.135$ A, while for the mean of the two regions $\lambda\lambda$ 3659–3561 and $\lambda\lambda$ 3535–3444 it is $W = 0.037$ A. The ratio is

$$\frac{W_{red}}{W_{violet}} = 4 .$$

The curve of growth has not been accurately determined for η Leonis, but it is sufficient for our purpose to assume[12] that

$$W \sim \sqrt{NH} .$$

Hence, we find for the ratio in κ at the two sides of the Balmer limit

$$\gamma = 16 .$$

This result may now be compared to that predicted by the theory. Assuming for η Leonis a temperature of about 10,000° K, so that $\theta = 5040/T = 0.5$, we find from Unsöld's data[13] that at the Balmer limit

$$\log \frac{\kappa_\nu'}{\bar{\kappa}} - \log \frac{\kappa_\nu''}{\bar{\kappa}} = -0.78 .$$

Hence, we should have expected a ratio

$$\gamma = \frac{\kappa_\nu''}{\kappa_\nu'} = 6 ,$$

instead of the observed value of 16. However, Unsöld's computations of κ are based upon his own mixture of elements, namely, 13.7 atoms of hydrogen to one atom of all other elements. The observational result suggests a greater abundance of hydrogen.

Referring again to Unsöld's work,[14] we find that for an atmosphere of pure hydrogen at $\theta = 0.5$.

$$\gamma = \frac{\kappa_\nu''}{\kappa_\nu'} = 21 .$$

This value is considerably larger than the observed result. Hence, the continuous absorption of the metals and of the free electrons (and perhaps also of the negative hydrogen ions) cannot be neglected. In principle, the observations should enable us to determine the abundance of hydrogen. In practice we can conclude only that this abundance is probably considerably greater than that originally suggested

[12] This would hold very closely for α Cygni and α Lyrae (*Ap. J.*, **78**, 409, 1934). It is probably a good approximation for lines of intermediate strength in any star.

[13] *Physik der Sternatmosphären*, p. 127, Table 30.

[14] *Ibid.*, p. 121, Table 28.

by Unsöld—a result which we believe to be essentially in accordance with Unsöld's latest (unpublished) findings. The observations are not accurate enough to verify Russell's mixture.

The assumption η = constant is fundamental in our discussion. For a stratified atmosphere the absorption coefficients enter not only in the form $[(\sigma_\nu + \kappa_\nu)/\kappa]$, and the formulae given by Swings and Chandrasekhar[5] must be used. Since the ionization potential of *Ti* II (13.6 volts) is almost identical with that of *H*, we are justified, in the present case, in considering η as a constant throughout the atmosphere.

The observational results for α Cygni and α Lyrae give similar values of γ:

$$\gamma \approx 10 .$$

It is not certain that the departure from η Leonis is real, and we have no reason, as yet, to suspect that hydrogen is less abundant in these stars than in η Leonis. The mean value of γ for these three stars would still be in excess of that computed from Unsöld's mixture, but the corresponding abundance of hydrogen may not be as large as in the Russell mixture.

The star υ Sagittarii shows a remarkably small value of γ:

$$\gamma \approx 2 .$$

This is much less than Unsöld's value of $\kappa_\nu''/\kappa_\nu' = 6$, indicating an unusually low abundance of hydrogen in the reversing layer of this star. This is also apparent from the absence of any measurable drop in the intensity of the continuous spectrum at λ 3647. The astrophysical consequences of this unusually low abundance of hydrogen are being discussed by Dr. Greenstein.[7] The great strength of *Fe* II, the presence of weak *Fe* I, and the absence of *Fe* III leave no doubt as to the state of ionization of υ Sagittarii. Hence, the weakness of the hydrogen continuous absorption cannot be explained in terms of ionization. It can mean only a real depletion of hydrogen atoms in the reversing layer.

YERKES OBSERVATORY
December 22, 1939

THE SPECTRUM OF υ SAGITTARII*

JESSE L. GREENSTEIN

ABSTRACT

The ultraviolet region of the spectrum of υ Sgr, from λ 3317 to λ 3975, has been investigated on plates taken at the McDonald Observatory. The measured wave lengths of 400 lines, together with intensities and identifications, are given in Table 1. The lines of hydrogen are very weak, while the lines of all series of helium are strong. The singly ionized metals are dominant, but a few weak lines of *Fe* I, *Mg* I, and *Cr* I are present. The *Fe* II spectrum is particularly strong and includes many new predicted lines from high-level transitions. Table 2 lists the elements identified. No indication of effects arising from dilution of the radiation can be found. The star is fairly massive and has an absolute magnitude near -7.

A comparison of the metallic spectrum with that of α Cyg suggests that the level of ionization is slightly higher in υ Sgr. The most striking difference between these two supergiants is the extreme weakness of the hydrogen lines in υ Sgr and the almost complete disappearance of the jump in intensity at the Balmer limit. An attempt has been made to determine the relative abundance of helium, hydrogen, and iron, on the basis of approximate theoretical predictions of line intensities. The effects of stratification are discussed. The equivalent widths given in Table 9 are used to determine the relative abundances given in Table 12. Estimates of f-values, together with the relative intensities of the *Fe* I, *Fe* II, and *Fe* III lines, fix the level of ionization. A model atmosphere with $T = 10{,}000°$ and with an electron pressure near 100 bars gives intensities similar to the observed values. The abundance of helium is nearly one hundred times that of hydrogen; hydrogen is one hundred times as abundant as iron. The presence of lines of other elements of very high excitation potential, notably *A* II, apparently indicates a higher excitation temperature for the extreme ultraviolet (Table 13). The low abundance of hydrogen would still persist if such deviations were real.

The contribution of helium to the continuous absorption coefficient is found to be greater than that of hydrogen and assists in reducing the jump at the Balmer absorption limit. An atmosphere in which helium is very abundant may exhibit absolute-magnitude effects, i.e., low electron pressure, for higher values of the surface gravity.

THE ULTRAVIOLET SPECTRUM

The spectral peculiarities of υ Sgr, HD 181615-6, have been recognized since Miss Cannon's description.[1] The spectrum was then classified as composite and variable, possibly arising from a triple system. A strong helium spectrum is superposed on a complex metallic spectrum;[2] the hydrogen lines are variable and sometimes multiple, with $H\alpha$ and sometimes $H\beta$ in emission. A spectroscopic orbit was obtained by R. E. Wilson[3] and was supplemented by measures by Plaskett[2] and McLaughlin.[4] The radial velocities of the

* *Contributions from the McDonald Observatory, University of Texas*, No. 21.

[1] *Harvard Ann.*, **56**, 108, 1912.

[2] J. S. Plaskett, *Pub. Dom. Ap. Obs.*, **4**, 1, 1927.

[3] *Lick Obs. Bull.*, **8**, 134, 1914.

[4] *Pub. A.A.S.*, **9**, 224, 1939.

helium, hydrogen, and metallic spectra all vary *in phase;* the period and orbital elements remain satisfactory. The star is apparently a bona fide spectroscopic binary, the fainter component of which is never visible in the spectrum. The stronger hydrogen lines are sometimes multiple, with components shifted to the violet. These components have velocities which also vary *in phase* with the primary spectrum. If they arise in an expanding shell, the shell must be connected with the primary star.

Plaskett[5] has measured the wave lengths of 300 lines in the photographic region of the spectrum. These measures and identifications have been supplemented by W. W. Morgan.[6,7] The present investigation covers the ultraviolet region of the spectrum, from λ 3317 to λ 3975. Three spectrograms have been obtained on Eastman Process plates with the Cassegrain spectrograph of the McDonald Observatory. Two quartz prisms yield a mean dispersion of 30 A/mm. All lines were measured on at least two plates; the derived wave lengths should have a mean error of the order of $\pm$0.05 A for good lines of intensity greater than 1. Weaker lines may be much less accurate. Because of varying orbital velocities on the three dates of observation (June 4, 5, and 30, 1939), it was necessary to correct the observed wave lengths for the radial-velocity shifts. The velocities were determined mainly from the metallic spectrum. The three plates were at mean phase 123 days, near the time of maximum positive velocity. The velocities agree moderately well with the spectroscopic radial-velocity curve. The ultraviolet region is extraordinarily rich in lines, 400 lines being measured within an interval of 600 A. Blending is a serious factor, and the wave lengths and identifications are, to that extent, uncertain. The star would repay investigation with higher dispersion.

The identifications and the laboratory intensity scales were taken from Miss Moore's *Multiplet Table of Astrophysical Interest*, supplemented in the case of *Fe* II, *Cr* II, *V* II, and *Ti* II by various unpublished lists of wave lengths and intensities kindly furnished by Mrs. Moore-Sitterly. Original laboratory investigations were also

[5] *Pub. Dom. Ap. Obs.*, **4**, 103, 1928.

[6] *Pub. Yerkes Obs.*, **7**, Part III, 1935.

[7] *Ap. J.*, **79**, 513, 1934.

consulted, and unidentified lines were searched for in Harrison's *M.I.T. Wave Length Tables*. Perhaps the single most useful list of new lines was kindly loaned by Mrs. Moore-Sitterly, giving predicted lines of the *Fe* II spectrum arising from combinations of known terms.

Table 1 contains the observed wave lengths and identifications of some 400 lines in υ Sgr. The first column gives the wave length, with a colon if uncertain. The intensities in the second column, I, are based on an arbitrary scale and are the means of four estimates on three plates. Lines of intensity 0 are doubtful; those of intensity 0–1 are fairly certain; and those of 1–0 are quite certain. Diffuse or blended lines are marked "n"; extremely diffuse, "nn"; double, "d"; blended on red or violet side, "nr" or "nv." The element is given in the third column, with laboratory wave length and intensity following. Uncertain identifications are in parentheses. The symbol "pr" denotes a predicted line, with the solar intensity in parentheses. The symbol π denotes predicted lines of *Fe* II, most of which have not been observed in the sun. Plaskett has found that the stronger hydrogen lines sometimes have components at -150, -200, and -300 km/sec. These are marked "*H* comp" in the table, where suspected. The relative contributions of various elements to a line have been estimated by means of the relation between laboratory intensities and stellar intensities of unblended lines. All known contributors which may give at least 25 per cent of the intensity of a line are listed. Lines which are too weak for their laboratory intensity are marked "wk"; too strong, "str." If it is probable that an unknown line contributes to the observed line, a question mark is added. If the major contributor is unknown, the double question marks (??) are given. If other known, but weaker, lines contribute to the observed line, the symbol plus (+) is used. In the last column, δI, is given a set of estimates on an arbitrary scale of the increase (or decrease) of intensity of the line, with respect to its intensity in α Cyg. Excellent plates of the latter were kindly supplied by Dr. Struve; they were taken on the same emulsion and given the same type of development. The δI is given only when well established; but if a line has no δI, it may be assumed generally to be enhanced, since some care was taken to find those lines that were weakened in υ Sgr.

TABLE 1

LINES IN THE ULTRAVIOLET SPECTRUM OF υ SAGITTARII

λ	I	Element	λ	I	Notes	δI	λ	I	Element	λ	I	Notes	δI
3317.93	3	*Ti* II	8.03	10	.....	.....	3358.43	6	*Cr* II	8.50	75	+	.....
3319.35	0–1	*Ti* II	9.08	1	.....	.....			*Fe* II	8.25	3	.....	.....
3321.60	5	*Ti* II	1.71	25	.....	.....	3360.23	5	*Cr* II	0.30	100	.....	.....
		V II	1.54	150	.....	.....			*Fe* II	0.10	3	.....	.....
3322.96	7	*Fe* II	3.07	8	+	.....	3361.46	7	*Ti* II	1.19	125	+	.....
		Ti II	2.93	75	.....	.....			*Cr* II	1.77	20	.....	.....
3324.42	6 nd	*Cr* II	4.05	20	+	.....	3362.80:	1 nn	*Cr* II	3.71	6	.....	.....
		Cr II	4.34	12	.....	.....			*Ti* II	2.65	1	.....	.....
		Fe II	5.01	1	.....	.....	3365.47	2 nn	*Ti* II	6.18	8	.....	.....
3326.74	3	*Ti* II	6.78	20	.....	.....			*Fe* II	5.41	1	.....	.....
3328.28	2	*Cr* II	8.35	12	.....	.....			*Fe* II	4.23	(−1)	pr	.....
3329.36	3	*Ti* II	9.47	70	.....	.....	3367.06	1 nn	*Fe* II	6.96	3	.....	.....
		Fe II	9.07	2	.....	.....			*Cr* II	7.42	10	.....	.....
3330.72	1–0	*Mn* II	0.81	3	.....	.....	3368.14	3 nn	*Cr* II	8.05	150	+	.....
									Fe II	8.63	0	.....	.....
3332.11	2	*Ti* II	2.11	30	.....	.....	3369.30	4 nn	*Cr* II	9.05	12	+	.....
									Fe II	9.35	3	.....	.....
3333.02	2	*Si* II	3.16	2	str	.....	3371.00	3	*Co* II	0.98	50	.....	.....
3335.29	6 n	*Ti* II	{5.22 5.17}	40	.....	.....	3372.64	5 n	*Ti* II	{2.77 2.86}	100	.....	.....
		Cr II	5.28	30	.....	.....			*Cr* II	2.13	10	.....	.....
		Cr II	5.17	20	.....	.....	3374.09	4	*Ni* II	3.98	4	.....	.....
3336.13	5 n	*Cr* II	6.33	35	.....	.....			*Ti* II	4.35	8	.....	.....
3337.52	2	*V* II	7.84	200	.....	.....	3374.99	1	*Cr* II	4.99	3	.....	.....
		Ti II	7.85	2	.....	.....	3376.38	3 n	*Cr* II	6.27	5	.....	.....
3338.59	2	*Fe* II	8.52	3	.....	.....			*Cr* II	6.72	3	.....	.....
									(*A* II	6.46	7)	.....	.....
3340.01	5 n	*Cr* II	9.80	50	+	.....	3378.31	2	*Cr* II	8.34	20	.....	.....
		Ti II	0.33	40	.....	.....							
		Si II	9.84	3	.....	.....	3379.79	8 n	*Cr* II	9.82	60	.....	.....
3342.09	4 nr	*Ti* II	1.84	150	.....	.....			*Cr* II	9.37	25	.....	.....
3342.59	4 nv	*Cr* II	2.51	50	.....	.....			*Ti* II	{0.26 0.31}	30	.....	.....
3343.68	2	*Ti* II	3.78	10	.....	.....	3381.16	4	*Fe* II	1.00	4	.....	.....
3346.79	2	*Ti* II	6.75	15	.....	.....	3382.62	4	*Cr* II	2.68	60	.....	+1
3347.90	3	*Cr* II	7.83	30	.....	.....	3383.78	4	*Ti* II	3.77	125	.....	=
3349.22	7 n	*Ti* II	{9.39 9.47}	125	+	.....	3386.51	1	*Fe* II	6.72	2	+	.....
		Ti II	9.00	75	.....	.....	3387.82	8 n	*Ti* II	7.85	50	+	+1
									Co II	7.72	60	.....	.....
3350.43	4	*Ni* II	0.41	5	.....	.....			*Co* II	8.18	50	.....	.....
									Fe II	8.13	2	.....	.....
3351.98:	1 nn	*Ti* II	2.07	5	+	.....	3389.96	2 n	*Ti* II	8.76	8	.....	+2
		(*Fe* II	1.90	π)	.....	.....			*Fe* II	0.08	2	.....	.....
3353.07:	3	*Cr* II	3.12	18	.....	.....	3391.40	4	*Cr* II	1.42	100	.....	+2
		Co II	2.83	30	.....	.....							
3354.45:	1 n	*Ti* II	4.64	60	.....	.....	3392.96	1	*Cr* II	3.00	25	.....	+1
		He I	4.52	.....	.....	.....							
3356.26	3 n	*Fe* II	6.27	2	?	.....	3394.19	7 n	*Cr* II	4.32	30	.....	+1
									Cr II	3.86	30	.....	.....
3357.52	4	*Cr* II	7.40	4	str, ?	.....			*Ti* II	4.55	40	.....	.....

TABLE 1—*Continued*

λ	*I*	Element	λ	*I*	Notes	δ*I*	λ	*I*	Element	λ	*I*	Notes	δ*I*
3395.40	3	*Fe* II	5.34	4	.....	+3	3444.07	7 n	*Ti* II	4.33	30	+, str	+2
		Cr II	5.02	15	.....	.....			*Fe* II	3.83	π	.....	.....
3396.58:	0–1	(*Lu* II	7.06	150)	?	.....	3445.48	0–1	*S* II	5.44	6	.....	.....
3398.07	5 n	*Fe* II	8.36	4	.....	+4			*Cr* II	5.06	2	.....	.....
		Ni II	7.84	1	.....	.....			*Fe* II	5.55	π	.....	.....
3399.75	2 n	*Cr* II	9.54	10	.....	+3	3446.39	2	*Co* II	6.40	100	.....	.....
		Mn II	0.16	2	.....	.....	3447.63	2 nn	*He* I	7.59	.....	?	+2
3401.95	6 n	*Cr* II	2.43	20	.....	+5	3448.39:	0–1	*Fe* II	8.43	1	.....	.....
		Ni II	1.77	2	.....	.....	3449.41	1	(*Cr* II	9.28	1)	??	+2
		Ti II	2.42	8	.....	.....							
3403.28	4	*Cr* II	3.32	100	.....	=, −	3451.25	4	*Fe* II	1.23	2	+	+4
3405.22	0–1	*Ti* II	4.97	1	.....	.....			*Fe* II	1.32	2	.....	.....
									Cr II	0.84	3	.....	.....
3407.14	6 n	*Ni* II	7.32	8	.....	+3	3452.38	0–1	*Ti* II	2.48	4	.....	.....
		Ti II	7.21	3	.....	.....							
3408.80	5	*Cr* II	8.77	150	.....	=, −	3454.09	5 n	*Ni* II	4.17	5	.....	+4
									Fe II	3.60	2	.....	.....
3410.16	0–1	*Ti* II	9.82	4	.....	.....	3455.01	1 nv	*Cr* II	4.98	25	.....	.....
3414.11	2 n	*Fe* II	4.14	2	.....	+2	3456.72	6 nr	*Fe* II	6.93	5	.....	+3
									Ti II	6.40	20	.....	.....
3415.94	4	*Fe* II	6.02	5	.....	+2							
		Co II	5.79	75	.....	.....	3457.74	3 nv	*Cr* II	7.62	25	.....	.....
									V II	7.15	300	.....	.....
3417.36:	0–1	*Ti* II	6.96	2	.....	.....							
		Fe II	8.03	π	.....	.....	3459.27	1	*Cr* II	9.29	18	.....	+2
3419.44	1	*Fe* II	0.18	0	?	+2	3460.24	6	*Mn* II	0.33	20	+	+1
		(*P* II	9.25	6)	.....	.....			*Mn* II	0.04	2	.....	.....
3421.29	4	*Cr* II	1.20	75	.....	−2	3461.56	3	*Ti* II	1.50	20	+	+1
3422.76	4	*Cr* II	2.74	125	.....	−2	3462.78	1	*Cr* II	2.73	4	.....	+
3423.91	3 n	*Co* II	3.84	75	.....	+3	3464.29	5 n	*Fe* II	4.50	3	+	+5
		Fe II	4.17	(−1)	pr	.....			*Fe* II	3.97	1	.....	.....
3425.59	3 n	*Fe* II	5.58	3	.....	+2	3465.70	4	*Ti* II	5.65	3	.....	+2
									Ni II	5.65	1	.....	.....
3426.91:	0–1	*Fe* II	6.82	(−3)	pr	.....			*Fe* I	5.88	60	.....	.....
									He I	5.89	.....	.....	.....
3428.60	4 n	*Al* II	8.92	6	.....	+4							
		Cr II	8.94	6	.....	.....	3466.85	2	*Cr* II	7.14	.....	+	+2
		Fe II	8.63	(−2)	pr	.....			*Fe* II	6.86	1	.....	.....
3430.52:	0	*Cr* II	0.42	2	+	.....	3468.68	5	*Fe* II	8.68	8	.....	+2
3432.01:	0–1	.....	.....	.....	??	.....	3470.15	1	*Fe* II	0.24	1	.....	+2
3433.45	5 nr	*Cr* II	3.30	75	.....	−	3471.51	6 nr	*Ni* II	1.35	2	str, ?	+4
									He I	1.78	.....	.....	.....
3433.99	3 nv	*Fe* II	4.31	π	?	+							
							3472.00:	1 n	*Cr* II	2.07	15	.....	+2
3436.13	5	*Fe* II	6.11	5	.....	+2			(*Lu* II	2.46	120)	.....	.....
3437.73:	0–1	*Cr* II	7.92	2	.....	.....	3474.02	6	*Mn* II	4.15	8	.....	−1
									Mn II	4.06	8	.....	.....
3438.97	2	*Mn* II	8.96	3	.....	.....			*Fe* II	3.82	2	.....	.....
3440.55	1–0	*Fe* I	0.63	150	wk	.....	3475.52	4 n	*Cr* II	5.13	10	+	+2
		Fe I	1.02	75	.....	.....			*Fe* II	5.74	1	.....	.....
		Fe II	0.25	π	.....	.....							
							3477.16	3	*Ti* II	7.19	15	.....	+1
3442.11	9	*Mn* II	1.98	30	.....	−1							
		Fe II	2.24	3	.....	.....							

TABLE 1—*Continued*

λ	*I*	Element	λ	*I*	Notes	δ*I*	λ	*I*	Element	λ	*I*	Notes	δ*I*
3478.58	2 n	*Fe* II	8.60	π	.....	+3	3517.27	3	*V* II	7.30	800	.....	+2
		He I	8.95	.....	.....	.....			*He* I	7.33	.....	.....	.....
		Cr II	8.17	2	.....	.....	3518.65	1 n	*Cr* II	8.65	2	?	+2
3479.90	2	*Fe* II	9.91	2	.....	+3	3520.14	4 n	*Ti* II	0.26	20	.....	+3
3481.61	1–0	*Fe* II	1.92	(−2)	pr	.....			*V* II	0.02	120	.....	.....
3482.78	8	*Mn* II	2.91	12	+	+1	3521.69	4 n	*Cr* II	2.15	7	.....	+3
		Fe II	2.43	2	.....	.....			*V* II	1.84	90	.....	.....
									Fe II	1.67	π	.....	.....
3484.14	3	*Cr* II	4.15	10	.....	+3			*Fe* II	2.11	(−3)	pr	.....
		Fe II	4.35	1	.....	.....	3523.45	2	.....	.....	.....	??	+2
3485.78	3 n	*V* II	5.92	250	.....	+3	3524.67	1	*V* II	4.71	200	.....	+2
		Fe II	5.73	1	.....	.....			(*Ni* I	4.54	200)	.....	.....
3488.53	10 nn	*Mn* II	8.68	10	.....	+	3526.36	8	.....	.....	.....	??	+6
		Fe II	7.99	3	.....	.....							
		Ti II	9.75	2	.....	.....	3530.57	4 nv	*V* II	0.76	500	.....	+5
		He I	7.72	.....	.....	.....			*He* I	0.50	.....	.....	.....
3490.92	5 n	*Ti* II	1.06	10	.....	+3	3531.75	1–0	(*Fe* II	1.59	π)	.....	.....
		He I	0.62	.....	.....	.....			(*Mn* I	2.00	130)	.....	.....
		Fe I	0.60	100	.....	.....							
3492.23	1–0	*Mn* II	2.29	2	.....	.....	3532.60	2	*Fe* II	2.65	2	.....	+3
3493.44	5	*Fe* II	3.47	10	.....	+2	3533.85	1	*Ti* II	3.86	2	.....	.....
		V II	3.16	150	.....	.....	3535.50	8	*Ti* II	5.41	40	.....	+5
3494.67	2	*Fe* II	4.67	5	.....	+2			*Fe* II	5.63	2	.....	.....
									Mg II	5.04	5	.....	.....
3495.70	4 n	*Fe* II	5.62	4	.....	+2	3536.69:	1	*He* I	6.81	.....	+	.....
		Mn II	5.84	7	.....	.....			*Fe* II	7.50	1	.....	.....
		Cr II	5.37	15	.....	.....							
3496.93	1 nr	*Mn* II	6.81	3	.....	.....	3538.67	2 n	*Mg* II	8.86	6	+	.....
		V II	7.03	200	.....	.....			*Cr* II	9.00	3	.....	.....
3497.69	4 nv	*Mn* II	7.53	6	.....	+3	3540.02	1	*Fe* II	9.55	3	.....	.....
		Fe II	7.72	3	.....	.....							
3498.63:	1–0	*He* I	8.63	.....	.....	.....	3541.26	1 n	*V* II	1.34	50	?	.....
							3543.24	3 n	*Fe* II	3.45	π	.....	.....
3500.00	3	*Fe* II	9.88	4	.....	+3							
							3545.10	4	*V* II	5.19	1000	.....	+3
3501.69	3	*Co* II	1.73	200	.....	+4			*Co* II	5.05	25	.....	.....
		He I	2.32	.....	.....	.....							
							3546.99	0–1	*Cr* II	7.12	3	.....	.....
3503.38	2	*Fe* II	3.47	2	.....	+3			*Fe* II	6.40	2	.....	.....
		Cr II	3.38	3	.....	.....							
							3548.00	3 n	*A* II	8.51	7	.....	+4
3504.79	5	*Ti* II	(4.88	80	.....	+3				(7.80			
			4.92)						*Mn* I	(8.03	110	.....	.....
		V II	4.43	400	.....	.....				8.19)			
									Fe II	8.55	π	.....	.....
3507.63	6 nr	*Fe* II	7.39	3	?	+8							
							3549.52	1–0	*S* II	9.85	4	+	.....
3508.26	5 nv	*Fe* II	8.21	1	??	.....			*Mg* II	9.61	4	.....	.....
3509.85	1	*Ti* II	9.85	3	.....	+1	3550.87:	0	.....	.....	.....	??	.....
3510.89	2	*Ti* II	0.85	60	.....	+2	3551.70	2	.....	.....	.....	??	.....
3511.98	1	*Cr* II	1.84	30	.....	=, +	3553.45	2 nr	*Mg* II	3.51	5	.....	.....
3512.82	1–0	*Cr* II	3.05	10	.....	=, +	3554.43	5 nv	*He* I	4.51	.....	.....	+5
		He I	2.50	.....	.....	.....			*Fe* II	5.08	(0)	pr	.....
									Fe II	4.50	1	.....	.....
3514.02	4	*Ni* II	3.94	8	.....	=			(*Lu* II	4.45	200)	.....	.....
3515.95	2 nn	*Fe* II	5.82	2	.....	+1	3556.86	3	*V* II	6.80	1500	.....	+2
		(*Ni* I	5.07	150)	.....	.....							

TABLE 1—*Continued*

λ	*I*	Element	λ	*I*	Notes	δ*I*
3557.44	1 nv	*Fe* II	7.55	2	.....	.....
3558.55:	0	*Fe* I	8.53	30	.....	.....
3559.38	0	*Fe* II	9.40	π	.....	.....
3560.30:	1 nr	*V* II	0.59	90	.....	.....
3561.22	4 nv	*Ti* II	1.58	3	?	+5
3562.96	1	*He* I	2.98	.....	.....	.....
3564.51	3	*Fe* II	4.52	3	.....	+3
3566.13	4	*Fe* II	6.16	3	.....	+3
		Fe II	6.05	2	.....	.....
		Ti II	5.97	6	.....	.....
		V II	6.18	200	.....	.....
3567.28:	0	*S* II	7.16	3	.....	.....
		Sc II	7.72	20	.....	.....
3568.94	2	(*Fe* II	8.95	π)	.....	+2
		Fe II	8.87	π	.....	.....
3570.24	1	*Fe* I	0.14	100	.....	=, −
		Mn I	0.05, 9.82, 9.51	120	.....	.....
3572.53	2	*Sc* II	2.48, 2.57	50	.....	=, +
3573.72	3	*Ti* II	3.74	20	.....	+1
3575.19	3	*Fe* II	5.27	π	.....	+3
3576.72	9	*Ni* II	6.76	3	str, ?	+4
		A II	6.62	10	.....	.....
		Sc II	6.33, 6.39	30	.....	.....
3578.04	2	*Co* II	8.00	30	.....	+2
		(*Mn* I	7.88	40)	.....	.....
		Cr I	8.69	200	.....	.....
3579.78	0–1	*Fe* II	9.66	π	.....	+
3581.05	3	*Fe* I	1.21	250	str, ?	−1
3583.81	1	*Fe* II	3.55	π	.....	.....
3585.47	15	*Cr* II	5.43	100	str	+3
3586.98	25	*He* I	7.35	.....	str	+15
		Ti II	7.15	12	.....	.....
		Al II	6.55	9	.....	.....
		Al II	7.06	8	.....	.....
		Al II	7.44	7	.....	.....
3589.66	3	*V* II	9.75	1000	.....	+2
3590.72:	0–1	(*C* II	0.87	2)	?	.....
3591.99	2	*V* II	2.01	800	.....	+2
3593.37	2	*V* II	3.32	600	.....	+2
		Ti II	3.08	2	.....	.....
3594.69	1 n	*S* II	4.45	3	str	+1
3596.10	3	*Ti* II	6.06	60	.....	+2
3597.65	2	*Fe* II	7.66	π	?	+2
3599.25	1	*He* I	9.39	.....	.....	+3
3601.45	2 nn	*Si* II	1.52	2	.....	.....
		(*V* II	0.74	300)	.....	.....
3602.56:	1–0	*Fe* II	2.61	π	.....	.....
3603.78	7	*Cr* II	3.64	15	.....	+3
		Cr II	3.80	30	.....	.....
		Cr II	3.86	10	.....	.....
3605.91	2 nr	*Fe* II	6.17	π	.....	+2
		Cr I	5.34	140	.....	.....
3606.98	1 nv	*Fe* II	7.07	π	.....	.....
3608.77	6	*Fe* II	8.49	π	?	+4
		Cr II	8.66	3	.....	.....
		Fe I	8.87	100	.....	.....
3610.28	3 n	*Fe* II	0.33	π	.....	+3
		(*Y* II	1.05	200)	.....	.....
3611.95	0–1	.....	.....	.....	??	.....
3613.46	8 n	*Cr* II	3.21	20	+	+4
		He I	3.64	.....	.....	.....
		S II	3.1	5	.....	.....
		Sc II	3.88, 3.81	100	.....	.....
3614.91	4	*Fe* II	4.87	5	.....	+3
3617.13	2 nn	*Cr* II	7.32	5	.....	+2
		S II	6.90	4	.....	.....
3619.15	2 nn	*V* II	8.92	200	.....	=, +
		Fe I	8.78	125	.....	.....
		Ni I	9.40	150	.....	.....
3621.25	7	*Fe* II	1.27	6	.....	+3
		Co II	1.20	100	.....	.....
3623.12	1 n	*Fe* II	2.82	π	+	+2
3624.85	6	*Ti* II	4.84	70	+	+3
		Fe II	4.89	5	.....	.....
3627.27	4 n	*Fe* II	7.17	1	??	+4
		V II	7.71	60	.....	.....
3631.76	12 n	*Cr* II	1.49	50	+	+2
		Cr II	1.72	25	.....	.....
		Fe II	2.29	3	.....	.....
		Sc II	0.75	100	.....	.....
3634.15	9 n	*He* I	4.30	.....	.....	+7
		Fe II	4.89	5	.....	.....
3636.68	1 n	*Fe* II	6.61	π	.....	+3
		Fe II	6.89	π	.....	.....
3638.58	2 nr	*Fe* II	8.88	π	?	.....
3639.45:	1–0 nv	*A* II	9.85	7	.....	.....
3641.33	4	*Ti* II	1.34	100	.....	+3
3643.11	4 n	*Cr* II	3.22	8	.....	+3
		Sc II	2.78, 2.83	50	.....	.....

TABLE 1—*Continued*

λ	*I*	Element	λ	*I*	Notes	δ*I*	λ	*I*	Element	λ	*I*	Notes	δ*I*
3644.56	1 nr	*Cr* II	4.70	8	.....	+	3696.52	2 nn	*Cr* II	6.78	5	.....	.....
									H	7.15	.....	*H*17	.....
3645.29	1–0 nv	*Sc* II	(5.29	15	.....	.....	3698.02	3	*Cr* II	8.00	15	.....	+
			5.34)										
3647.56	2 nn	*Cr* II	7.40	5	.....	+3	3700.13	1	*V* II	0.34	200	.....	+
		Fe I	7.85	100	.....	.....			*Fe* II	9.91	(−2)	pr	.....
3650.14	4 n	*Cr* II	0.37	20	.....	+4	3701.56	1–0 nn	*Cr* II	1.90	2	.....	.....
3651.79	4 n	*He* I	2.06	.....	.....	+4	3703.90	1	*H*	3.86	.....	*H*16	−15
		Cr II	1.68	8	.....	.....							
		Sc II	1.80	20	.....	.....	3704.96	3 n	*He* I	5.07	.....	.....	+3
									Fe I	5.58	100	.....	.....
3653.61:	0	(*Fe* II	2.75	1)	.....	.....	3706.11	4	*Ca* II	6.04	10	.....	−1
		(*Ti* I	3.50	100)	.....	.....			*Ti* II	6.22	20	.....	.....
3655.07	2	*Al* II	4.99	12	.....	+2	3708.11	1	(*Fe* I	7.83	20)	??	+
3656.70	1 n	*Fe* II	6.79	π	.....	+2	3710.11	1	*Fe* II	0.14	π	.....	+
		Fe II	6.50	π	.....	.....			(*V* II	0.29	500)	.....	.....
3658.15	2	*Cr* II	8.19	12	.....	+2	3711.98	2 n	*H*	1.97	.....	*H*15	−15
3659.72	2	*Ti* II	9.76	60	.....	+1			*Fe* II	1.97	1	.....	.....
3661.01	1–0	*V* II	1.38	200	+	.....	3713.00	5 n	*Cr* II	2.97	40	.....	.....
3662.33	2 n	*Ti* II	2.24	40	.....	+2	3715.26	6	*V* II	5.48	1200	.....	.....
3664.93	3	*Cr* II	4.95	20	.....	+3			*Cr* II	5.45	18	.....	=, +
3667.05	1	.....	.....	.....	??	.....	3717.47	1 nn	*V* II	8.16	60	?	.....
3669.20	4 n	*V* II	9.41	300	.....	+3	3720.16	2 n	*Fe* II	0.17	(0)	pr	+
		S II	9.03	4	.....	.....			*Fe* I	9.95	250	.....	.....
3670.77:	0	.....	.....	.....	??	.....	3721.74	3	*Ti* II	1.64	15	.....	−15
									H	1.94	.....	*H*14	.....
3672.07	1	*S* II	2.11	1	.....	.....	3723.47	1	*Fe* II	3.91	(−1)	pr	+
		(*H*	1.48	.....	*H*24)	.....			*Cr* II	3.40	7	.....	.....
3673.59	0–1	*Fe* II	3.35	π	+	.....	3725.26	3	*Fe* II	5.30	3	.....	+2
		(*H*	3.76	.....	*H*23)	.....	3727.15	4	*V* II	7.35	1000	.....	+2
3674.91:	0–1	*Cr* II	5.00	(−3)	pr	.....			*Fe* II	7.03	(0)	pr	.....
									Cr II	7.37	10	.....	.....
3676.42	1–0	*H*	6.36	.....	*H*22	−15	3728.54:	0	*V* II	8.34	200	.....	+
3677.82	8	*Cr* II	7.86	30	.....	+4	3730.67	1 nn	.....	.....	.....	??	.....
		Cr II	7.69	20	.....	.....	3732.82	3	*He* I	2.92	.....	.....	+3
		Cr II	7.93	10	.....	.....			*V* II	2.76	800	.....	.....
3679.67	1	*Ti* II	9.69	(2)	pr	−15	3734.64	2 n	*H*	4.37	.....	*H*13	−15
		H	9.36	.....	*H*21	.....			*Fe* I	4.88	300	.....	.....
3681.25	1	*Fe* II	0.99	π	.....	+2	3737.00	5	*Ca* II	6.92	11	+	−1
3682.64	0–1	*Fe* II	2.67	(0)	pr	−15			*Fe* I	7.14	150	.....	.....
		H	2.81	.....	*H*20	.....	3738.21	4	*Cr* II	8.38	15	.....	+2
3684.15	1–0	*Cr* II	4.25	15	.....	.....	3741.62	5	*Ti* II	1.65	50	.....	=, +
3685.20	6	*Ti* II	5.20	250	.....	−2			*Fe* II	1.55	(0)	pr	.....
3686.51	3 n	*Cr* II	6.67	12	.....	−15	3743.59	3 n	*Fe* II	2.94	π	?	+1
		H	6.83	.....	*H*19	.....							
3691.46	1–0 n	*H*	1.56	.....	*H*18	−15	3746.22	7 nn	*V* II	5.81	800	.....	+2
									Fe II	5.36	(2)	pr	.....
3693.10:	0–1	.....	.....	.....	??	.....			*Fe* II	6.56	1	.....	.....
									Fe I	5.58	100	.....	.....
3695.64:	0–1	*Cr* II	4.98	2	.....	.....							
		(*Fe* II	6.10	π)	.....	.....							

TABLE 1—*Continued*

λ	*I*	Element	λ	*I*	Notes	δ*I*
3748.41	7	*Ti* II	8.00	10	.....	+1
		Fe II	8.49	8	.....	.....
		Cr II	8.68	5	.....	.....
3750.35	6 nn	*H*	0.15	.....	*H*12	−10
		V II	0.88	600	.....	.....
		Fe I	9.50	200	.....	.....
3753.13:	0–1	.....	.....	.....	??	.....
3754.81	3 nr	*Cr* II	4.58	2:	?	+2
3755.61	3 nv	*Fe* II	5.56	4	.....	+4
		He	6.09	.....	.....	.....
3757.79	2	*Ti* II	7.69	30	.....	−1
		Fe I	8.25	150	.....	.....
3759.39	5	*Ti* II	9.30	200	.....	−1
		Fe II	9.46	6	.....	.....
3761.48	7	*Ti* II	1.32	200	+	−1
		Cr II	1.90	4	.....	.....
		Cr II	1.69	4	.....	.....
3763.03	2	*Fe* II	2.89	5	.....	+2
3763.94	3	*Fe* II	4.11	3	.....	+1
3765.49	1	*Cr* II	5.62	8	.....	+2
3767.23:	0 n	*Cr* II	6.65	2	.....	.....
		Fe I	7.21	80	.....	.....
3769.36	8	*Ni* II	9.47	5	str	+
		He I	8.80	.....	.....	.....
3770.73	4	*H*	0.63	.....	*H*11	−12
		He I	0.57	.....	.....	.....
		V II	0.97	400	.....	.....
3773.94:	1 nn	*V* II	2.96	80	.....	.....
		(*V* II	4.34	300)	.....	.....
3776.07	2	*Ti* II	6.06	6	.....	=, +
3778.40	2	*V* II	8.36	100	str	+2
3779.66	2	*Fe* II	9.57	(0)	pr	+2
3781.41	2	*Fe* II	1.51	1	.....	+3
3783.35	4	*Fe* II	3.35	4	+	+2
3784.79	1	*He* I	4.88	.....	.....	+3
3786.45	1	*Ti* II	6.33	.....	pr	+
		(*Fe* II	6.41	*r*)	.....	.....
3787.75	1–0	*He* I	7.49	.....	.....	+
		V II	7.24	150	.....	.....
3792.00:	1 nn	.....	.....	.....	d, ??	.....
3795.24	2 nn	*Fe* I	5.01	60	?	+
		(*H*	4.10	.....	comp)	.....
3796.66:	0	*Ti* II	6.89	2	.....	+
3798.12	13	*H*	7.90	.....	*H*10, ?	−10
		Fe II	8.60	*r*	.....	.....
		Fe II	8.40	*r*	.....	.....
3801.37	1–0	.....	.....	.....	??	+1
3805.70	5 n	*He* I	5.75	.....	?	+5
		(*Fe* II	5.57	*r*)	.....	.....
3806.91	1 n	*Fe* II	6.82	*r*	.....	+
3809.48	2	*He* I	9.17	.....	+	+3
		A II	9.49	7	.....	.....
3811.88	1–0	.....	.....	.....	??	+
3814.15	7	*Fe* II	4.12	4	str, ?	+4
		Ti II	4.60	4	.....	.....
3815.78	1	*V* II	5.38	200	.....	−1
		Fe I	5.85	100	.....	.....
3817.35	1	.....	.....	.....	??	+
3819.67	10 n	*He* I	9.68	.....	str, ?	+6
3821.99	3	*Fe* II	1.97	(0)	pr	+2
		Fe II	2.74	3	.....	.....
3824.87	4	*Fe* II	4.91	4	.....	+2
3827.18	4	*Fe* II	7.08	4	.....	+3
		Fe II	7.69	(1)	pr	.....
3830.51:	2 nn	(*N* II	9.80	3)	??	−
		(*Mg* I	9.37	40)	.....	.....
3833.44	5 nn	*He* I	3.56	.....	.....	+1
		(*H*	3.45	.....	comp)	.....
		Fe II	3.02	(0)	pr	.....
		(*Mg* I	2.31	80)	.....	.....
3835.26	8 n	*H*	5.39	.....	*H*9, ?	−15
3838.22	2	*He* I	8.09	.....	.....	−3
		Fe II	8.04	2	.....	.....
		(*Mg* I	8.30	100)	.....	.....
3841.06:	0–1	*Fe* II	1.36	(−1)	pr	−
		Fe I	1.06	80	.....	.....
3843.12:	0	*Mn* II	2.98	1	.....	+
3844.98	6	*Fe* II	5.18	3	?	+4
3848.25	2	*V* II	7.32	100	.....	+2
		Mg II	8.24	7	.....	.....
3849.93	6 nr	*Mg* II	0.40	6	str	+3
		Si II	0.91	3	.....	.....
		A II	0.57	15	.....	.....
3853.56	8	*Si* II	3.66	3	str	+4
		Si II	3.08	2	.....	.....
3855.99	11	*Si* II	6.02	8	.....	+2
3860.17	2 n	*Fe* II	0.11	(0)	pr	+1
		Fe II	0.92	3	.....	.....
		Fe I	9.92	300	.....	.....
3862.57	9	*Si* II	2.59	6	.....	+3
3863.84	2	*Fe* II	3.41	1	.....	+2
		Fe II	3.95	1	.....	.....

TABLE 1—*Continued*

λ	*I*	Element	λ	*I*	Notes	δ*I*
3865.74	2	*Cr* II	5.59	20	+	+1
3867.39	3	*He* I	7.54	.....	.....	+4
3872.23	8 nn	*He* I	1.80	.....	.....	+4
		(*La* II	1.65	200)	.....	.....
		Fe II	2.98	π	.....	.....
		Fe II	2.77	2	.....	.....
3875.65	0–1	*Fe* II	5.69	π	.....	=, +
		(*C* II	6.19	4)	.....	.....
3878.52	4 nn	*He* I	8.18	.....	+	+2
		V II	8.72	300	.....	.....
		Fe I	8.58	100	.....	.....
3881.88	1 n	(*Fe* II	0.78	1)	?	=, +
3884.69	1	*Mn* II	3.28	3	.....	+1
		(*Fe* II	4.67	π)	.....	.....
		(*H*	5.10	.....	comp)	.....
3886.23:	0	(*La* II	6.33	150)	.....	+
		Fe I	6.30	40	.....	.....
		(*H*	6.40	.....	comp)	.....
3887.63	1–0	(*H*	7.10	.....	comp), ?	+
3888.87	15	*He* I	8.65	.....	.....	−10
		H	9.05	.....	*H*8	.....
3892.11	2	*Cr* II	2.14	2	.....	+3
		S II	2.28	5	.....	.....
3893.29:	0–1	.....	.....	.....	??	+
3894.53	1–0	*Fe* II	4.58	π	.....	.....
3896.14	1	*V* II	6.16	60	?	+
		Fe I	5.67	25	.....	.....
3898.47	3 nn	*V* II	9.14	200	.....	+
		Fe II	8.63	π	.....	.....
		Fe II	8.46	π	.....	.....
3900.53	5	*Al* II	0.66	10	.....	=
		Ti II	0.54	70	.....	.....
3903.38	3 nn	*V* II	3.27	250	.....	+1
		Fe II	3.79	π	.....	.....
		Fe II	3.82	π	.....	.....
3905.83	6	*Fe* II	6.04	5	.....	+3
		Cr II	5.64	18	.....	.....
3908.31	0–1	*Fe* II	8.55	π	.....	+
3911.45	2	*Fe* II	1.59	π	.....	+2
3913.47	9	*Ti* II	3.47	60	.....	=
3914.34	3	*Fe* II	4.48	2	.....	+2
		V II	4.33	250	.....	.....
3916.55	1	*V* II	6.42	200	.....	+
3918.49	3	*Mn* II	8.32	3	.....	+3
		(*C* II	8.98	6)	.....	.....
		Fe II	8.25	π	.....	.....
		Fe II	8.51	π	.....	.....
3920.51	2	*Fe* II	0.66	π	.....	+2
		(*C* II	0.68	8)	.....	.....
3923.55	1	*S* II	3.43	6	.....	+
3925.04:	0–1	.....	.....	.....	??	.....
3926.54	5 n	*He* I	6.53	.....	.....	+4
		Mn II	6.46	4	.....	.....
3927.90:	0	*Fe* I	7.94	30	.....	.....
3930.22	2	*Fe* II	0.32	π	?	+1
3931.94:	1–0	*Ti* II	2.02	2	.....	.....
		S II	1.90	5	.....	.....
3933.35	30	*Ca* II	3.68	400	.....	.....
3935.89	3	*He* I	5.91	.....	.....	+2
		Fe II	5.94	6	.....	.....
3938.56	7	*Fe* II	8.97	4	.....	+3
		Fe II	8.29	2	.....	.....
3942.18	1	.....	.....	.....	??	+
3944.04	0–1	*Mn* II	3.82	1	.....	+
		A II	4.27	8	.....	.....
3945.12	2	*Fe* II	5.23	(1)	pr	+1
3947.20	0	*Fe* II	7.90	π	?	.....
3949.14	0–1	*Fe* II	8.83	π	.....	.....
		(*La* II	9.16	600)	.....	.....
		(*Y* II	0.36	200)	.....	.....
3952.13	1	*V* II	1.97	500	.....	+1
3954.27	2	(*O* II	4.37	7)	??	+2
3960.88	4	*Fe* II	0.90	3	.....	+1
3962.91	1–0	*S* II	3.09	2	.....	+
3964.61	4	*He* I	4.73	.....	.....	+3
3966.38	1	*Fe* II	6.45	π	.....	+
		(*H*	6.25	.....	comp)	.....
3968.37	17	*Ca* II	8.49	350	.....	.....
3969.72	11	*H*	0.08	.....	*H*7	−10
3972.24	0–1	*Fe* II	2.29	π	.....	+
3974.38	5 n	*V* II	3.64	300	.....	+2
		Fe II	4.16	3	.....	.....

A summary of the elements identified in the present investigation is given in Table 2. All elements possibly present were searched for, and absence from Table 2 means that the elements cannot be identified or that the evidence is not conclusive. Table 2 contains remarks on the nature of the identification and, in some cases, the laboratory intensity of the weakest lines, I'. The identifications of *A* II, *C* II, and *N* II depend essentially on the photographic region

TABLE 2

ELEMENTS IDENTIFIED IN υ SAGITTARII

Element	Remarks	Element	Remarks
H.....	*Hα* to *H*22	*Ti* II...	Strong, $I'=1$
He I....	2^1S-7^1P, 2^1P-14^1S, 2^1P-12^1D, 2^3S-3^3P, 2^3P-14^3S, 2^3P-15^3D	*V* II....	Moderate, $I'=75$
		Cr I....	Weak, $I'=300$
		Cr II...	Strong, $I'=2$
C II....	Possible, Morgan in blue	*Mn* I...	Possible, one line
N II....	Possible?, Morgan in blue	*Mn* II..	Strong, $I'=2$
O II....	Probably absent	*Fe* I....	Weak, $I'=30$
Ne I....	Merrill, in visual	*Fe* II...	Very strong
Mg I...	Possible, very weak	*Fe* III...	Probably absent
Mg II..	Strong, $I'=2$	*Co* II...	Strong, $I'=30$
Al II...	Strong	*Ni* II...	Strong, all lines
Si II...	Strong, $I'=2$	*Sr* II...	Possible?, Morgan in blue
P II....	Possible?, one line	*Y* II....	Doubtful
S II....	Strong, $I'=6$	*Zr* II...	Probably absent
A II....	Present, Morgan in blue	*La* II...	Weak, $I'=250$
Ca II...	Strong	*Lu*II ...	Doubtful
Sc II...	Weak, $I'=20$		

studied by Morgan;[6,7] *Ne* I depends on Merrill's report of the visual region.[8] There are few important or unexpected differences between the new identifications and those of Morgan. *Al* II and *V* II are strong in the ultraviolet region and were not found in the blue. The presence of neutral metallic elements, *Fe* I, *Cr* I, *Mn* I, and *Mg* I is definite.

The spectrum of *Fe* II is of particular interest. Using Dobbie's table of observed *Fe* II lines,[9] a large number of the laboratory lines, to $I' = 1$, were identified. The laboratory lines arise dominantly from the lower excited levels. In the low-pressure atmosphere of a supergiant a number of additional lines arising from excited

[8] *Pub. A.S.P.*, **51**, 218, 1939.

[9] *Ann. Solar Phys. Obs., Cambridge*, **5**, Part I, 1938.

levels may be expected. Of such predicted lines found in the solar spectrum with intensities greater than -2, most can be identified in υ Sgr. The table of Mrs. Moore-Sitterly gives predicted lines from still higher levels and has made possible the tentative identification of 80 lines. The lack of even rough guides to the expected intensity and the breakdown of the selection rules for *L-S* coupling make some of these identifications uncertain. A cursory investigation of the blue region of the spectrum suggests that these high-level transitions may contribute to perhaps 100 other lines. Some of the

TABLE 3

PREDICTED HIGH-LEVEL MULTIPLETS OF *Fe* II

λ'	λ	Designation	χ	I	Blends
3531.59.....	1.75	$c^2D_{3/2}-x^4F^\circ_{5/2}$	4.7 V	1–0	(*Mn* I)
3543.45.....	3.24	$D_{5/2}-F_{7/2}$	4.7	3 n	.....
3583.55.....	3.55	$a^2I_{11/2}-z^4G^\circ_{9/2}$	4.1	1	.....
3602.61.....	2.56:	$I_{13/2}-G_{11/2}$	4.1	1–0	.....
3607.07.....	6.98	$I_{11/2}-G_{11/2}$	4.1	1 nv	(*Fe* I)
3894.58.....	4.53	$z^4G^\circ_{5/2}-e^4F_{3/2}$	7.5	1–0	.....
3898.63.....	8.47	$G_{7/2}-F_{5/2}$	7.5	3 nn	*V* II, *Fe* II
3903.79.....	3.38	$G_{9/2}-F_{7/2}$	7.5	3 nn	*V* II, *Fe* II
3911.59.....	1.45	$G_{5/2}-F_{5/2}$	7.5	2	.....
3920.66 ...	0.51	$G_{11/2}-F_{9/2}$	7.5	2	(*C* II)
3948.83 ..	9.14	$G_{9/2}-F_{9/2}$	7.5	0–1	(*La* II, *Y* II)
3972.29 ...	2.24	$G_{7/2}-F_{9/2}$	7.5	0–1	.....

lines attain considerable intensity, reaching $I=3$ in υ Sgr. Table 3 lists three sample multiplets observed. The first column gives the predicted wave length, λ'; the next, the observed stellar wave length, λ; the third, the spectroscopic designation. The excitation potential, χ, follows in electron volts, V, with the observed intensity next. The last column suggests possible blends, which are given in parentheses if unimportant. The existence of lines arising from both normal and metastable levels is confirmed by the occurrence of these high-level lines, as well as by the *Fe* II lines observed in the laboratory.

The presence of high-excitation lines in the *Fe* II spectrum points to low pressure. The relative intensities of lines of a wide range of excitation could be used to determine the excitation temperature. A complete spectrophotometric analysis and a determination of the

curve of growth is required. A simple inspection of the available data, however, shows that the correlation of line intensity in the star and Rowland intensity in the sun is a function of excitation potential, χ. *Fe* II lines of solar intensity 0 to -2 have a mean intensity of $I = 1.4$ in υ Sgr for $\chi < 3.1$ V, $I = 2.1$ for $3.1 < \chi < 4.3$ V, and 2.8 for $\chi > 4.3$ V. There exist at least 11 lines with $\chi > 4.3$ V, and with stellar intensities greater than 1, which are absent in the sun. The excitation temperature is therefore a good deal higher than that of the sun.

The comparison with the supergiant A2 star, α Cyg, indicates that almost all lines are enhanced in υ Sgr. The visual estimates, δI, in Table 1 have been grouped by excitation potential to exhibit any possible systematic effects. Lines in the region of the strong continuous hydrogen absorption in α Cyg have been omitted. Table 4 gives the mean increase, δI, υ Sgr *minus* α Cyg, as a function of excitation potential, χ. The number of lines is given in parentheses. It is apparent that there is very little difference between the relative populations of the higher levels; the excitation temperatures should not differ by more than 1000°.

The metallic spectrum of υ Sgr resembles that of α Cyg rather closely. The identifications in Table 1 differ little from those by Struve in the latter star.[10] Almost all lines are stronger in υ Sgr, and more lines have been measured. Besides the obvious great relative strength in υ Sgr of lines to the violet of the Balmer series limit, shown by the prevalence of large positive δI's, a few interesting effects are obvious in Table 1. The mean δI for the *Fe* II spectrum is +2.2 for 33 lines, while for 25 lines of *Ti* II, *Cr* II, *Mn* II, and *Ca* II, δI is +0.9. *Sc* II and *Ca* II seem particularly weakened, probably because of their low ionization potential. Lines which arise in α Cyg from neutral elements are very definitely weaker in υ Sgr. As examples we may take λ 3570 of *Fe* I and *Mn* I, λ 3581 of *Fe* I and *Sc* II, λ 3816 of *Fe* I and *V* II, and the *Mg* I multiplet $\lambda\lambda$ 3829, 3832, and 3838. These lines are weakened in υ Sgr; since most lines of the ionized metals are strengthened, it is certain that the level of ionization is higher in υ Sgr. Certain other features of the metallic

[10] *Ap. J.*, **90**, 699, 1939.

PLATE IV

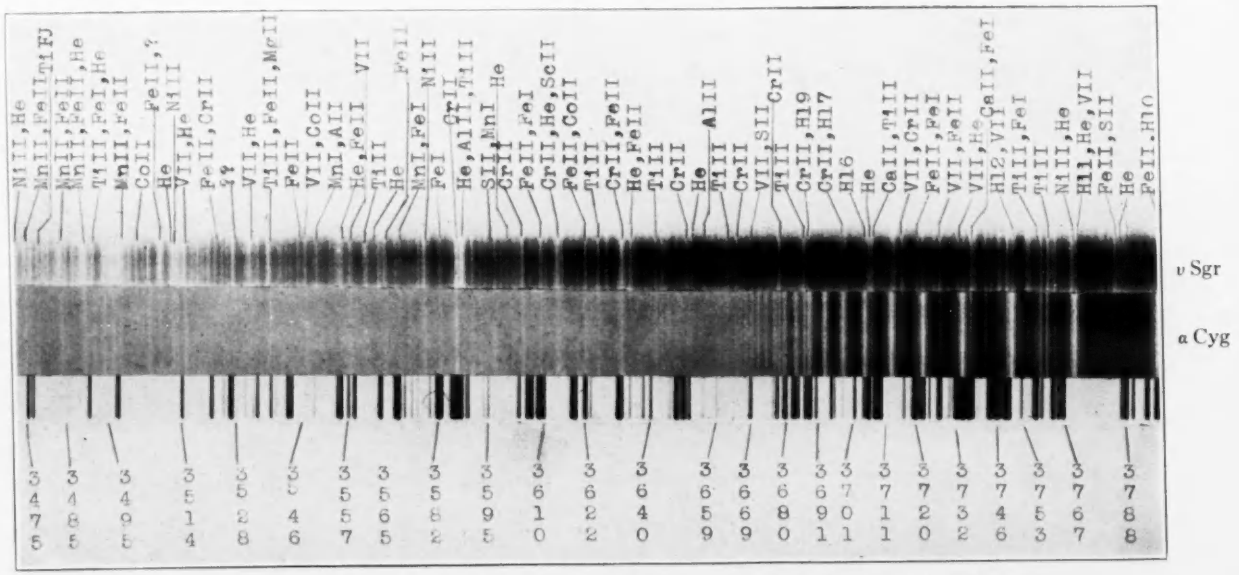

REPRODUCTIONS OF McDONALD OBSERVATORY SPECTROGRAMS OF υ SGR (*top*) AND α CYG (*bottom*)

The identifications of the lines refer to their appearance in υ Sgr. Rough wave lengths for the iron arc comparison spectrum are given below. The weakness of the Balmer continuous absorption in υ Sgr and the strength of the lines beyond the Balmer series limit are obvious by comparison with α Cyg. Eastman Process plates, developed under similar conditions, were used.

spectrum require a spectrophotometric analysis. For example, lines that are particularly strong in α Cyg seem actually to be weaker in υ Sgr. Such an effect may have its origin in the method of making the estimates of δI. For 25 *Ti* II, *Cr* II, and *Mn* II lines the δI is $+2$ for lines with intensity $\leqslant 1$ in α Cyg (Struve's estimates), $+1.3$ for $I = 2, 3, 4$, $+0.5$ for $I = 5, 6$, and -2 for $I = 7$. If this systematic effect is real, a difference in curve of growth is suggested, in the sense that the curve of growth is steeper in α Cyg. The other striking effects in the δI's in Table 1 are the obvious great increase in the strength of the helium lines in υ Sgr. The hydrogen lines are all very greatly weakened.

TABLE 4

INCREASE OF *Fe* II LINE INTENSITIES, δI
υ SGR *minus* α CYG

x	$I \leqslant 2$	$I = 3, 4$	$I \geqslant 5$	All
<3.1	1.5 (4)	2.0 (4)	.....	1.7 (8)
3.1–4.3	1.1 (7)	2.5 (2)	2.3 (3)	1.7 (12)
>4.3	1.4 (5)	3.0 (3)	2.7 (3)	2.2 (11)

The number of unidentified lines in Table 1 is not large, but not all identifications are completely satisfactory. The successful results obtained with the use of the theoretical wave lengths in the *Fe* II spectrum and the comparative incompleteness of laboratory data for excited levels of other common once-ionized metals suggest the need for further laboratory investigations of these spectra.

The hydrogen lines in the ultraviolet region are of particular interest and importance. The weakness of the hydrogen lines up to $H\epsilon$ had been noticed; but because of curve-of-growth phenomena the intensity of the lower members of the Balmer series is not a good criterion of the number of absorbing atoms. The hydrogen lines are sharp and show no Stark effect. The higher series members, while still sharp, become very weak and fade out long before they approach confluence. For example, $H16$ is of intensity $I = 1$; $H22$ is $I = 1$–0; $H23$ is $I = 0$–1; and the higher members are invisible. The region between these higher members is not obviously affected by any increase of the continuous absorption coefficient by

the overlapping wings of the lines. The weakness of the lines is obviously correlated with the lack of any detectable change of intensity of the continuous spectrum to the violet of the Balmer series limit at λ 3647. In Figure 1 is reproduced a microphotometer tracing of the ultraviolet region of the spectrum of υ Sgr. A jump corresponding to 0.2 mag. is indicated at the Balmer limit. The general level of the continuous spectrum is difficult to estimate, because of the number and strength of the lines; but it seems improbable that any discontinuity greater than 0.2 mag. is present. We must conclude that the actual number of hydrogen atoms in the second level is remarkably low. Struve and Sherman[11] have determined the decrease in the intensity of metallic lines in the region of Balmer continuous absorption for several A stars. υ Sgr shows the smallest decrease of any of the stars.

Some of the components of the hydrogen lines described by Plaskett[2] may exist as far as $H10$, although they seem very weak at this epoch. It may be profitable to consider their reality in the light of the new identifications of metallic lines. Plaskett finds that components appear at radial velocities of -300, -200, and -150 km/sec. Table 5 gives the wave lengths of the various components corresponding to these mean velocities, together with the observed wave lengths, and possible lines of other substances which might appreciably contribute to these lines. The last column suggests the importance of blending in the appearance of the component. On the basis of the evidence in Table 5, it seems probable that the component at -300 km/sec is present and that the one at -150 km/sec may possibly be present.

The helium spectrum is the most striking feature. The helium lines are very strong, and a comparison of the measured equivalent widths of some of the higher series members suggests that they are stronger than in any normal B star. Both the singlet and triplet series can be traced to about their fourteenth members. Because of the severe blending, it is difficult to make any definite estimate of relative population of the metastable triplet and normal singlet levels, but it is certain that there is no *large* overpopulation of the

[11] *Ap. J.*, this issue, p. 428.

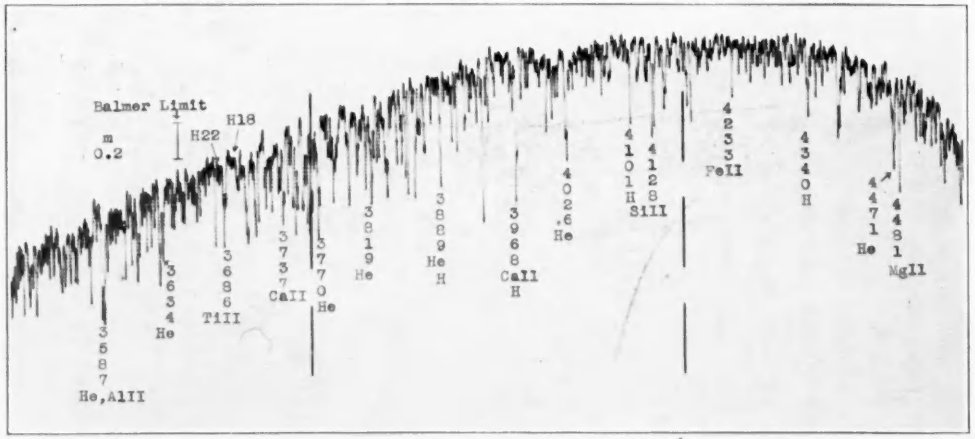

FIG. 1.—Microphotometer tracing of the spectrum of υ Sgr, with identifications of some of the stronger lines. Two weak lines are higher members of the Balmer series of hydrogen. The vertical bar at the Balmer series limit indicates the change in intensity corresponding to 0.2 mag.

triplet levels. The problem of the excitation and abundance of helium will be considered later, in detail.

THE STATE OF IONIZATION IN THE ATMOSPHERE OF υ SAGITTARII

In a spectrum of considerable variability it is rather dangerous to compute the ionization and the abundances of various elements.

TABLE 5

COMPONENTS OF THE HYDROGEN LINES*

λ′ Predicted	λ Obs.	Other Lines	I	Blending
4856.48.....	.....	6.20 (1) *Cr* II; 6.71 (π) *Fe* II	.....	Partial
4858.17.....	.....	7.96 (π) *Fe* II	.....	Partial
4858.98.....	.....	.....	.....	None
4336.14.....	.....	.....	.....	None
4337.46.....	.....	7.32 (1) *Ti* II; 7.76 (π) *Fe* II	.....	Partial
4338.10.....	.....	7.92 (50) *Ti* II; 8.70 (π) *Fe* II	.....	Dominant
4097.66.....	7.29	7.51 (1) *Fe* II	2	Partial
4099.75.....	9.97	*S* II, *Mn* II, weak	2	None
3966.25.....	6.38	6.45 (π) *Fe* II	1	Partial
3887.10.....	7.63	7.63 (15) *Fe* I	1–0	None
3886.40.....	6.23:	6.23 (40) *Fe* I; 6.33 (150) *La* II	0	Dominant
3885.10.....	4.69	4.67 (π) *Fe* II; 3.28 (3) *Mn* II	1	Partial
3833.45.....	3.44	3.56, *He* I; 3.02 (1) *Fe* II	5 nn	Dominant
3794.10.....	5.24	5.01 (60) *Fe* I	2 nn	Partial

*The data for $H\beta$ and $H\gamma$ are not given in Morgan's compilation.

At the present epoch, the spectrum observed seems to arise in one atmosphere—and, in fact, in an atmosphere which does not exhibit marked departures from thermodynamic equilibrium. $H\alpha$ is the only line in the spectrum which is certainly in emission. The absorption lines are sharp and deep and do not show rotation. Except for the weak components of the hydrogen lines, there is no sign at present of an expanding shell. Struve[12] has investigated the effects of an extended atmosphere, with considerable dilution of radiation, on the spectra of various elements. The most important effects arise

[12] *Proc. Amer. Phil. Soc.*, **81**, 211, 1939.

from the increase of the populations of excited metastable levels with reference to excited normal levels. Interesting examples occur in the case of helium, where the 2^3S and 2^3P levels may gain tremendously in population over the 2^1P level. In the case of P Cygni[13] the 2^3P level is overpopulated by a factor of 3; the triplet series can be traced to the twenty-first member, while the singlet series reaches the eleventh member. Cases of more extreme dilution are known. Within the observational error, in υ Sgr there is no sign of such an effect.

In the spectra of the ionized metals there are many which have lines arising from excited metastable levels, e.g., *Ti* II, *Mn* II, *Cr* II, and *Fe* II. In the spectrum of the shell of 17 Lep these lines are found to be strong.[13] The dominant lines of *Mg* II and *Si* II, however, arise from excited levels which communicate with the ground level; these lines are weakened nearly to disappearance in 17 Lep. In υ Sgr, on the other hand, the lines of *Si* II are among the strongest in the spectrum (e.g., λλ 4128, 4131, 3854, 3856, and 3863); *Mg* II, λ 4481, is also extremely strong. The great development of the *Fe* II spectrum, in which lines arising from both high metastable and normal levels appear, is further evidence that dilution plays a negligible role in the formation of the lines. We may therefore apply, with some confidence, the usual theory of ionization in stellar atmospheres.

Some physical data concerning the star are available. The spectroscopic orbit yields a mass function of 1.582, and the secondary spectrum is never visible. If we assume that $m_1/m_2 = 2$, the minimum mass is 10 ⊙; values up to 100 ⊙ are not excluded. No data on possible variability of light are available. A rough value of the color temperature has been obtained by J. S. Plaskett,[5] who used a slit spectrograph to compare the intensity distribution between λ 4500 and λ 4950 with that in various B, A, and F stars. The intensity-curve obtained fits that of a star of spectral type Fo. The result is rather uncertain, and an accurate redetermination of the color temperature and energy distribution would be valuable. The absolute magnitude has been roughly estimated by McLaughlin[4] as

[13] Struve and Roach, *Ap. J.*, **90**, 727, 1939.

-7^m from the strength of the interstellar K line. Another estimate can be obtained from the radial velocity, on the assumption that the star takes part in the simple galactic rotation. Corrected for solar motion, the mean velocity of the star is +27 km/sec. The galactic latitude is $-15°$; the longitude, 350°; and the rotational term, rA, is +45 km/sec. If we adopt the value of the rotational constant, $A = 17$ km/sec/kpc, the distance is $r = 2700$ psc, and the absolute magnitude is -7^m6. The galactic latitude is high for so luminous an object; the corrections for interstellar absorption and reddening will be small. No significant parallax or motion can be detected.

The gravitational acceleration, g, at the surface lies in the range 50–500 cm/sec/sec. The gravitational acceleration is reduced by radiation pressure in the amount $20\bar{\kappa}$, where $\bar{\kappa}$ is the mass absorption coefficient. Since $\bar{\kappa}$ is greater than 0.1, and may be as high as 2, the effective acceleration, g_e, is unknown and must be carried as one of the variables of the problem. The existence of the components of the hydrogen lines suggests that radiation pressure is of some importance in the support of the atmosphere. The radius is roughly seventy times that of the sun.

Prediction of the level of ionization and of the actual strengths of absorption lines depends on a knowledge of the continuous absorption coefficient and requires a theory of line formation. We will make the following simplifying assumptions in our theoretical discussion: (1) The populations of excited levels are given by the Boltzmann distribution factor, with the excitation temperature equal to the ionization temperature. (2) The equivalent width of a line is proportional to the number of atoms in the level from which the line arises (weak lines on the straight-line portion of the curve of growth). (3) The monochromatic line absorption coefficient, l_ν, is small compared to the continuous absorption coefficient, κ_ν, so that we may employ Unsöld's form[14] of the weighting function, $G(\tau)$. This function measures the effectiveness of an atom at optical depth, τ, in reducing the emergent flux, H, i.e., in producing the line. The theory is usually applied to the wings of a line and is only a first approximation when equivalent widths are used. The lines used are weak, and the relative intensities should be accurate. Kirchhoff re-

[14] *Zs. f. Ap.*, **4**, 339, 1932.

emission ($\eta = 1$), accompanying true absorption, is assumed in the formation of the line. (4) The continuous absorption arising from hydrogen and the metals will be taken equal to that given in the tables of Unsöld.[15] Unsöld has used, for the ratio of the number of atoms of hydrogen to those of the metals, 14:1. This low value has been adopted in preference to the values of Russell or Pannekoek (1000:1) because of the nature of the hydrogen spectrum and the Balmer continuous absorption. Unsöld's lower value of the hydrogen abundance reduces the jump at the Balmer limit (for A stars negative hydrogen-ion corrections are irrelevant). Further, it will be shown that the actual hydrogen abundance is low. Unsöld's tables of absorption coefficients should properly be corrected for an appreciable bound-free absorption by helium. This correction is correlated with the high abundance of helium. The present investigation will limit itself to a first approximation, where the helium absorption is neglected. The absolute line intensities predicted will then be only approximate; the relation between the effective surface gravity, g_e, and the electron pressure is also rendered uncertain.

The measured equivalent widths will be converted into the number of atoms in the given level, and we shall want to compute that number theoretically. Unsöld's form of the Milne-Eddington theory of a stellar atmosphere yields the number of atoms above an effective photosphere. The ionization temperature, T, the effective electron pressure, P_e, and the effective optical depth, τ_0, of an equivalent homogeneous reversing layer can be obtained as functions of the effective temperature, T_e, and of the effective surface gravity, g_e. The Rosseland mean absorption coefficient, $\bar{\kappa}$, is taken from Unsöld's Table 6, and the other parameters of the equivalent atmosphere from his Table 12,[15] with some extrapolation. Also obtained from these data is the number of atoms per square centimeter above the "effective photosphere," (N). We wish to predict effective abundances of various elements in relevant stages of ionization and excitation. We shall adopt a set of total abundances, to be adjusted later by comparison with observations. Let us assume that the number of hydrogen atoms is half the total number, the number of helium atoms also half the total, and the number of iron atoms

[15] *Ibid.*, **8**, 225, 1934.

0.0136 that of hydrogen (the latter value according to Unsöld). The number of atoms in various stages of ionization were computed, as well as the number of neutral hydrogen atoms in the second level (H^*) and the number of helium atoms in the excited second levels (He^*). I have replaced the various helium levels by one level of statistical weight, $\omega = 16$, and excitation potential, $\chi = 20.69$ V. In the case of *Fe* I and *Fe* II the total numbers of atoms in these stages of ionization were derived. For *Fe* III, I computed (*Fe* III*), the number in the excited a^5P levels at $\chi = 8.22$ V, since the only lines that may be expected arise from that level.[16] The parameters of the computation were $\theta_e = 5040°/T_e$, and g_e, the effective temperature and surface gravity. Tables 6, 7, and 8 give the resultant predicted numbers of atoms for $g_e = 1$, 10, and 100, respectively. The results of Table 6 are subject to considerable uncertainty in the Rosseland mean absorption coefficient. For these low pressures and high temperatures, scattering by free electrons becomes of importance. The parameters θ and P_e are those derived theoretically from θ_e and g_e and are used in the ionization and excitation formulae.

Estimates of the population of the second levels of hydrogen and helium and of the excited levels of various other elements have been obtained by the measurement of equivalent widths of the lines on the three available plates. Table 9 gives the observational data for all measured lines. Because of the low dispersion and the crowded and blended nature of the spectrum, these equivalent widths give only the order of magnitude of the populations of the various levels. It was assumed that all the lines measured were on the straight-line portion of the curve of growth, an assumption probably justified for lines weaker than 0.2 A. The number of atoms, (N), is given by

$$(Nf) = 10^{13} \times W \times \left(\frac{3340}{\lambda}\right)^2. \qquad (1)$$

The equivalent width in angstrom units is W; the oscillator strength is f. The internal probable error of an equivalent width is about 10 per cent of its value, for the weakest lines. The absolute intensity is more seriously affected by the uncertainty of drawing the back-

[16] Swings and Edlén, *Ap. J.*, **88**, 618, 1938.

TABLE 6

PREDICTED NUMBERS OF ATOMS ABOVE THE EFFECTIVE PHOTOSPHERE

$g_e = 1$

θ_e	θ	log (N)	log P_e	log (He^*)	log (H^*)	log (Fe I)	log (Fe II)	log (Fe III*)
0.71	0.70	24.20	+0.18	10.7	17.4	18.7	22.0	13.4
.65	.65	23.53	− .23	10.9	17.0	16.5	21.4	14.4
.60	.60	23.25	− .08	11.8	16.3	15.8	20.9	15.4
.55	.55	23.34	− .30	12.8	15.8	14.8	20.5	16.4
.51	.50	23.70	+ .06	14.3	16.2	14.0	20.1	17.2
.45	.45	23.88	+ .24	15.5	16.3	13.4	19.4	17.8
.39	.40	23.95	+ .31	16.6	15.8	12.1	18.6	18.2
0.33	0.35	23.96	+0.32	17.6	15.5	10.7	17.7	18.7

TABLE 7

$g_e = 10$

θ_e	θ	log (N)	log P_e	log (He^*)	log (H^*)	log (Fe I)	log (Fe II)	log (Fe III*)
0.71	0.70	23.92	+0.64	10.3	17.1	18.1	21.8	13.0
.65	.65	23.87	+0.82	11.3	17.5	17.9	21.7	14.0
.60	.60	23.77	+1.01	12.2	17.6	17.5	21.6	15.0
.55	.55	23.65	+0.96	13.2	17.3	16.8	21.4	16.1
.51	.50	23.57	+0.93	14.1	17.1	15.8	20.8	16.9
.45	.45	23.57	+0.93	15.2	16.8	14.5	20.0	17.5
.39	.40	23.64	+1.00	16.3	16.5	13.2	19.3	17.9
0.33	0.35	23.70	+1.07	17.4	16.3	11.9	18.5	18.4

TABLE 8

$g_e = 100$

θ_e	θ	log (N)	log P_e	log (He^*)	log (H^*)	log (Fe I)	log (Fe II)	log (Fe III*)
0.71	0.70	23.29	1.08	9.7	16.5	18.7	21.1	11.9
.65	.65	23.19	1.16	10.6	16.8	17.6	21.0	13.0
.60	.60	23.07	1.20	11.5	17.3	17.1	20.9	14.2
.55	.55	23.07	1.27	12.6	17.0	16.6	20.8	15.5
.51	.50	23.08	1.38	13.6	16.9	15.9	20.6	16.3
.45	.45	23.15	1.44	14.7	16.8	14.9	20.1	17.0
.39	.40	23.22	1.51	15.9	16.6	13.4	19.3	17.4
0.33	0.35	23.22	1.67	16.9	16.5	12.7	18.6	18.0

ground in the crowded spectrum. Small corrections have been applied to the observed W when the line is suspected of blending. The oscillator strengths for helium and hydrogen in Table 9 are known from theoretical investigations.[17,18] The interpretation of the iron spectra is not possible without some f-values for the lines observed. The values given have been computed in several indirect ways, described below.

TABLE 9

EQUIVALENT WIDTHS AND POPULATIONS OF LOWER LEVELS OF SELECTED LINES

λ	Element	Transition	log f	W in Angstroms	log (N)
3563	*He*	2^3P-10^3S	−3.0	0.070	14.80
3599	*He*	2^3P-9^3S	2.9	0.088	14.75
3785	*He*	2^1P-12^1D	2.7	0.120	14.68
3676	*H*	2−22	3.5	0.036	14.96
3691	*H*	2−18	3.2	0.053	14.87
3703	*H*	2−16	3.1	0.103	15.00
3570	*Fe* I	$a^5F_4-z^3G^\circ_5$	1.2	0.031	12.34
4045	*Fe* I	$a^3F_4-y^3F^\circ_4$	0.8	0.064	12.15
3945	*Fe* II	$a^4P_{3/2}-z^6D^\circ_{3/2}$	4.0	0.207	16.48
4119	*Fe* II	$a^2D_{5/2}-z^4D^\circ_{5/2}$	4.1	0.122:	15.78:
4122	*Fe* II	$b^4P_{5/2}-z^4F^\circ_{5/2}$	4.3	0.236	16.23
4296	*Fe* II	$b^4P_{3/2}-z^4F^\circ_{5/2}$	3.9	0.279	16.36
3933	*Ca* II	$4^2S_{1/2}-4^2P^\circ_{3/2}$	−0.2	1.21	.....
3333	*Si* II	$4^2P^\circ_{1/2}-6^2S_{1/2}$	.....	0.110:	.....
3655	*Al* II	$4^3P^\circ_2-5^3D_{2,3}$	.....	0.146	.....
3923	*S* II	$4p^2D^\circ_{3/2}-4d^2F_{5/2}$	.....	0.157	.....

In the case of *Fe* I the relative f-values by King[19] indicate that the lines λ 3570 and λ 4045 are among the most probable transitions; Russell[20] has estimated the absolute f-values for similar lines. A rather indirect method must be used for *Fe* II. The level of ionization in the solar atmosphere and the abundance of iron are known, the latter from the knowledge of the absolute f-values for *Fe* I. Lines of *Fe* II with measured equivalent widths in the solar spectrum[21] were selected, which were weak in υ Sgr. One method of estimating the f-values of these lines depends on Russell's[20] abundance of iron in the sun. The other depends on the observed relative strengths of *Fe* I and

[17] Menzel and Pekeris, *M.N.*, **96**, 77, 1935.

[18] Goldberg, *Ap. J.*, **90**, 414, 1939.

[19] *Ap. J.*, **87**, 24, 1938.

[20] *Ap. J.*, **78**, 238, 1933.

[21] *Mem. Comm. Sol. Obs.*, **1**, No. 5, 1934; **2**, No. 6, 1938.

Fe II and the level of ionization, and therefore on the absolute *f*-values of *Fe* I. The two results are very accordant and, to a certain extent, independent. An error in the absolute *f*-values for *Fe* I will appear in those for *Fe* II; the ratio of *Fe* II/*Fe* I is, therefore, well determined. The small values given in Table 9 are not surprising, since all the lines violate, in some fashion, the selection rules for *L-S* coupling. The lines λ 4296 and λ 4122 involve $\delta L = 2$, together with a change in parent ion, $(^3P)4s\,^4P - (^5D)4p\,^4F^\circ$; λ 4119 and λ 3945 are intersystem combinations, without change of parentage.

It is also necessary to make an estimate of the absolute *f*-value for the transitions in the observable multiplet of *Fe* III. This is a transition of the form $(^4P)4s\,^5P - (^6S)4p\,^5P^\circ$ and will have a small *f*-value because of the change in the parent ion. The weakness of the transition is further supported by the fact that the strongest lines of this low-lying multiplet at λλ 4350–4430, with $\chi_1 = 8.22$ V, have intensities estimated between 1 and 3 in γ Peg,[16] a B2 star. Some lines arising from the level $5p\,^7P^\circ$, with $\chi_2 = 20.5$ V, are actually stronger—e.g., λ 4141, $I = 1$–2; λ 4123, $I = 3$–4; λ 4165, $I = 7$. If the high-level transitions are observed with the same intensity as the low $a\,^5P$ transitions, the latter will have *f*-values, f_1, given by

$$f_1 = f_2 10^{-\theta(\chi_2 - \chi_1)} \frac{\omega_2}{\omega_1}, \tag{2}$$

$$f_1 \approx 10^{-12.3\theta}, \tag{3}$$

where f_2 has been taken as ≈ 1, and the ratio of the weights also ≈ 1. Such considerations give f_1 of the order of 10^{-4}, for an assumed temperature of 17,000° for γ Peg. Another estimate can be obtained by assuming that the actual abundance of iron in the B stars is of the order of 10^{-4} of the total, i.e., of the Russell mixture having a high abundance of hydrogen. If this is done and the usual ionization theory is applied to γ Peg, the observed intensities of the lines from the low multiplet also correspond to $f \approx 10^{-4}$. This small *f*-value is of great significance, since otherwise the multiplet would appear in B8 stars and perhaps even later. No line of the *Fe* III spectrum is, with certainty, visible on the McDonald Observatory plates, and Plaskett lists none as an unblended line. The strongest line at

λ 4419.61 is blended with *Fe* II and *Mn* II, while the next lines of the multiplet, also variously blended, are not certainly seen. It is unfortunate that no positive decision can be made as to the presence or absence of *Fe* III, but certainly no line has an intensity as great as $I = 2$. A rough calibration would indicate that $W < 0.2$ A and that log (*Fe* III*) is less than 16.15.

The populations of the lower levels for each line, as given in Table 9, must be converted into the total numbers of atoms of *Fe* I and *Fe* II and into total populations of the second levels of *H* and *He*. This has been done in Table 10, which provides the essential data for a comparison with theory. The adopted value of $\theta = 0.5$,

TABLE 10

OBSERVED POPULATIONS

Element	Level	log (*N*)	Element	Level	log (*N*)
*H**	2 nd	14.95	*Fe* II	All	18.52
*He**	2 nd	15.16	*Fe* III*	a^5P	<16.15
Fe I	All	13.51			

$T = 10{,}000°$, is not very critical in the computation of the total numbers. The relative numbers in the three stages of the iron spectrum are decisive in fixing the level of ionization in the atmosphere. The estimated uncertainty of these values should not be larger than ± 0.3 in the logarithm.

The analysis of the observed intensities gives us a set of observational parameters, which, by comparison with Tables 6–8, would permit us to determine the relative abundances of *He*, *H*, and *Fe*, as functions of the assumed θ_e and g_e. It is immediately apparent that an immensely high abundance of helium will be required, of the order of one thousand times that of hydrogen. We will therefore investigate one obvious mechanism for increasing the relative strength of the helium lines.

STRATIFICATION

In the approximation used for the computation of the strength of an absorption line it was found possible to replace the actual atmosphere, in which l_ν/κ_ν, θ and P_e vary with optical depth, by an

equivalent homogeneous atmosphere. This approximation involved the use of the weighting function, $G(\tau_\nu)$, which measures the contribution of atoms at various optical depths to the formation of the line. Unsöld[14] has shown that in the case of true absorption the weight function $G(\tau_\nu)$ is given by

$$G(\tau_\nu) = \frac{3\beta}{3 + 2\beta} 2K_3(\tau) , \tag{4}$$

where $K_3(\tau)$ is the third exponential integral, and β is

$$\beta = \frac{3}{8} \frac{h\nu}{kT_0} \frac{\bar{\kappa}}{\kappa_\nu} , \tag{5}$$

where T_0 is the boundary temperature. The effective number of atoms in a given energy level is

$$(N^*) = \int_0^\infty G(\tau_\nu) \frac{\zeta(\tau_\nu)}{\mu_0 m_H \kappa_\nu(\tau_\nu)} d\tau_\nu . \tag{6}$$

Here, $\zeta(\tau_\nu)$ is the fraction of all atoms in the given level of the element, and $1/\mu_0 m_H$ is the number of all atoms per gram. Now, if $\zeta(\tau_\nu)$ is not sharply dependent on τ, and since $\kappa_\nu(\tau_\nu)$ is nearly constant, we may define an effective optical depth, τ_0, by

$$\tau_0 = \int_0^\infty G(\tau_\nu) d\tau_\nu , \tag{7}$$

and the effective number of atoms by

$$(N^*) = \frac{\zeta}{\mu_0 m_H} \frac{\tau_0}{\kappa_\nu} . \tag{8}$$

The essence of the approximation is the slow variation of $\zeta(\tau_\nu)$, since $K_3(\tau)$ decreases very rapidly with depth, roughly as $e^{-\tau}/\tau$. At temperatures of the order of 10,000°, $\zeta(\tau_\nu)$ varies slowly with depth for most elements. But for helium, with a very high excitation potential of 20.69 V, the increase of temperature with increasing τ is of primary importance. This will also be true for any element on the low-temperature side of its maximum. While τ_0 for most of the ele-

ments is of the order of 0.5 mag., for helium it is found that the maximum contribution to the integral (eq. [6]) arises at $\tau = 2.5$. We must therefore consider, in the case of helium, the behavior of a stratified atmosphere.

The detailed investigation of stratification has been carried through for only one model, $g_e = 100$ and $\theta_e = 0.5$. Unsöld's tables of the continuous absorption coefficient were used, with $\bar{\kappa}/\kappa_\nu = 1$. A résumé of the results is given in Table 11, with a comparison of the predicted numbers of atoms in the stratified and unstratified cases. The pressure, absorption coefficient, and temperature vary with depth, the important variation being in the temperature, which increases as the fourth root of the optical depth. The large increase in

TABLE 11

EFFECT OF STRATIFICATION, $g_e = 100$, $\theta_e = 0.50$

	log (*He**)	log (*H**)	log (*Fe* I)	log (*Fe* II)	log (*Fe* III*)
Stratified	14.63	16.72	16.03	20.59	16.35
Nonstratified	13.82	16.88	15.76	20.53	16.40

helium, by a factor of seven times, is most striking. Smaller effects are noticeable in the other elements. Another, and very rough, estimate of the effect of stratification has been obtained in a simplified model, in which the variation of the continuous absorption coefficient with depth was neglected and only the effect on the helium atoms was computed. The ratio of increase of the number of excited helium atoms in this model over the nonstratified case was found to be 28 for $\theta_e = 0.60$, 7 for $\theta_e = 0.50$, and 8 for $\theta_e = 0.40$. These factors have been applied in the final predicted values $(He^*)'$ in Table 12; for other elements the effects of stratification are omitted.

The observational data of Table 10 can now be compared with the predicted values. Only a small range of ionization is compatible with the observed intensities of *Fe* I and *Fe* II (and the absence of *Fe* III), which essentially fix the possible ranges of temperature and surface gravity. The predicted numbers of excited helium and hydrogen atoms, given in Table 12, are obtained by varying the relative abundance of hydrogen and helium to give a predicted ratio in agreement with the observed ratio of intensities.

This, of course, will not affect the absolute intensities. The relative abundance required to obtain the observed ratio is also given. The predicted number of iron atoms in various stages of ionization has been obtained by using the fixed ratio $Fe/H = 0.0136$, as given by

TABLE 12

LOGARITHMS OF THE PREDICTED NUMBERS OF ATOMS

θ_e	$g_e = 1$	$g_e = 10$	$g_e = 100$
0.65	(He*)′ 12.8 (Fe I) 12.2 (Fe II) 17.1 (H*) 12.7 (Fe III*) 10.1 log He/H = 4.6		
0.60	(He*)′ 13.4 (Fe I) 12.7 (Fe II) 17.8 (H*) 13.2 (Fe III*) 12.3 log He/H = 3.4		
0.55	(He*)′ 14.1 (Fe I) 12.9 (Fe II) 18.6 (H*) 13.9 (Fe III*) 14.5 log He/H = 2.2	(He*)′ 14.5 (Fe I) 13.7 (Fe II) 18.3 (H*) 14.2 (Fe III*) 13.0 log He/H = 3.4	
0.51	(He*)′ 15.3 (Fe I) 12.9 (Fe II) 19.0 (H*) 15.1 (Fe III*) 16.1 log He/H = 1.4	(He*)′ 15.2 (Fe I) 13.7 (Fe II) 18.7 (H*) 15.0 (Fe III*) 14.8 log He/H = 2.4	(He*)′ 14.7 (Fe I) 13.6 (Fe II) 18.2 (H*) 14.5 (Fe III*) 13.9 log He/H = 2.7
0.45		(He*)′ 16.1 (Fe I) 13.6 (Fe II) 19.1 (H*) 15.9 (Fe III*) 16.6 log He/H = 1.2	(He*)′ 15.7 (Fe I) 13.7 (Fe II) 18.9 (H*) 15.6 (Fe III*) 15.8 log He/H = 1.5
0.39		(He*)′ 16.8 (Fe I) 13.3 (Fe II) 19.4 (H*) 16.6 (Fe III*) 18.0 log He/H = −0.3	(He*)′ 16.7 (Fe I) 13.2 (Fe II) 19.1 (H*) 16.4 (Fe III*) 17.2 log He/H = 0.3
0.33			(He*)′ 17.1 (Fe I) 13.0 (Fe II) 18.9 (H*) 16.8 (Fe III*) 18.3 log He/H = −0.9
Observed numbers	(He*)′ 15.2 (Fe I) 13.5 (Fe II) 18.5 (H*) 15.0 (Fe III*) <16.2		

Unsöld. The relative abundance He/H is the only disposable parameter of each atmosphere. It can be seen that a satisfactory fit to the observed numbers of absorbing atoms can be obtained from several model atmospheres. For $g_e = 1$, $\theta_e = 0.52$, the mean electron pressure is ≈ 1 bar, and the ratio He/H is about 80. For $g_e = 10$, the fit is good at $\theta_e = 0.51$, $P_e = 10$, and He/H is 250. For $g_e = 100$, $\theta_e = 0.48$, $P_e = 25$, and He/H is about 100. A small differential

effect on the predicted intensity of *Fe* III exists, but it is insufficient as an observational criterion to distinguish which of these models is to be preferred. The existence of highly excited lines of other elements (see below) leads me to prefer the model with the higher pressure and temperature: $g_e = 100$, $T_e = 10{,}500°$.

The very high abundance of helium compared to hydrogen may be subject to the uncertainties, discussed below, which arise because of the large difference of excitation potential between the two elements. In the case of iron, however, the strength of *Fe* II and the apparent absence of *Fe* III are probably sufficient to establish the relative abundance of iron and hydrogen. The abundance seems close to the value tentatively adopted, i.e., of the order of 1 per cent by number of atoms. This is much closer to the range of values usually adopted for stellar interiors than to the value adopted for stellar atmospheres (less than one-thousandth). A high abundance of helium may also be compatible with conditions in stellar interiors.

SUPEREXCITATION

Deviations of the energy distribution of the exciting radiation from a black-body curve have been suggested as the origin of anomalous ionization and excitation in stars. A low continuous absorption coefficient in the far ultraviolet would not be implausible, or local variations of "surface temperature" might exist in connection with turbulent motions. In either case the spectroscopic evidence would take the form of an excessive range of ionization and excitation in the line spectrum of the star. The identification of lines of *Fe* I in υ Sgr is certain, and lines of other neutral metals probably exist. The presence of lines of very high excitation, *S* II and *A* II, is also established. Several unsolved spectroscopic problems in this connection make it difficult to present direct evidence for abnormal intensities of highly excited lines. A brief review of the interesting cases is given below.

Si II.—All lines of *Si* II are very strong, and the curve of growth is needed for proper interpretation. The line at λ 3333 arises from a level at 10.02 V, and has $I = 2$. The lines from the lower level at 6.83 V, λ 3856 and λ 3863, are exceedingly strong, $I = 11$ and 9, respectively. No abnormality of excitation is obvious. *Si* II is just past its maximum and is becoming slightly ionized.

Al II.—The lines of *Al* II are strong; λ 3655 has $I = 2$, and $\chi = 13.02$. This line and λ 3333 of *Si* II are undoubtedly weak transitions, picked for measurement of equivalent width because they will be near the straight-line portion of the curve of growth. Their *f*-values must be low. The group of *Al* II lines at λλ 3586.55, 7.06, and 7.44, with $\chi = 11.80$ V, are blended with *He* and *Ti* II; but the observed blended line has the amazing intensity of $I = 25$ and is nearly as strong as the K line. The line is very greatly enhanced over α Cyg. The intensity of the higher-level *Al* II line is therefore not anomalous. At the adopted temperatures and pressures, *Al* II is becoming partly ionized.

S II.—The lines of *S* II, according to Morgan, are stronger than in any other star. The line at λ 3923 is weak but unblended, with $I = 2$. It arises from a level at 16.13 V. Nearly all *S* is singly ionized.

Ne I.—Merrill[8] reports the presence of the strong lines of *Ne* I in the visual region. These arise from excited levels near $\chi = 16.55$ V. I have arbitrarily assumed that the strongest line, λ 6402, has an equivalent width corresponding to $(Nf) = 10^{12}$. *Ne* is nearly all neutral.

C II.—The identification of *C* II is difficult. The strongest line at λ 4267 seems to be present, as well as λ 3919 and possibly λ 3921. The identification would be more certain if the lower lines at λ 6578 and λ 6583 could be measured. If present, *C* II would indicate appreciable populations of levels at 18.0 V. All *C* would be singly ionized. I have taken the arbitrary estimate that *C* II contributes one-half of the line at λ 4267 and have estimated its equivalent width.

A II.—Perhaps the most striking feature in the spectrum is the identification by Morgan[7] of *A* II in the blue region of the spectrum. Little extra weight can be obtained from the ultraviolet lines, but the identification seems satisfactory. Dr. Morgan informs me that the lines may vary in intensity; at the present epoch they seem to be weak, and the equivalent width has been estimated. The excitation potential is 18.34 V for λ 4042. All *A* would be singly ionized.

N II.—The strongest line at λ 3995 may be present, $I = 2n$; no strong blending line can be identified at this wave length. Lines of similar nature (e.g., λλ 3437 and 3956) are absent. λ 3437 should

have been seen if its equivalent width were greater than 0.02 A, and should not be much weaker than λ 3995. It would be important to establish the existence of some of the lines of lower excitation potential in the visual region of the spectrum. I have estimated the equivalent width of λ 3995, assuming it to be present.

He and *H*.—Helium is obviously most subject to the effects of any possible anomalous excitation, and its excessive abundance might be illusory. It should be remembered, however, that the relative weakness of the hydrogen lines cannot be explained in this manner. Hydrogen, with an ionization potential of 13.5 V, is mainly ionized; but metals such as *Fe* II, with an ionization potential of 16.5 V, are also mainly ionized. If we assume that hydrogen is weakened by excessive ionization, the metals would be similarly affected. The great strength of the metallic lines, compared to hydrogen, is evidence for the absence of any very large deviations from equilibrium conditions up to energies of the order of 16 V.

In Table 13 an attempt has been made to summarize the evidence for deviations from equilibrium conditions of excitation in the extreme ultraviolet. The measured equivalent widths have been used to obtain estimates of the populations of excited levels of the various elements. Some of the lines which could not be measured are arbitrarily assigned maximum populations, given in parentheses in the fourth column. The Boltzmann distribution was assumed, in order to compute the total abundances ζ, for two temperatures, in the fifth and sixth columns. These fractional abundances are given in terms of the total theoretical number of all atoms (N) above an effective photosphere. The unknown f-values for the various lines present a serious difficulty. For *S* II, *Ne* I, *C* II, *A* II, and *N* II the f-values should be of the order of unity, since the lines are among the strongest laboratory lines. For *Si* II and *Al* II the f-values are low. We cannot neglect the effect of stratification for lines of such high excitation potential. A detailed solution in the stratified case was available only for $g_e = 100$, $\theta_e = 0.50$. The increase in this case is as large as 3, for *N* II, over the unstratified case. As a first approximation these theoretical factors have also been applied to the predictions for the unstratified atmosphere with $\theta_e = 0.40$.

The computed abundances, ζ, for a temperature of 10,000° show

some indication of a systematic increase with excitation potential and are not completely in agreement with the usually accepted values. It is unfortunate that the presence of *C* II, *A* II, and *N* II is not more certainly established. At 10,000° they appear to be more abundant than *Fe*. At a temperature of 12,500° these relative abundances would seem more normal. But the ionization then seems too high, and we would expect *Fe* III to be stronger than *Fe* I, in contradiction to the observations. Until definite evidence for the high-

TABLE 13

ABUNDANCE OF THE ELEMENTS AS FUNCTION OF EXCITATION POTENTIAL

$g_e = 100$

ELEMENT	LINE	χ	LOG (Nf)	LOG ζ		f
				$\theta_e = 0.50$	$\theta_e = 0.40$	
Fe I	.....	Low	.....	−4.7	−2.6	.....
Fe II	.....	Low	.....	−4.3	−3.1	.....
Fe III	.....	8.82	.....	<-2.3	<-3.3	.....
Si II	3333	10.02	12.0	$-5.1-\log f$	$-4.9-\log f$	Small
H	.....	10.16	.....	−2.0	−1.9	.....
Al II	3655	13.02	12.1	$-4.7-\log f$	$-4.9-\log f$	Small
S II	3923	16.13	12.1	$-3.4-\log f$	$-4.9-\log f$	≈ 1
Ne I	6402	16.55	(12)	$(-3.7-\log f)$	$(-4.4-\log f)$	≈ 1
C II:	4267	18.0	(11.7)	$(-3.3-\log f)$	$(-4.8-\log f)$	≈ 1
A II	4042	18.34	(11.5)	$(-2.5-\log f)$	$(-4.0-\log f)$	≈ 1
N II:	3995	18.42	(11.0)	$(-2.3-\log f)$	$(-3.9-\log f)$	≈ 1
He	.....	20.69	.....	+0.3	−1.6	.....

excitation lines and for the presence of *Fe* III and other doubly ionized elements is forthcoming, it seems unprofitable to speculate on the meaning of this discrepancy between the temperature obtained from elements of high and of low excitation potentials. The energies at 20 V differ by a factor of 100 between 12,500° and 10,000. It should be emphasized that the observed spectroscopic features cannot be described with the higher temperature. The intensity of the predicted lines of both hydrogen and helium would be much greater than that of the observed lines, and a new source of continuous absorption would be required to reduce the discrepancy. (The nature of this discrepancy is shown in Table 13 by the low absolute abundances of hydrogen and helium for $\theta_e = 0.40$.) All elements

with lines of low excitation potential—*Fe* II, *Cr* II, *Ti* II—would then have excessively high abundances compared to hydrogen.

The high abundance of helium in υ Sgr is indicated by a comparison of its strength with that of *C* II, *N* II, and *O* II. The helium lines are as strong as in B stars, while the other elements are weak or absent. In B stars these elements have intensities more nearly comparable to helium. No matter how high a temperature is used to describe the excitation of high-energy lines, the strength of the helium lines would still indicate an abnormally high abundance of helium relative to *C*, *N*, and *O*.

THE CONTINUOUS ABSORPTION COEFFICIENT

The present theoretical discussion has been based on the normal abundance of hydrogen and the metals. No great weight can be placed on the predicted intensities of the absorption lines, but it is obvious that the great strength of all lines requires an extremely deep atmosphere with a low absorption coefficient. The weakness or absence of a jump in intensity at the Balmer limit is confirmation of the relative unimportance of the absorption by hydrogen. Struve and Sherman[11] have shown that the absorption lines beyond the Balmer limit are only slightly weakened. There must be only a small change in τ_0/κ_ν, according to equation (8). The hydrogen may be so highly ionized that electron scattering is large and serves to smooth out the discontinuity in the absorption by the neutral hydrogen. In the model atmosphere with $g_e = 100$, electron scattering is negligible, although it may be of importance at lower pressures.

The contribution of excited helium atoms has not been taken into account in Unsöld's tables of the continuous absorption coefficient, nor has it received much theoretical attention. If the helium lines are of appreciable intensity compared to the hydrogen lines, the continuous absorption by helium must be appreciable in comparison with that of hydrogen. The helium absorption limits fall in the near infrared, as close to the normal photographic region of the spectrum as the Paschen series limit of hydrogen. Let us assume, as a first approximation, that the continuous absorption coefficient per atom in an excited level of helium is the same as for an atom in an excited level of hydrogen. We can express the relative populations of the

third levels in terms of the observed populations of the second levels. The helium atom is idealized in that the third level is given weight $\omega = 36$, $\chi_3 = 22.93$ V; the second level, weight $\omega = 16$, $\chi_2 = 20.69$ V. The relative populations of the third levels of helium and hydrogen are given by

$$\frac{(He^*)_3}{(H^*)_3} = 2 \times 10^{-0.36\theta} \frac{(He^*)_2}{(H^*)_2}. \tag{9}$$

The observed value of $(He^*)_2/(H^*)_2$ is about 1.6, so that there are about 1.4 times as many helium atoms active in continuous absorption processes as hydrogen atoms. This amount must be added to the metallic absorption in its effect on the jump at the series limit of hydrogen.

As long as electron scattering can be neglected, at a temperature of 10,000°, Unsöld's ratio of hydrogen to the metals (14:1) predicts a jump of 0.6 mag. at the Balmer limit. The addition of the helium absorption is roughly equivalent to doubling the amount of metallic absorption and reduces the jump to 0.5 mag. This seems insufficient but suggests that a theoretical computation of the absorption coefficient of helium may have interesting applications. According to Struve and Sherman,[11] line intensities in multiplets beyond the Balmer series limit are slightly decreased by the increase of a continuous absorption coefficient, but less so in υ Sgr than in any normal star. The Balmer jump, according to Figure 1, seems actually to be less than 0.2 mag. This low value would suggest that the absorption by helium, metals, and electrons should be ten times as large as by hydrogen.

The effect of a large abundance of helium on other features of the atmosphere may be outlined. If we adopt the ratio of hydrogen to the metals as 14 and the abundance factor of helium to hydrogen as 100, the most important effect is the reduction in the number of free electrons per atom. As long as we can neglect the ionization of helium, the electron pressure will be of the order of one-hundredth of the gas pressure instead of one-half for Unsöld's mixture. For a given surface gravity and temperature the electron pressure will be lower and the ionization higher than normal. A given temperature

and electron pressure can occur at higher surface gravities. High helium abundance produces the same effects as low surface gravity and could be a source of absolute-magnitude effects. Russell[20] has suggested this possibility in connection with the spectrum of α Cyg, a less extreme case than υ Sgr. Finally, a high abundance of helium in the interior of a star will make it overluminous for its mass.

Several interesting problems are suggested by this preliminary investigation. The computation of the continuous absorption coefficient of helium would be valuable in connection with evolutionary speculations. Its effect on the energy distribution would be of interest in connection with the observation of the energy distribution in the continuous spectrum. The low color temperature derived by Plaskett[5] might well be reinvestigated, with possible extensions to the infrared and ultraviolet. Some method for the determination of mass is badly needed, and traces of the secondary star might be searched for in the energy distribution or in the spectrum in other wave-length regions. Finally, it would be important to investigate the possible variability of light.

The present investigation was started at the suggestion of Dr. Otto Struve, during the author's tenure as National Research Council Fellow. I am deeply indebted to Dr. Struve for his advice and insight and for his many valuable suggestions. The loan of unpublished spectroscopic data by Mrs. Moore-Sitterly is gratefully acknowledged. I am indebted also to Professor Henry Norris Russell for an inspiring discussion of this problem.

YERKES OBSERVATORY
January 20, 1940

NOTES

ON THE EVOLUTION OF COMETS

The purpose of this note is to show that those comets which are now inside the system of planets (mean distance a between 2 and 10 a.u.), i.e., the short-period comets, have arrived there in comparatively recent times from more distant regions, where they were long-period comets.

The presence of the tail suggests that the short-period comets are unlikely to have existed for a very long time in the present state. We may, therefore, confine ourselves to the study of the recent history of these comets. In particular, we shall consider the changes in the elements of their orbits. In the comparatively short interval of time during which the perturbation due to Jupiter may have considerably changed a comet's elements, the perturbation due to the other planets may be neglected. Thus, we can apply Jacobi's integral of the restricted problem of three bodies,

$$I_1 - a_{\text{Jup}}^{-3/2} I_2 = \text{constant},$$

where $a_{\text{Jup}}^{3/2}$ is the period of revolution of Jupiter, which is supposed to have a circular orbit.

$$I_1 = -\frac{1}{2a} = -\frac{1-e}{2q}$$

and

$$I_2 = \sqrt{a}\cos\phi\cos i = \sqrt{q(1+e)}\cos i$$

represent the energy and the z-component of the moment of momentum per unit mass of the comet relative to the center of gravity of the solar system.

Let us plot the comets in a *Lindblad diagram*. Hyperbolic, parabolic, and elliptic orbits correspond to $I_1 \gtreqless 0$, respectively. Circular orbits of inclination 0° (direct) and 180° (retrograde) correspond to the full-drawn lines on the right and left sides, marked $\cos\phi\cos i =$

$+1$ and -1, respectively. The domains outside (below) these two lines are inaccessible (unreal domains). Comets which have been observed several times ("periodic" comets) are represented by triangles; the other elliptical comets, by dots. Parabolic and hyperbolic comets are omitted in this diagram. We notice four characteristics of the distribution of the comets in this diagram: (1) there are

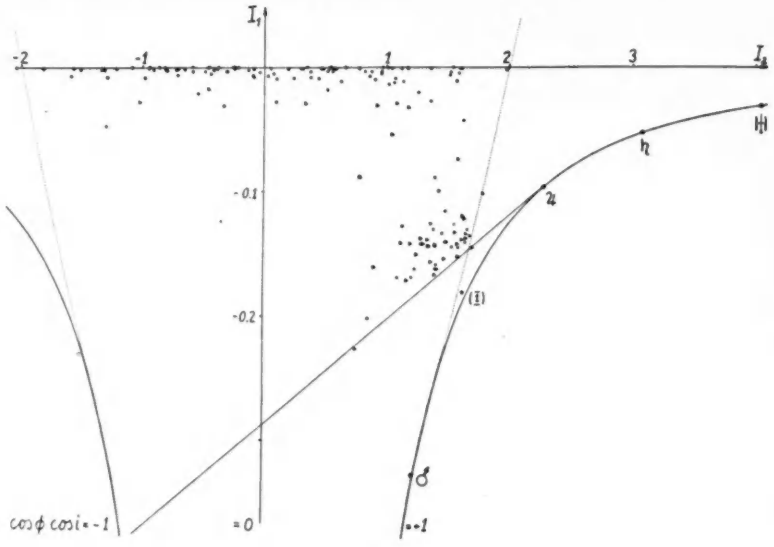

FIG. 1

no comets outside the two dotted lines; (2) there are no comets under the oblique straight line; (3) there are no short-period comets of small and of negative (retrograde) moment of momentum; and (4) there are no strongly hyperbolic comets (in the diagram the hyperbolic comets would practically lie on the line $I_1 = 0$).[1] These features are explained as follows:

1. Outside the two dotted lines the perihelion distance q is always greater than 2; therefore, comets of these domains are likely to escape observation.[2]

[1] Cf. Charlier, *Application de la théorie des probabilités à l'astronomie*, Paris, 1931; L. Fabry, *Etude sur la probabilité des comèts hyperboliques et l' origine des comètes* (thèse), Marseille, 1893.

[2] Cf. Bourgeois and Cox, *B.A.*, **9**, 349, 1936.

2. According to Jacobi's integral, the comets can move in this diagram along straight lines parallel to the oblique line. If we make the hypothesis that the comets have arrived along these lines from the upper part of the diagram, i.e., from long-period domains, then it follows that they were able to reach only the domains above the oblique line (and, of course, above the adjoining parts of the full-drawn boundary lines $\cos\phi \cos i = \pm 1$), since the upper part of the boundary line $\cos\phi \cos i = +1$ acts as a screen. This hypothesis offers the most reasonable explanation of (2).[3] What happens to short-period comets which stay a rather long time in the lower part of the diagram? Owing to the proximity of the sun, they lose their tails. Furthermore, the disturbances from the other planets cause the comets to move also in directions different from that given by the Jacobi integral due to Jupiter. Thus, the older short-period comets may cross the oblique straight line (Comet Encke has already crossed it) and become minor planets.[4] The minor planets are situated near the line $\cos\phi \cos i = +1$, nearly all of them lying between this line and the oblique line. To establish the latter conclusion, however, it should be proved by statistical mechanics that there exists a tendency toward a diminution of the inclinations and eccentricities of small particles in the solar system.

3. The lack of retrograde short-period comets[5] is probably due to the instability of any retrograde swarm of particles, as will be shown elsewhere.[6]

HERBERT JEHLE

DEPARTMENT OF PHYSICS
UNIVERSITY COLLEGE, SOUTHAMPTON,

INSTITUT D'ASTRONOMIE
UNIVERSITÉ DE BRUXELLES

[3] Mentioned by Schulhof, *A.N.*, **124**, 195, 1890.

[4] Cf. Leuschner, *Pub. A.S.P.*, **39**, 275, 1927; Bobrovnikoff, *Lick Obs. Bull.*, No. 408, 1929.

[5] A. Newton, *Mem. Nat. Acad.*, **6**, 7, 1893; H. N. Russell, *A.J.*, **33**, 49, 1920.

[6] Jehle, *La mécanique statistique en astronomie*, **6**, 7, 1893.

THE CONTOURS OF $H\gamma$ IN A-TYPE STARS

ABSTRACT

The contours of $H\gamma$ in 14 A-type stars are measured, and their half-widths and those of additional stars are found. The half-width shows a strong dependence on the absolute magnitude, increasing from 1.6 A for giants, to 26.6 A, for white dwarfs.

For the purpose of measuring the contours of the hydrogen lines in A-type stars, Dr. W. H. Wright, director of the Lick Observatory, kindly placed at my disposal a number of spectrograms obtained in

TABLE 1

MEASURED HALF-BREADTHS OF $H\gamma$ IN ANGSTRÖM UNITS

Star	Plate	0.9	0.8	0.7	0.6	0.5	0.4	0.3	r_0
η Leo	Y570I, slitless	7.75	5.35	2.75	.....	.....	.....	.....	0.605
κ U Ma	Y247U, slit	11.8	8.3	6.02	4.59	2.81	.....	.....	.41
β Aur	Y550E, slitless	20.5	13.8	8.4	5.8	2.2	.....	.....	.48
α^2 C Vn	Y406E, slitless	12.7	9.0	6.0	4.2	2.2	.....	.....	.42
γ Gem	Y505, slitless	20.5	15.0	10.5	7.6	5.1	2.0	.....	.36
λ Oph	Y370E, slitless	18.0	14.85	9.7	7.25	4.45	.....	.....	.405
γ U Ma	Y218I, slit	16.2	11.4	8.4	6.5	4.8	3.4	1.5	.265
β U Ma	Y401B, slitless	15.8	11.1	7.6	4.8	2.8	.....	.....	.37
β U Ma	Y217H, slit	16.0	10.3	7.7	5.8	4.1	2.8	1.2	.255
α Cr B	Y315F, slit	7.75	5.21	3.88	2.55	0	.....	.....	.50
α C Ma	Y545B, slitless	17.1	13.4	9.0	6.0	3.4	.....	.....	.44
7 Lac	Y441B, slitless	20.3	15.6	11.4	8.4	4.8	.....	.....	0.41
van Maanen 1166	Slitless	50	31	22	15	.....	.....	.....	.....
Wolf 1346	Slitless	57	33	20	.....	.....	.....	.....	.....

1925–1926 by C. S. Yü with the Crossley reflector, some with the UV glass lenses and slit, and others with the quartz lenses without slit. The dispersion near $H\gamma$ is about 90 A/mm for the slit, and 115 A/mm for the slitless, spectrograms. Two microphotometer tracings were made of each plate, except in the case of κ U Ma and α Cr B. The scale on the tracings near $H\gamma$ is 0.98 mm/A for the slit spectrograms and 0.78 mm/A for the slitless spectrograms. The half-breadths at various residual intensities and the central residual intensities are listed in Table 1. Included in this list are the data

derived from measurements of two white dwarf stars, made by Y. Öhman.[1]

The half-widths δ' of the measured stars and of additional stars, taken from the large observational material published by C. T.

TABLE 2

VALUES OF δ' FOR $H\gamma$ IN A-TYPE STARS OBTAINED FROM THE EQUIVALENT BREADTH AND CENTRAL INTENSITY

Star	Observer	M	δ' (A.U.)	Star	Observer	M	δ' (A.U.)
Boss 786	G	−5	1.4	α Lyr	G	+0.6	6.2
σ Cyg	G	−4	1.8	β U Ma	E	+0.8	7.3
Mean	(2)	−4.5	1.6	β U Ma	G	+0.8	5.8
				β U Ma	K	+0.8	5.6
η Leo	E	−3.4	3.0	β U Ma slit	K	+0.8	6.4
η Leo	G	−3.4	2.4	α Cr B	E	+0.9	7.8
η Leo	K	−3.4	4.0	α Cr B	G	+0.9	5.4
13 Mon	G	−3	2.7	α Cr B	K	+0.9	3.8
γ Lyr	G	−2	2.8	ε U Ma	G	+1.0	5.1
Mean	(5)	−3.0	3.0	Mean	(9)	+0.8	5.9
				α C Ma	E	+1.3	8.8
κ U Ma	K	−0.6	4.5	α C Ma	G	+1.3	6.5
ϑ Aql	E	−0.2	5.5	α C Ma	K	+1.3	6.7
ε U Ma	E	−0.2	5.7	α^2 Gem	E	+1.3	6.6
β Aur	E	−0.1	7.6	α^2 Gem	G	+1.3	5.9
β Aur	G	−0.1	7.0	7 Lac	K	+1.9	9.2
β Aur	K	−0.1	7.7	α′ Gem	E	+2.2	6.7
α^2 C Ven	E	−0.1	4.1	Mean	(7)	+1.5	7.2
α^2 C Ven	K	−0.1	5.0				
δ Cyg	G	0.0	4.2	van Maanen 1166	O	+8.6	23.0
λ Oph	K	+0.1	6.9	Wolf 1346	O	+9.8	30.2
γ Gem	E	+0.1	7.2	Mean	(2)	+9.2	26.6
γ Gem	G	+0.1	6.1				
γ Gem	K	+0.1	7.5				
ϑ Aur	G	+0.3	4.1				
α And	G	+0.4	4.1				
γ U Ma	G	+0.4	6.8				
γ U Ma	K	+0.4	5.5				
Mean	(17)	0.0	5.9				

Elvey[2] and S. Günther,[3] were determined by one of the three methods described by the author.[4]

In Table 2 are shown the values of δ' for $H\gamma$ for the entire list

[1] *Arkiv för matematik, astronomi och fysik*, **25**B, No. 21, 1937.

[2] *Ap. J.*, **71**, 191, 1930.

[3] *Zs. f. Ap.*, **7**, 106, 1933.

[4] *Pub. A.A.S.*, **9**, 263, 1939.

of stars, arranged according to absolute magnitude. Group means are also given. A general increase of δ' with absolute magnitude is noted, although there is some scatter of the individual data, owing to the dispersion used, the quality of the spectrograms, the manner in which the continuous background was drawn in, etc.

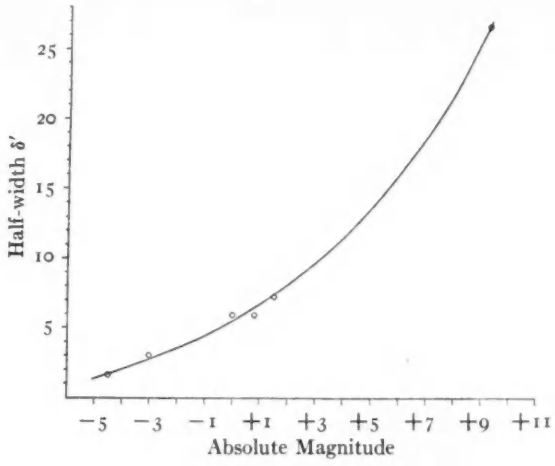

FIG. 1

The results are shown graphically in Figure 1. The absolute magnitudes of the stars measured by the author were calculated from mean parallaxes kindly furnished by Professor Frank Schlesinger.

It is a pleasure to acknowledge my indebtedness to Dr. W. H. Wright, director of the Lick Observatory, for the loan of spectrograms; to Dr. Otto Struve, director of the Yerkes Observatory, for numerous helpful discussions; and to Professors H. N. Russell and A. Unsöld for helpful advice.

C. J. KRIEGER

ST. LOUIS UNIVERSITY
September 7, 1939

REVIEWS

Atlas der Restlinien von 30 chemischen Elementen; 28 photographische Tafeln. By A. GATTERER and J. JUNKES. Specola Vaticana. Castel Gandolfo, 1937.

Two years ago the astrophysical laboratory of the Specola Vaticana published this atlas of the ultimate lines (*raies ultimes, Restlinien*) of the spectra of thirty elements, in 28 photographic plates. Its importance for spectroscopic research, especially in astrophysics, does not seem to have been sufficiently recognized. A review of two of the preceding papers by the same authors has already appeared in this journal.[1]

To reach a greater precision in the determination of the wave lengths of the various lines, it is necessary to have a comparison spectrum, such as that of the iron arc or spark, for which the authors have published (in 1935) two useful and precise maps. The direct comparison of the iron spectrum with those of the thirty elements makes it convenient to use the existing spectroscopic tables—for example, those of the *Handbuch der Spektroskopie* by Kayser and Konen.

The *Atlas*, which goes from the infrared (8000 A) to the ultraviolet (2200 A) with a dispersion varying from 12 to 1.1 A/mm., is composed of 28 photographic plates on Agfa Lupex paper of size 30×40 cm. On each plate the authors give six chemical elements in six horizontal strips, so arranged that the same wave lengths are exactly on the same vertical lines. The strip of each element is again composed of six strips in the following order: (1) a comparison spectrum of iron; (2) the spectrum of the element with a short exposure; (3) a space for the wave lengths of the more intense lines; (4) the spectrum of the element with an average exposure; (5) the iron comparison spectrum; (6) the spectrum of the element with long exposure. The wave lengths are given in international angstrom units to the hundredth of an angstrom. The scheme to give three exposures of the spectrum of the element is particularly suitable for the investigation and identification of the more intense lines, as well as of the faintest. To make these photographs, which are really exceptional for the precision and clearness in all wave lengths, the rich instrumental equipment of the astrophysical laboratory of the Specola Vaticana has been

[1] *Ap. J.*, **86**, 108, 1937.

employed: for the infrared, a three-prism Steinheil spectrograph; for the first part of the ultraviolet, the same instrument with quartz optical parts; for the farthest ultraviolet, a two-prism Halle spectrograph.

To judge the resolving-power obtained in the plates, we may say that, in the violet, three components of an iron triplet, separated by 0.1–0.2 A, are well resolved; with the naked eye, lines 0.5 A apart are distinctly visible in the ultraviolet; and one can estimate lines whose separation is only 0.05 A.

The explanatory text of the *Atlas* gives the quality and the degree of purity of the employed elements, with indications about other elements contained in traces and about spurious lines visible in the spectra; there are also tables of the exposure times, of the electrodes employed, and of the conditions of excitation of the electric arc. In another pamphlet we find a list of the wave lengths of the principal lines for each element and of the photographic tables in which they may be found, with an indication whether the line is due to the neutral atom or to the ion. The most important lines are underlined. The intensities for the single lines are not given, as these may be taken directly from the photographs.

The atlas of the iron spectrum and the new atlas of the ultimate lines, by the astrophysicists of the Specola Vaticana, supplement one another, because the first allows an exact and easy reading of the scale (iron comparison spectrum) for the second. To facilitate the combined use of the two atlases there are given, at the bottom of each table of the second atlas, the number of the corresponding table of the first.

GIORGIO ABETTI